

Site-directed mutagenesis in photosystem I complex: Functional analysis of
P700

by

Maria Pantelidou

A dissertation submitted to the graduate faculty
in partial fulfillment of the requirements for the degree of

DOCTOR OF PHILOSOPHY

Major: Biochemistry

Program of Study Committee:
Parag R. Chitnis, Major Professor
Arun B. Barua
Basil J. Nikolau
David J. Oliver
Robert W. Thornburg

Iowa State University

Ames, Iowa

2004

Copyright © Maria Pantelidou, 2004. All rights reserved.

UMI Number: 3139257

INFORMATION TO USERS

The quality of this reproduction is dependent upon the quality of the copy submitted. Broken or indistinct print, colored or poor quality illustrations and photographs, print bleed-through, substandard margins, and improper alignment can adversely affect reproduction.

In the unlikely event that the author did not send a complete manuscript and there are missing pages, these will be noted. Also, if unauthorized copyright material had to be removed, a note will indicate the deletion.

UMI[®]

UMI Microform 3139257

Copyright 2004 by ProQuest Information and Learning Company.

All rights reserved. This microform edition is protected against unauthorized copying under Title 17, United States Code.

ProQuest Information and Learning Company
300 North Zeeb Road
P.O. Box 1346
Ann Arbor, MI 48106-1346

Graduate College
Iowa State University

This is to certify that the doctoral dissertation of
Maria Pantelidou
has met the dissertation requirements of Iowa State University

Signature was redacted for privacy.

Committee Member

Signature was redacted for privacy.

Major Professor

Signature was redacted for privacy.

For the Major Program

TABLE OF CONTENTS

ABSTRACT	iv
CHAPTER 1. GENERAL INTRODUCTION.....	1
CHAPTER 2. SITE-DIRECTED MUTAGENESIS OF AMINO ACIDS HYDROGEN BONDING TO THE PRIMARY ELECTRON DONOR OF PHOTOSYSTEM I.....	19
CHAPTER 3. FTIR SPECTROSCOPY OF <i>SYNECHOCYSTIS</i> 6803 MUTANTS AFFECTED ON THE HYDROGEN BONDS TO THE CARBONYL GROUPS OF THE PsaA CHLOROPHYLL OF P700 SUPPORTS AN EXTENSIVE DELOCALIZATION OF THE CHARGE IN P700+.....	45
CHAPTER 4. SITE-DIRECTED MUTAGENESIS OF AMINO ACIDS IN PsaB SURROUNDING THE PRIMARY ELECTRON DONOR OF PHOTOSYSTEM I.....	76
CHAPTER 5. GENERAL CONCLUSIONS.....	102
APPENDIX. DISRUPTION OF <i>crtX</i> GENE, ENCODING A HYPOTHETICAL ZEAXANTHIN GLYCOSYL TRANSFERASE IN <i>SYNECHOCYSTIS</i> SP. PCC 6803.....	105
ACKNOWLEDGEMENTS.....	118

ABSTRACT

Photosynthesis is the process by which plants and cyanobacteria convert light to chemical energy. Photosystem I and photosystem II are the two photosynthetic reaction centers that perform light-driven electron transport across thylakoid membranes. Using photon energy, photosystem I oxidizes plastocyanin in the lumen, transfers electron through a series of cofactors, and finally reduces ferredoxin on the stromal side of the thylakoid membranes. Photosystem I is a pigment-protein complex that consists of 12 or more proteins, 96 chlorophyll α molecules, 22 beta-carotenes, two phylloquinones, two lipid molecules, and three iron-sulfur clusters. PsaA and PsaB, the largest subunits, surround the electron transfer chain cofactors with a two-fold symmetry. These cofactors are: P700, the primary electron donor chlorophylls, another pair of molecules of Chl α (A_0), two phylloquinone molecules (A_1) and the iron-sulfur cluster Fx. Between P700 and Fx, A_0 and A_1 are symmetrically arranged in pairs, thus forming two branches of electron transfer chain. The directionality of electrons down one or both branches has been questioned. P700, a dimer of chlorophylls may play an important role in the determination of the electron directionality since P700 itself exhibits asymmetry, both in its structure and in its interaction with the protein. This asymmetry may influence the electron spin distribution over the two chlorophylls. This dissertation tests the functional significance of the asymmetric protein interactions of photosystem I.

P700 is a heterodimer of two chemically different chlorophyll α molecules. The chlorophyll molecule that is coordinated by PsaA is the C13² epimer of chlorophyll α . PsaB coordinates Chl α , the other half of P700. Thus, there are five hydrogen bonds between PsaA and Chl α' (some through a water molecule) that are not present on the other half of the dimer. To understand the importance of protein environment to the biophysical properties of P700, the hydrogen bonding residues in PsaA and the homologous positions in PsaB were altered using site-directed mutagenesis of the *psaA* and *psaB* genes of *Synechocystis* sp. PCC 6803. Fourier transform infrared (FTIR) spectroscopy was used to study the protein-cofactor binding interaction in P700. The electron spin density distribution over P700⁺ was determined by electron nuclear double resonance spectroscopy (ENDOR). Our results show

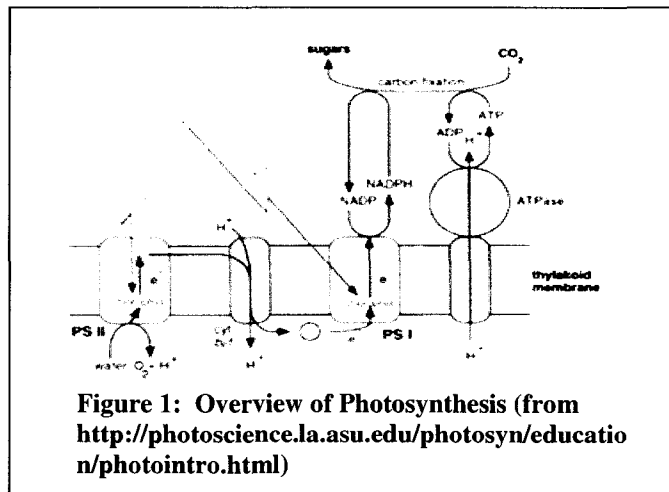
that changes of the hydrogen bonding residues in PsaA and the respective amino acids in PsaB, has not only altered the bonding pattern between P700 and the protein but has affected its electronic structure as well.

CHAPTER 1: GENERAL INTRODUCTION

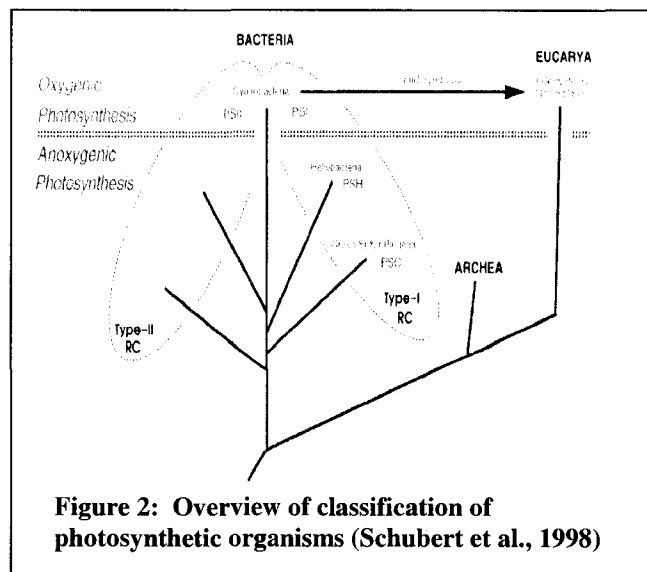
I. PHOTOSYNTHESIS

Photosynthesis is the conversion of solar energy to chemical energy by plants, algae and certain bacteria. This biological process, which is the primary source of food and oxygen on the planet, has made the existence and evolution of more complex organisms possible. Oxygenic photosynthesis takes place in two phases: the light reactions and the dark reactions. The light reactions utilize

four protein complexes: Photosystem II (PSII), Cytochrome *b6/f*, Photosystem I (PSI) and ATP synthase (Figure 1). These proteins are bound to the thylakoid membranes of photosynthetic organisms. During the light reactions of photosynthesis, energy in the form of photons is captured by PSII and PSI. This energy



is used for electron transfer and for the formation of a proton gradient across the thylakoid membrane. As a result, ATP and NADPH are produced. These molecules are finally used in dark reactions to reduce CO₂ to carbohydrates. Nature shows a diversity of photosynthetic organisms. Purple bacteria, green nonsulfur bacteria, heliobacteria and green sulfur bacteria are classified as anoxygenic photosynthetic organisms and they possess only one reaction center. Oxygenic photosynthetic organisms, such as cyanobacteria, algae and green plants, utilize two reaction centers, PSI



and PSII (Figure 2). These two types of reaction centers (RCs) have many similarities in the arrangements of their cofactors in the electron transfer chain, but they have a major difference in their terminal electron acceptors. As shown in Figure 3, in type I RC (photosystem I and RC of heliobacteria and green sulfur bacteria) the terminal electron acceptor is a Fe_4S_4 cluster, whereas quinones are the final electron acceptors in type II RC photosystem II and RC of purple bacteria and green nonsulfur bacteria).

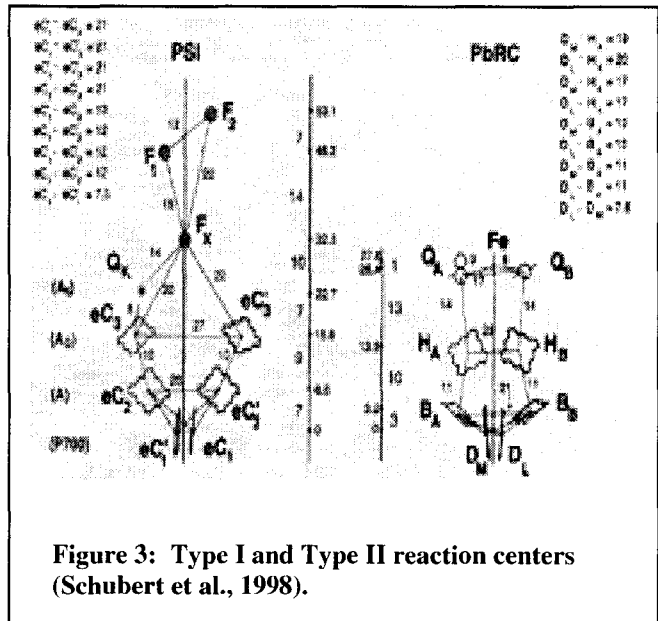
It is believed that the RCs in cyanobacteria, algae and green plants have evolved from a fusion between two types of bacterial ancestors, one with type I RC and another with type II RC (Blankenship, 1992; Buttner et al., 1992). These photoreaction centers are PSI and PSII in cyanobacteria. Algae and higher plants (Eukarya) have incorporated cyanobacteria as their

chloroplasts through endosymbiosis (Woese et al., 1990; Pace, 1997). Type I RC in cyanobacteria, algae and higher plants is the heterodimer PsaA and PsaB of PSI. Type II RCs consist of heterodimers D1 and D2 and core-antenna-binding proteins CP43 and CP47. In addition, both types of RCs contain small peripheral and transmembrane proteins with different roles.

II. PHOTOSYSTEM I

1. General introduction

PSI is a protein-pigment complex. Its overall function is to take an electron from plastocyanin on the luminal side of the thylakoid membrane, and reduce ferredoxin on the stromal side. In the past 17 years PSI has been studied in order to determine its structure and functional role in photosynthesis. Research efforts using biochemistry, biophysics and molecular genetics approaches have helped determine the subunit and cofactor composition



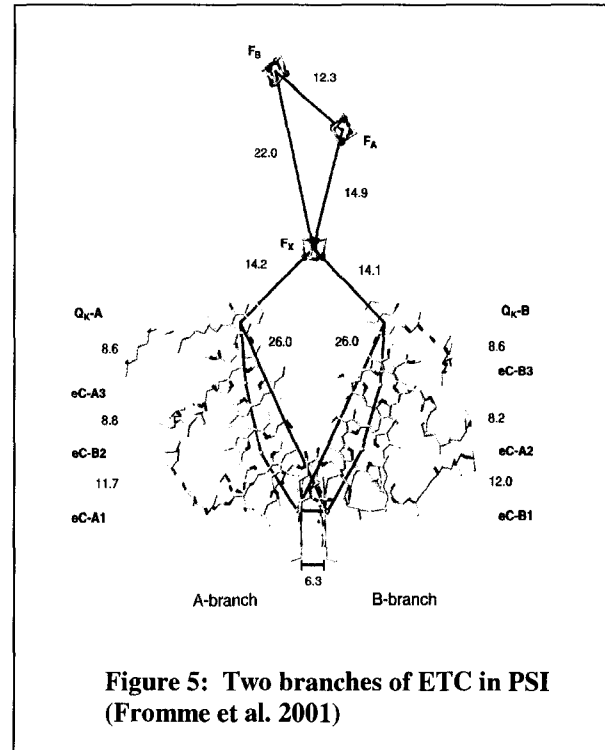
of this photoreaction center and give information on structure-function relations (Chitnis, 2001). The electron transfer chain of PSI has also been studied through various spectroscopic techniques. X-ray crystallography has been used to obtain even more information on the structural organization of PSI. In 1993, the three-dimensional structure of PSI from *Synechococcus elongatus* was proposed at 6 Å resolution (Krauß et al., 1993). Later a 4 Å resolution of the structure was released (Schubert et al., 1997) giving more information on the helices and the cofactors involved in the complex.

In 2001, the 2.5 Å crystal structure of cyanobacterial photosystem I was published which elucidated detailed interactions between the protein and its cofactors (Jordan et al., 2001). According to this structure, the monomeric PSI complex is a 356 kDa protein-cofactor complex and it can form trimers with its threefold rotation axis perpendicular to the thylakoid membrane. It is composed of 12 subunits (PsaA, B, C, D, E, F, I, J, K, L, M and X), 96 chlorophyll α (Chl α) molecules, 22 beta-carotenes, two phylloquinones, three [Fe₄S₄] clusters (F_X, F_A and F_B), four lipids and a Ca²⁺ ion (Jordan et al., 2001). Subunits PsaA and PsaB enclose the electron transfer chain, which consists of six chlorophyll cofactors, the phylloquinone pair and the three [Fe₄S₄] clusters. The rest of the 90 chlorophylls are the antenna chlorophylls that trap and harvest photons to P700, the primary electron donor of PSI. After P700 goes in its excited state (P700*) an electron is transferred to another chlorophyll molecule and eventually to a phylloquinone. The electron goes through the three clusters and is eventually used to reduce ferredoxin, the final electron acceptor of PSI (Chitnis et al., 2001, Fromme et al. 2001). The carotenes absorb photons of wavelength other than the chlorophylls and also protect the cells from photooxidation.

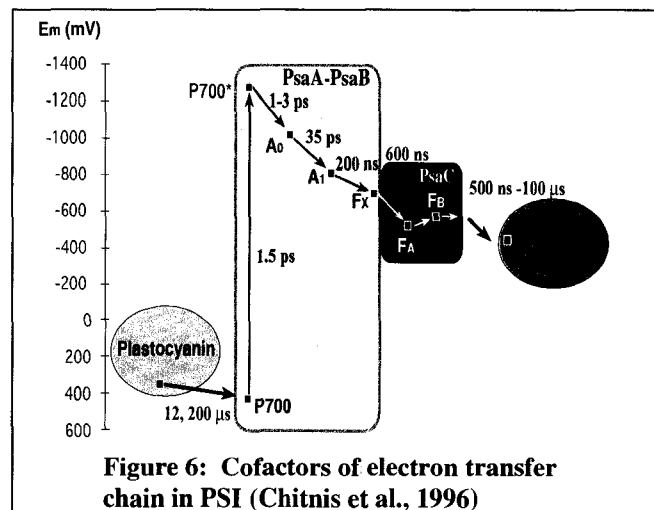
2. Subunit organization

PSI consists of nine transmembrane and three stromal subunits (Figure 4). Subunits PsaA and PsaB are homologous in their sequence and transmembrane topography. These 83kDa transmembrane proteins form the core of PSI reaction center. In each PSI monomer, they are related by a two symmetry (pseudo-C₂) axis which is parallel to the PSI trimer's C₃ axis (Jordan et al., 2001). Each subunit consists of eleven transmembrane α -helices, six amino-terminal and five carboxy-terminal. The carboxy-terminal helices of the two subunits

form two branches (nomenclature according to crystal structure): branch A (chlorophylls A₁, B₂, A₃ and phylloquinone Q_A), coordinated primarily by PsaA; and branch B (chlorophylls B₁, A₂, B₃ and phylloquinone Q_B), coordinated primarily by PsaB (Figure 5). P700 (or A₁/B₁), the “special” chlorophyll pair of PSI, is the primary electron donor of PSI. It is located near the luminal side of the membrane and interacts with both PsaA and PsaB subunits in a symmetric way. The photon energy trapped by the antenna chlorophylls eventually is trapped



in P700 which is the excited to P700* (Figure 6). P700*, then donates an electron to A₀ (or A₃/B₃), another molecule of Chl α , and A₀⁻-P700⁺ is formed. The electron is then transferred to A₁ (Q_A/Q_B), a phylloquinone molecule, and then to three iron-sulfur clusters F_X, F_A and F_B (Figure 6). After the reduction of ferredoxin, the electron finally reaches NADP⁺ reductase at the stromal (cytoplasmic) side of the membrane (Chitnis, et al. 2001). The chlorophyll pair A₂/B₂ shown in Figure 5, is the only point in the ETC where the subunits crossover and coordinate cofactors of the opposite branch (A₂ by PsaB and B₂ by PsaA). This pair of chlorophylls is in



close proximity to the chlorophyll pair A₃/B₃ or A₀ but it has not been shown whether it is directly or indirectly involved in the electron transfer (Fromme et al., 2001). Although there are two branches for electron transfer of similar structure, it is not clear whether both of

them are active during electron flow. The unidirectionality or bidirectionality of the PSI electron transfer has been a controversial issue in the field of photosynthesis for years and a lot of experiments have been performed in order to resolve this issue. The experimental data collected so far may support one theory but cannot completely exclude the other. A great deal of research is still being performed in order to further resolve this matter.

3.2 Evidence for directionality of electron flow in PSI

Whether both or one branch of electron transfer chain is active in PSI, has been a controversial issue in the literature. Although the two branches are approximately symmetrical, there are a few small differences regarding the location and orientation of the cofactors that are usually related to slight differences in the protein environment of the cofactors. These differences could affect the properties of the cofactors and thus the electron transfer along one branch. The main evidence concerning the directionality of electron transfer along the two branches of PSI comes from studies regarding the phylloquinones, A₁. Pulsed EPR (Electron Paramagnetic Resonance) was initially performed on PSI crystals of *Synechococcus elongatus* and a signal from one phylloquinone molecule was detected (Bittl et al., 1997) indicating that only one phylloquinone is active. This result, however, can also suggest that there are two active phylloquinones that are indistinguishable or that only one phylloquinone can be detected by EPR (Chitnis et al., 2001). Further experiments showed that the A₁ EPR signal is altered in PsaE and PsaF less mutants and since these subunits are located near the PsaA phylloquinone, it is suggested that this quinone is the active one (Yang et al., 1998). More evidence favoring unidirectionality is based on the fact that one phylloquinone can be extracted with a dry organic solvent, whereas extraction of the second one required a more hydrophilic solvent. Based on this method, a study showed that the removal of the first phylloquinone does not alter PSI activity. However, the activity is completely lost by removal of both (Malkin, 1986). Nevertheless, this result cannot prove that the second branch is not active. More recently, EPR and ENDOR (Electron Nuclear Double Resonance spectroscopy) data from point mutations in the A₁ binding pockets of cyanobacterial cells, suggest that the signal detected is from the phylloquinone on the A-side and thus electron transfer in PSI is unidirectional (Xu et al., 2003). Similar conclusions are

reached in studies of the eubacterial system *Chlamydomonas reinhardtii* (Purton et al., 2001; Boudreaux et al., 2001). Optical difference spectroscopy and transient EPR spectroscopy on the same mutants, however, show a slow (associated with PsaA mutants) and a fast kinetic rate component (associated with PsaB mutants) of forward electron transfer from A_1 , and suggest that PsaA branch is predominantly active but does not exclude PsaB branch from participating (Xu et al., 2003). Similar biphasic kinetic rate components (halftimes ~ 13 ns and ~ 140 ns), are observed in time-resolved optical spectroscopic measurements of reoxidation of A_1^- in *Chlamydomonas reinhardtii*. Site-directed mutagenesis in A_1 pocket of PsaA shows an increase in the slow component (140ns) and the analogous mutations on PsaB affects the fast (13ns) component (Guergova-Kuras et al., 2001). These halftimes are ~ 18 and ~ 180 ns in analogous measurements performed on algal cells (Joliot and Joliot, 1999). The two kinetic components can be evidence that both phylloquinones are involved in electron transfer with different rates. However, site directed mutagenesis could be misleading, since point mutations applied on either side could initiate or affect transfer on the other side. Bidirectionality of electron transfer is also supported by vibrational spectroscopy. FTIR (Fourier Transform InfraRed spectroscopy) spectra associated with $P700^+A_1^-$ in *Synechocystis* sp. PCC 6803 and demonstrate the detection of two reduced phylloquinones (Hastings et al., 2001).

The issue of electron transfer directionality in PSI has also been approached through studies involving A_0 (or A_3/B_3), the pair of chlorophylls preceding the phylloquinones in the ETC. Pulsed EPR and ENDOR analysis of single point mutants of the axial ligands (methionyl residues) to the Mg^{2+} of A_3/B_3 in *Chlamydomonas reinhardtii*, show that electron transfer through PsaB and not PsaA side is essential for phototrophic growth (Fairclough et al., 2003). The same axial ligands were mutated to leucines in cyanobacterial cells (*Synechocystis* sp. PCC 6803) and only mutations on the PsaA side significantly affect the physiological and spectroscopic properties of the cells and thus the electron transfer in this organism is asymmetric favoring the PsaA branch (Golbeck et al., 2003; W. Xu, personal communication).

P700, the chlorophyll dimer that is the primary electron donor of PSI, is another important cofactor of the ETC that is also under study. The most significant structural

differences between the two branches are in the binding pockets P700. This observation suggests that P700 can be associated with an asymmetry in the ETC in PSI. Many studies that have been performed support this theory. This dissertation primarily focuses on P700 and the asymmetry in its structure in relation to its function.

3.3 P700 Asymmetry

(a) Chemical and physical structure

According to the most crystal structure of PSI in *Synechococcus elongatus*, P700 is a pair of chlorophylls (A_1/B_1) positioned perpendicular to the membrane plane and parallel to each other with an interplanar distance of about 3.6\AA (Jordan et al., 2001). The chlorin planes overlap only at the A and B rings (Figure 7A), and they are both coordinated through their Mg^{2+} ions to histidine (His) residues on PsaA and PsaB (Jordan et al., 2001, Mac et al.,

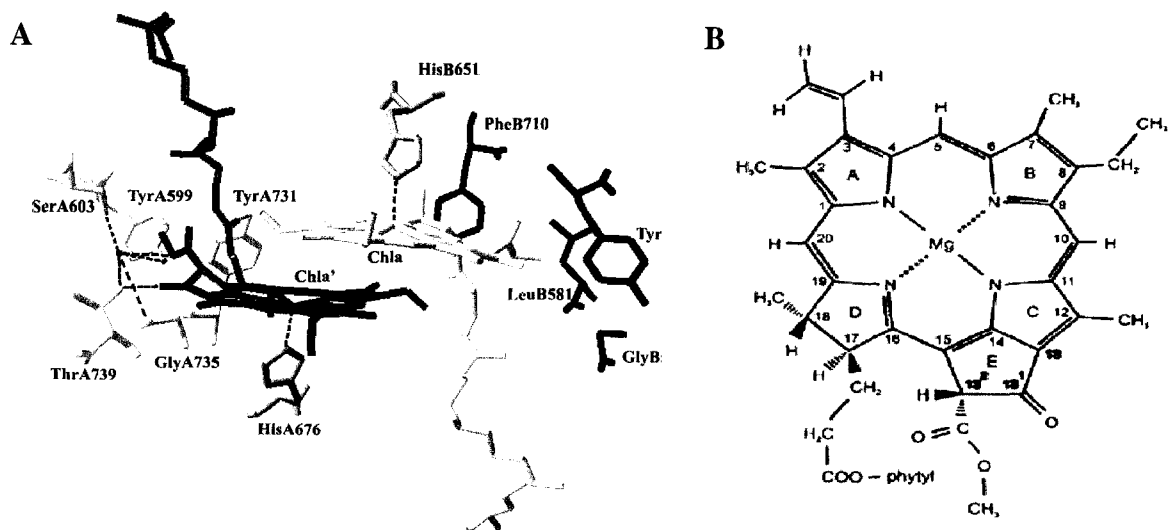


Figure 7: (A) Local protein environment of P700 (numbering is according to *Synechocystis* sp. PCC 6803). HisA676 and HisB651 are the coordinating ligands of P700. Putative hydrogen bonds between $\text{Chl}\alpha'$, the water molecule and surrounding PsaA residues are shown by dotted lines. The respective residues on PsaB side are also shown. The figure was drawn using the program Swisspdbviewer based on the coordinates of *S. elongatus*. **(B) Molecular structure and IUPAC numbering of $\text{Chl}\alpha$.**

1996). Both molecules are chlorophyll α ($\text{Chl}\alpha$) but the one coordinated by PsaA (called $\text{Chl}\alpha'$) is the C13² epimer (Figure 7B). Thus P700 is a heterodimer. It is not known how epimerization occurs and how the $\text{Chl}\alpha'$ is assembled to form P700. Previous experiments

show that Pchl α' cannot occur naturally and cannot be produced from Chl α by photoreduction. Moreover, chlorophyll synthetase does not catalyze the prenylation of Chl α' and therefore the epimerization must occur after Chl α prenylation (Helfrich et al., 1994; Helfrich et al., 1996). A possible theory is that epimerization occurs during the assembly of the reaction center and a H-bond to 13¹ keto oxygen makes the 13² proton more acidic and promotes epimerization at that position (Webber et al., 2001).

Another significant structural difference that makes P700 different from other chlorophyll pairs, is the asymmetry in the interaction of the two chlorophylls with the protein environment. Subunit PsaA coordinates Chl α' and PsaB coordinates Chl α (this nomenclature will be used to distinguish the two chlorophyll molecules throughout the text). The subunits interact with the chlorophylls in a similar fashion, except for the presence of a H-bonding network on A side. Figure 7A, shows the differences in pigment-protein subunit H-bond interactions. According to the crystal structure of cyanobacterial PSI (Jordan et al., 2001), Thr A739 is capable of donating a H-bond to the 13¹ keto oxygen and to a water molecule (numbering will be according to *Synechocystis* throughout the text). This water molecule, which is also involved in a H-bonding network with residues Ser A603 and Tyr A599 and G A735, donates a H-bond to the 13² methyl ester oxygen of Chl α' . Moreover, Tyr A731 donates a H-bond to the phytyl ester-carbonyl oxygen of Chl α' (Figure 7). The respective positions in PsaB are occupied by different residues (Tyr B718, Gly B585, Leu B581 and Phe B710) that do not form H-bonds with Chl α . The presence of this H-bonding network between P700 (Chl α') and PsaA, and its absence in the interaction of P700 (Chl α) and PsaB, is a significant structural asymmetry and it may have a great effect on the electronic structure and function of P700. The presence of the H-bonds are thought to stabilize the ground state and thus increase the redox potential of P700/P700⁺. It is most probable that the electron spin density above P700, is affected by this structural asymmetry.

(b) Electronic structure

The antenna chlorophyll molecules of PSI absorb photons and the exciton energy is transferred to P700 forming P700*. P700* is probably the most reducing compound found in natural systems with a negative redox potential of about 1200mV. P700⁺, or simply P700⁺

radical (carrying an unpaired electron) is formed after donation of an electron to A_0 , the primary acceptor of the ETC. Finally, the cation radical uptakes an electron from plastocyanin and goes back to the singlet (ground) state.

The $P700^{+}$ radical of PSI has been studied extensively by EPR spectroscopy. The EPR signal of $P700^{+}$ gives a single line centered at a g-factor of 2.0025. A very similar result is obtained from a chlorophyll radical in vitro with a difference in the linewidth of this signal because $P700^{+}$ of the reaction center is a dimer with an unpaired electron spin delocalized over it (Norris et al., 1971). A direct measurement of the distribution of this spin over $P700$ can be given by electron nuclear hyperfine couplings or hfcs [i.e. hyperfine couplings with magnetic nuclei (^1H , ^{14}N) that interact with the electron spin]. These hfcs can be resolved by Electron Nuclear DOuble Resonance (ENDOR) or Electron Spin Envelope Echo Modulation (ESEEM). Unfortunately, only the hfcs from three methyl groups (positions 2, 7, and 12 according to Figure 7B) from one chlorophyll of $P700^{+}$ can be detected ($\text{Chl}\alpha$), which makes a final decision for the spin localization of the radical, rather difficult. Initially hfcs obtained from $P700^{+}$ were compared to hfcs obtained from a chlorophyll radical ($\text{Chl}\alpha^{+}$) in different solvents. However, due to solvent effects these hfcs assignments cannot be absolutely reliable and therefore other methods were developed, such as studies on labeled samples or mutants, which further confirmed the approximate location of this spin density.

Initial EPR and ENDOR studies were performed in order to investigate whether the $P700^{+}$ radical is of monomeric or dimeric nature (i.e. the electron spin density is delocalized above one chlorophyll or a dimer of chlorophyll molecules). First, ENDOR studies confirmed that the delocalization of the spin is equal over a chlorophyll dimer based on comparisons with $\text{Chl}\alpha^{+}$ in different solvents (Norris et al., 1974, Norris et al. 1975). However, an EPR study on ^{13}C enriched chlorophyll in vitro or $P700^{+}$, suggested a monomeric nature of $P700^{+}$, i.e. the unpaired electron is localized over one chlorophyll molecule (Wasielewski et al., 1981). ^1H -ENDOR experiments show that about 85% of the electron spin density is residing on $\text{Chl}\alpha$ (Käss et al., 2001; Rigby et al., 1994). This leaves ~15% of the spin on the other half of the dimer ($\text{Chl}\alpha'$ in Figure 7A). These results were confirmed by the same group from ENDOR and ESEEM hfcs assigned to $^{14}\text{N}/^{15}\text{N}$ $P700^{+}$ (

Käss et al., 1995; Käss and Lubitz, 1996a). Results of Davis et al., 1993 show that this ratio is 3:1 or 4:1 favoring Chl α , instead. Moreover, the $^{14}\text{N}/^{15}\text{N}$ hfcs were found to result from five nitrogen nuclei (Käss et al., 1996b). The fifth nitrogen was identified to come from the histidine ligand (Mac et al, 1996). This histidyl residue, the coordinating ligand to the spin carrying Chl α , was later identified to belong to PsaB (Webber et al., 1996; Redding et al., 1998; Krabben et al., 2000) through site-directed mutagenesis studies.

In contrast to EPR and ENDOR studies, which predict a more asymmetric electron spin density favoring the chlorophyll molecule of P700 on B side (Chl α), FTIR spectroscopy supports a more symmetrical distribution over the dimer. P700 has been studied by vibrational spectroscopy since 1986 (Breton, 2001 for review). In this technique, the light minus dark (or P700 $^+$ -P700) difference spectra can give information on the chlorophyll interactions with their environment upon charge separation. Through ^2H or ^{15}N global and specific labeling experiments (Breton et al., 1999), as well as site-directed mutagenesis (Redding et al. 1998, Breton et al., 2002), bands at 1600-1800 cm^{-1} frequencies are now recognized to be due to vibrational modes from the 13^1 keto and 13^2 methyl ester C=O groups from both chlorophylls of P700 (Figure 7B). These vibrational modes can be distinguished due to the H-bonding network associated with Chl α' of P700 that is absent in Chl α -PsaB interactions (Figure 7A). The H-bonds associated with Chl α' of P700 are the reason why the vibrational modes coming from this chlorophyll are of lower frequency (Breton et al., 1999). In addition to protein-chlorophyll interactions, FTIR spectra can give information on charge density above the chlorophyll dimer. If the charge density on ring E of the chlorophyll macrocycle, measured by perturbations of 13^1 keto and 13^2 methyl ester C=O vibrations, reflects the spin density over the dimer upon oxidation, then the charge is shared equally over the dimer with a 1:1 or 2:1 ratio, favoring Chl α on B side. This result is in contrast to the electron spin density distribution given by EPR and ENDOR studies (85:15 favoring Chl α). Of course, there are differences between the techniques that should be taken under consideration when comparing results. For example, FTIR investigates charge localization, whereas ENDOR studies electron spin density. Moreover, FTIR detects the change of bond order of 13^1 keto and 13^2 methyl ester C=O groups on ring E of the

chlorophyll macrocycle, ENDOR detects the excess spin density mainly on three methyl groups (positions 2, 7, 12 on the macrocycle) at another location on the macrocycle.

Although P700 has been a subject of great focus in the photosynthetic community, to this day, there is a great deal of ambiguity about the electronic structure. Further studies still need to be performed in order to determine the distribution of electron spin over the P700 with more certainty and most importantly to determine its effect on the directionality of electron flow through the ETC. Differences in the protein environment surrounding the chlorophyll dimer have great effects on the properties of P700.

III. ORGANIZATION OF DISSERTATION

This dissertation includes five chapters and one appendix. Chapter one (this chapter) is an introduction to photosynthesis and PSI. The main focus of this chapter is the process of electron transport in PSI with an emphasis on P700, the primary electron donor of PSI. Chapter two is a manuscript to be submitted to *Biochemistry*. It is a global study on hydrogen bonding of PsaA to Chl α' of P700. In this work, H-bonding amino acids of PsaA in *Synechocystis* sp. PCC 6803, were changed to the respective homologues in PsaB by site-directed mutagenesis. P700 in these mutants is studied by FTIR and ENDOR spectroscopy. Chapter three is a manuscript to be submitted to *Biochemistry* and focuses on the FTIR spectroscopy analysis of the PsaA H-bonding mutants with a detailed analysis of the spectra. Chapter four is a manuscript to be submitted to the *Biochemistry*. This work presents a study of PsaB point mutants. In these mutants, the PsaB amino acids that do not H-bond to P700, were changed to the corresponding H-bonding amino acids of PsaA. The physiological and electronic structure of P700 is studied in these mutants. General conclusions about the work presented in this dissertation are discussed in chapter five. Finally the appendix describes another project regarding mutagenesis in a late step of the carotenoid biosynthetic pathway in *Synechocystis* sp. PCC 6803. Carotenoids, are pigments that protect *Synechocystis* and other photosynthetic organisms from photooxidation. The gene encoding for zeaxanthin glycosyl transferase was disrupted in the mutant and the carotenoid content is studied.

IV. REFERENCES

- Barth P., Lagoutte B., Setif P. (1998). Ferredoxin reduction by photosystem I from *Synechocystis* sp. PCC 6803: toward an understanding of the respective role of the subunits PsaD and PsaE in ferredoxin binding. *Biochemistry*, *37*, 16233-16241.
- Bittl R., Zech S.G., Fromme P., Witt H.T. and Lubitz W. (1997). Pulsed EPR structure analysis of photosystem I single crystals: Location of the phylloquinone acceptor. *Biochemistry*, *36*, 12001-12004.
- Blankenship R.E. (1992). Origin and early evolution of photosynthesis. *Photosynth. Res.*, *33*, 91-111.
- Boudreaux B., Macmillan F., Teutoll C., Rufat A., Gu F., Grimaldi S., Bittl R., Brettel K. and Redding K. (2001). Mutations in both sides of the photosystem I reaction center identify the phylloquinone observed by electron paramagnetic resonance spectroscopy. *J. Biol. Chem.*, *276*, 37299-37306.
- Breton J., Nabdryk E. and Leibl W. (1999). FTIR study of the primary electron donor of photosystem I (P700) revealing delocalization of the charge in P700⁺ and localization of the triplet character in ³P700. *Biochemistry*, *38*, 11585-11592.
- Breton J. (2001). Fourier Transform Infrared Spectroscopy of primary electron donors in type I photosynthetic reaction centers. *Biochim Biophys Acta*, *1507*, 180-193.
- Buttner M., Xie D.-L., Nelson H., Pinther W., Hauska G. and Nelson N. (1992). Photosynthetic reaction center genes in green sulfur bacteria and in photosystem I are related. *Proc. Natl Acad. Sci. USA*, *89*, 8135-8139.
- Chitnis V.P. and Chitnis P.R. (1993). PsaL subunit is required for the formation of photosystem I trimers in the cyanobacterium *Synechocystis* sp. PCC 6803. *FEBS Lett.*, *336*, 330-334.
- Chitnis P.R., Xu Q., Chitnis V.P. and Nechushtai R. (1995). Function and organization of photosystem I polypeptides. *Photosynth. Res.*, *44*, 23-40.
- Chitnis P.R. (1996). Photosystem I. *Plant Physiol.*, *111*, 661-669.
- Chitnis P.R. (2001). Photosystem I: function and physiology. *Annu. Rev. Plant Physiol. Plant Mol. Biol.*, *52*, 593-626.

- Davis I.H., Heathcote P., MacLachlan J. and Evans M.C.W. (1993). Modulation analysis of the of the electron spin echo signals of in vivo oxidized primary donor ^{14}N chlorophyll centers in bacterial, P870 and P960 and plant Photosystem I, P700, reaction centers. *Biochim. Biophys. Acta*, 1143, 183-189.
- Fairclough W.V., Forsyth A., Evans M.C.W., Rigby S.E.J., Purton S. and Heathcote P. (2003). Bidirectional electron transfer in photosystem I electron transfer on the PsaA side is not essential for phototrophic growth in *Chlamydomonas*. *Biochim. Biophys. Acta*, 1606, 43-55.
- Fromme P., Jordan P., Krauss N. (2001). Structure of photosystem I. *Biochim. Biophys. Acta*, 1507, 5-31.
- Golbeck J.H. (2003). The binding of cofactors to photosystem I analyzed by spectroscopic and mutagenic methods. *Annu. Rev. Biophys. Biomol. Struct.*, 32, 237-256.
- Guergova-Kuras M., Boudreaux B., Joliot A., Joliot P. and Redding K. (2001). Evidence for two active branches for electron transfer in photosystem I. *PNAS*, 98, 4437-4442.
- Hatanaka H., Sonoike K., Hirano M. and Katoh S. (1993). Small subunits of Photosystem I reaction center complexes from *Synechococcus elongatus*. I. Is the psaF gene product required for oxidation of cytochrome c-553? *Biochim. Biophys. Acta*, 1141, 45-51.
- Hastings G. and Sivakumar V. (2001). A fourier transform infrared absorption difference spectrum associated with the reduction of A_1 in photosystem I: are both phylloquinone involved in electron transfer? *Biochemistry*, 40, 3681-3689.
- Helfrich M., Schoch S., Lampert U., Cmeil E. and Rüdiger W. (1994). Chlorophyll synthetase cannot synthesize chlorophyll a'. *Eur. J. Biochem.*, 219, 267-275.
- Helfrich M., Schoch S., Schäffer W., Ryberg M. and Rüdiger W. (1996). Absolute configuration of protochlorophyllide *a* and substrate specificity of NADPH-protochlorophyllide oxidoreductase. *J. Am. Chem. Soc.*, 118, 2602-2611.
- Hippler M., Drepper F., Rochaix J.D. and Muhlenhoff U. (1999). Insertion of the N-terminal part of PsaF from *Chlamydomonas reinhardtii* into photosystem I from *Synechococcus elongatus* enables efficient binding of algal plastocyanin and cytochrome C6. *J. Biol. Chem.*, 274, 4180-4188.

- Jensen P.E., Gilpin M., Knoetzel J., Sceller H.V. (2000). The PSI-K subunit of photosystem I is involved in the interaction between light harvesting complex I and the photosystem I reaction center core. *J. Biol. Chem.*, 275, 24701-24708.
- Joliot P. and Joliot A. (1999). In vivo analysis of the electron transfer within photosystem I: are two phylloquinones involved? *Biochemistry*, 38, 11130-11136.
- Jordan P., Fromme P., Witt H.T., Klukas O., Saenger W. and Krauß N. (2001). Three-dimensional structure of cyanobacterial photosystem I at 2.5Å resolution. *Nature*, 411, 909-917.
- Käss H., Bittersmann-Weidlich E., Andréasson E.-E. and Lubitz W. (1995). ENDOR and ESEEM of the ¹⁵N labeled radical cations of chlorophyll a and the primary donor P700 in photosystem I. *Chem Phys.*, 194, 419-432.
- Käss H. and Lubitz W. (1996a). Evaluation of 2D-ESEEM data of ¹⁵N-labeled radical cations of the primary donor P700 in photosystem I and chlorophyll a. *Chem. Phys. Lett.*, 251, 193-203.
- Käss H., Fromme P. and Lubitz W. (1996b). Quadruple parameters of nitrogen nuclei in the cation radical P700⁺ determined by ESEEM of single crystals of photosystem I. *Chem. Phys. Lett.*, 257, 197-206.
- Käss H., Fromme P., Witt H.T. and Lubitz W. (2001). Orientation of electronic structure of the primary donor radical cation P700⁺ in photosystem I: a single crystals PER and ENDOR study. *J. Phys. Chem.*, 105, 1225-1239.
- Krabben L., Schlodder E., Jordan R., Carbonerra D., Giacometti G., Lee H., Webber A.N. and Lubitz W. (2000). Influence of the axial ligands on the spectral properties of P700 of photosystem I: a study of site-directed mutants. *Biochemistry*, 39, 13012-13025.
- Krauß N., Hinrichs W., Witt I., Fromme P., Pritzkow W., Dauter Z., Betzel C., Wilson K.S., Witt H.T. and Saenger W. (1993). Three-dimensional structure of system I of photosynthesis at 6Å resolution. *Nature*, 361, 326-331.
- Lelong C., Setif P., Lagoutte B., Bottin H. (1994). Identification of the amino acids involved in the functional interaction between photosystem I and ferredoxin from *Synechocystis* sp. PCC 6803 by chemical cross-linking. *J. Biol. Chem.*, 269, 10034-10039.

- Mac M., Tang X.S., Diner B.A., McCracken J and Babcock G.T. (1996). Identification of histidine as an axial ligand to P₇₀₀⁺. *Biochemistry*, 35, 13288-13293.
- Malkin R. (1986). On the function of two vitamin K molecules in the PSI electron acceptor complex. *FEBS Lett.*, 208, 343-346.
- Meimberg K., Lagoutte B., Bottin H., Muhlenhoff U. (1998). The PsaE subunit is required for complex formation between photosystem I and flavodoxin from the cyanobacterium *Synechocystis* sp. PCC 6803. *Biochemistry*, 37, 9759-9767.
- Norris J.R., Uphaus R.A., Crespi H.L. and Katz J.J. (1971). Electron spin resonance of chlorophyll and the origin of signal I in photosynthesis. *Proc. Nat. Acad. Sci. USA*, 68, 625-628.
- Norris J.R., Scheer H., Druyan M.E. and Katz J.J. (1974). An electron-nuclear double resonance (ENDOR) study of the special pair model for photo-reactive chlorophyll in photosynthesis. *Proc. Nat. Acad. Sci. USA*, 71, 4897-4900.
- Norris J.R., Scheer H. and Katz J.J. (1974). Models for antenna and reaction center chlorophylls. *Ann. N.Y. Acad. Sci.*, 244, 260-280.
- Ourton S., Stevens D.R., Muhiuddin I.P., Evans M.C.W., Carter S., Rigby S.E.J. and Heathcote P. (2001). Site-directed mutagenesis of PsaA residue W693 affects phylloquinone binding and the function in the photosystem I reaction center of *Chlamydomonas reinhardtii*. *Biochemistry*, 40, 2167-2175.
- Pace N.R. (1997). A molecular view of microbial diversity and the biosphere. *Science*, 276, 734-740.
- Redding K., MacMillan F., Leibl W., Brettel K., Hanley J., Rutherford W.A., Breton J. and Rochaix J.D. (1998). A systematic survey of conserved histidines in the core subunits of photosystem I by site-directed mutagenesis reveals the likely axial ligands of P700. *EMBO J.*, 17, 50-60.
- Rigby S.E.J., Nugent J. and O'Malley P.J. (1994). ENDOR and special triple resonance studies of chlorophyll cation radical in photosystem 2. *Biochemistry*, 33, 10043-10050.
- Schubert W.D., Klukas O., Krauss N., Saenger W., Fromme P., Witt H.T. (1997). Photosystem I of *Synechococcus elongatus* at 4 Å resolution: comprehensive structural analysis. *J. Mol. Biol.*, 272, 741-769.

- Shubert W.D., Klukas O., Saenger W., Witt H.T., Fromme P. and Krauss N. (1998). A common ancestor for oxygenic and anoxygenic photosynthetic systems: a comparison based on the structural model of photosystem I. *J. Mol. Biol.*, 280, 297-314.
- Shen G., Boussiba S. and Vermaas W. F. (1993). *Synechocystis* sp. PCC 6803 strains lacking photosystem I and phycobilisome function. *Plant Cell*, 5, 1853-1863.
- Sun J., Xu W., Hervás M., Navarro J.A., De La Rosa M.A. and Chitnis P.R. (1999). Oxidizing side of cyanobacterial photosystem I: Evidence for interaction between the electron donor proteins and the luminal surface helix of the PsaB subunit. *J. Biol. Chem.*, 274, 19048-19054.
- Webber A.N., Su H., Bingham S.E., Käss H., Krabben L., Kuhn M., Jordan R., Echlodder E. and Lubitz W. (1996). Site-directed mutations affecting the spectroscopic characteristics and midpoint potential of the primary donor in photosystem I. *Biochemistry*, 35, 12857-12863.
- Webber A.N. and Lubitz W. (2001). P700: the primary electron donor of photosystem I. *Biochim. Biophys. Acta*, 1507, 61-79.
- Wasielewski M.R., Norris J.R., Crespi H.L. and Harper J. (1981). Photo induced ESR signals from the primary electron donors in deuterated highly carbon-13 enriched photosynthetic bacteria and algae. *J. Am. Chem. Soc.*, 103, 7664-7665.
- Woese C.R., Kandler O. & Wheelis M.L. (1990). Towards a natural system of organisms: proposal for the domains Archaea, Bacteria, and Eucarya. *Proc. Natl Acad. Sci. USA*, 87, 4576-4579.
- Xu Q., Armbrust T.S., Guikema J.A. and Chitnis P.R. (1994). Organization of photosystem I polypeptides (a structural interaction between the PsaD and PsaL subunits). *Plant Physiol.*, 106, 1057-1063.
- Xu Q., Jung Y.S., Chitnis V.P., Guikema J.A. Golbeck J.H. and Chitnis P.R. (1994a). Mutational analysis of photosystem I polypeptides in *Synechocystis* sp. PCC 6803. Subunit requirements for reduction of NADPH⁺ mediated by ferredoxin. *J. Biol. Chem.*, 269, 21512-21518.
- Xu W., Chitnis P., Valieva A., Est A., Pushkar Y.N., Krzystyniak B., Teutloff C., Zech S.G., Bittl R., Stehlik D., Zybailov B., Shen G. and Golbeck J.H. (2003a). Electron transfer in

cyanobacterial photosystem I: I. Physiological and spectroscopic characterization of site-directed mutants in a putative electron transfer pathway from A_0 through A_1 to F_x . *J. Biol. Chem.*, 278, 27864-27875.

Xu W., Chitnis P., Valieva A., Est A., Brettel K., Guergova-Kuras M., Pushkar Y.N., Zech S.G., Stehlik D., Shen G. Zybailov B. and Golbeck J.H. (2003). Electron transfer in cyanobacterial photosystem I: II. Determination of forward electron transfer rates of site-directed mutants in a putative electron transfer pathway from A_0 through A_1 to F_x . *J. Biol. Chem.*, 278, 27876-27887.

Yang F., Shen G., Schluchter W.M., Zybailov B.L., Ganago A.O., Bryant D.A. and Golbeck J.H. (1998). Detection of the PsaF polypeptide modifies the environment of the redox-active phylloquinone (A_1). Evidence for unidirectionality of electron transfer in photosystem I. *J. Phys. Chem. B*, 102, 8288-8299.

**CHAPTER 2. SITE-DIRECTED MUTAGENESIS OF AMINO ACIDS HYDROGEN
BONDING TO THE PRIMARY ELECTRON DONOR
OF PHOTOSYSTEM I^{1*}**

A paper to be submitted to *Biochemistry*

Maria Pantelidou, Huadong Tang, Tanya Konovarova, Kevin Redding, Jacques Breton,
Parag R. Chitnis^{2**}

ABSTRACT

P700, the primary electron donor of photosystem I, is a heterodimer comprised of chlorophyll α (Chl α) and chlorophyll α' (Chl α'). Chl α' is hydrogen bonded to several amino acids of the PsaA protein. To study the effects of these hydrogen bonds on the properties of P700, we used site-directed mutagenesis in the cyanobacterium *Synechocystis* sp. PCC 6803. In the single mutant PsaA T739F, the threonine at this position, which in wild type hydrogen bonds to the Chl α' 13¹ keto oxygen, was changed to phenylalanine. In the triple mutant, PsaA Y599L/S603G/T739Y, the threonine at the same position, was mutated to tyrosine. The additional mutations in this strain include replacement of tyrosine 599 and serine 603 in PsaA by leucine and glycine, respectively. In the wild type photosystem I, these two amino acids provide a hydrogen bond through a water molecule, to the 13²-methyl ester oxygen of Chl α' . Both the single and triple mutant strains grew photoautotrophically, with slower rates than the wild type strain. The total chlorophyll content in the mutant cells was reduced compared to the wild type. Fourier Transform InfraRed (FTIR) spectroscopy showed that the targeted mutations affected the hydrogen bonding interaction between PsaA and Chl α' . High Performance Liquid Chromatography (HPLC) analysis of the triple mutant showed that, although in lower amounts, Chl α' was present in the mutant photosystem I complexes. Finally, the electronic structure of P700⁺ in the mutants, was studied by Electron Nuclear Double Resonance (ENDOR) spectroscopy, and the hfcs of the 12-methyl protons

¹ This work was supported by a grant from US National Science Foundation (MCB 0078268)

² To whom correspondence should be addressed. Tel: 703-292-7132; Fax: 703-292-9061; Email: pchitnis@nsf.gov

of Chl α' were found to be reduced significantly. This result provides evidence for redistribution of electron spin density between Chl α and Chl α' in the mutant complexes. Finally, a mutant of the tyrosine at position PsaA 731, which provides a hydrogen bond to the phetyl ester carbonyl oxygen of Chl α' , was also studied. Growth of this mutant was indistinguishable from that of the wild type strain and the FTIR spectroscopy showed no detectable effects in the hydrogen bonding between P700 and the PsaA protein.

INTRODUCTION

Oxygenic photosynthetic organisms, such as cyanobacteria, algae and plants, utilize two reaction centers, photosystem I (PSI) and photosystem II (PSII). Both of these centers are protein-pigment complexes, with a similar architecture of their electron transfer chain, but have different terminal electron acceptors. PSI is a type-1 reaction center with a Fe₄S₄ cluster as the terminal electron acceptor, whereas PSII, a type-2 reaction center, has a quinone as the terminal electron acceptor. In PSI, an electron is transferred from plastocyanin on the luminal side of the thylakoid membrane, to ferredoxin on the stromal side (1). According to the 2.5 Å crystal structure of the protein in *Synechococcus elongatus* (2), PSI is composed of 12 subunits (PsaA, B, C, D, E, F, I, J, K, L, M and X), 96 chlorophyll α (Chl α) molecules, 22 beta-carotenes, two phylloquinones and three [Fe₄S₄] clusters (F_X, F_A and F_B).

The two largest subunits, PsaA and PsaB, show 45-50% sequence identity with each other, and their tertiary structure is very similar. These two subunits are related by a pseudo-C2 symmetrical axis. Their five carboxy-terminal helices of PsaA and PsaB subunits form two semicircles and symmetrically engulf the cofactors of the electron transfer chain (ETC) cofactors (3). These cofactors consist of a) the primary electron donor of PSI, which is a chlorophyll pair called P700, b) the primary acceptor A₀ (another chlorophyll pair), c) a phylloquinone pair and d) the three [Fe₄S₄] clusters. P700, A₀, and the two phylloquinones are pairs forming two branches A and B. These branches are related by the same pseudo-C2 symmetry, and interact with PsaA and PsaB symmetrically (1).

The issue of directionality of electrons along one or both the two branches of the electron transfer chain, has been under investigation in the recent years (4 for review). Electron Paramagnetic Resonance (EPR) and Electron Nuclear DOuble Resonance

(ENDOR) characterization of the site-directed mutants of the phylloquinone –binding sites in the PsaA and PsaB proteins shows that the electron transfer chain is unidirectional, primarily along PsaA (5-7). However, transient optical spectroscopy studies on the reoxidation of phylloquinone indicate the activity of both branches in electron transfer (8). In general, it has been concluded that although there is a great symmetry in the arrangement of cofactors along the ETC of PSI, the electron transfer does not necessarily occur equally along both branches. This asymmetry of electron transfer could be due to an asymmetry in cofactor-cofactor or cofactor-protein interactions. P700, the primary electron donor of PSI, could possibly contribute to the imbalanced electron transfer along the two branches, due to an asymmetry in its own structure and the interaction with the protein surrounding it.

P700 is a pair of chlorophylls located near the luminal side of the membrane. The two chlorophyll molecules are positioned perpendicular to the membrane plane and parallel to each other with an interplanar distance of about 3.6Å. The chlorin planes overlap only at the A and B rings, and they are both coordinated through their Mg²⁺ ions to histidine (His) residues on PsaA and PsaB (2, 3). The electron transfer process starts when photon energy is harvested by the antenna chlorophylls of PSI and is trapped in P700. The dimer is the excited to P700* and donates an electron to A₀. The electron is then transferred to the phylloquinone and then to the three iron-sulfur clusters F_X, F_A and F_B of the ETC. Finally, after reduction of ferredoxin, the electron reaches NADP+ reductase at the stromal (cytoplasmic) side of the membrane (1). The chlorophyll molecules that form the P700 pair are not identical. They are both chlorophyll α molecules (Chl α), but the one coordinated by PsaA (called Chl α') is the C13² epimer of Chl α (Figure 1). PsaB, on the other hand, coordinates Chl α , the other half of P700 (Chl α' /Chl α will be used to distinguish the two chlorophyll molecules).

Subunits PsaA and PsaB interact with Chl α' and Chl α , respectively, in a similar way, except for the presence of a hydrogen bonding network on the A side. As shown in Figure 2, based on the 2.5Å crystal structure of PSI in *Synechococcus elongatus* (2), Thr at PsaA 739 (numbering will be according to *Synechocystis*), is capable of donating a hydrogen bond to the 13¹ keto oxygen the Chl α' and to a water molecule. This water molecule, which can be hydrogen bonded to residues Ser A603, Tyr A599 and Gly A735, forms a hydrogen bond to

the bridging oxygen of the 13² carbomethoxy group of Chl α' . Moreover, Tyr A731 is within hydrogen bond distance with the phytyl ester-carbonyl oxygen of Chl α' . The homologous positions on PsaB are occupied by different residues that do not form hydrogen bonds with Chl α (Figure 2). The hydrogen bonds are thought to stabilize the ground state and thus increase the redox potential of P700/P700⁺ (9). The absence of this bonding pattern between Chl α and PsaB results in a significant structural asymmetry in P700 and it possibly has a great effect on its biophysical properties.

Functional asymmetry in P700 could play a key role in the directionality of electron transfer along the two branches of the ETC. The electronic structure of P700 has been studied extensively during the past and recent years. ENDOR and EPR studies, have shown that the electron spin distribution over the oxidized state of P700 (P700⁺), is asymmetrical, favoring the PsaB coordinated chlorophyll (Chl α) by ratios \geq 4:1 (10). However, Fourier Transform InfraRed (FTIR) difference spectroscopy, measures a more equally distributed positive charge over the two chlorophylls with ratios of 1:1 or 2:1, favoring B-side Chl α (11). Regardless of these differences it is expected that the chlorophyll-protein interaction to affect the electronic structure of P700. It is therefore, important to investigate, the effects of this hydrogen bonding interaction of PsaA and Chl α' on the electronic structure of P700.

In this study, we used site-directed mutagenesis to generate three mutants in *Synechocystis* sp. PCC 6803. In the single mutant, PsaAY731F, the Tyr residue was replaced with Phe to disrupt the hydrogen bond to the phytyl ester carbonyl oxygen of Chl α' . Two additional mutants were constructed to potentially remove the hydrogen bond between Thr (at position PsaA 739) and the Chl α' 13¹ keto oxygen. This particular hydrogen bond is expected to be important since the keto group is part of the conjugated π system. The single mutant PsaA T739F and the triple mutant PsaA Y599L/S603G/T739Y were produced. The latter has two additional mutations involving a hydrogen bonding network to the 13² methyl ester oxygen of Chl α' . The bonding pattern upon P700 oxidation was studied by FTIR difference spectroscopy. PsaA T739F and PsaA Y599L/S603G/T739Y were further studied by HPLC, in order to test whether chlorophyll isomerization (formation of Chl α'), still occurs. Finally, the electronic structure of the P700⁺ in the mutants was investigated by ENDOR spectroscopy.

EXPERIMENTAL PROCEDURES

Site-directed mutagenesis. The recipient strain of *Synechocystis* pWX was used for making site-specific mutations in PsaA. In this strain, the 1130-bp C-terminal region of PsaA, the region between PsaA and PsaB and the PsaB coding region of the wild type are replaced by a spectinomycin-resistance gene cassette. Therefore, pWX lacks a part of PsaA and the whole PsaB gene (5). pIBC was the donor plasmid used for transforming pWX. This construct consists of a 1527-bp C-terminal region of PsaA, the region between PsaA and PsaB, the PsaB gene and its 760-bp downstream region incorporated into the pBluescript II KS vector. A chloramphenicol resistance gene cassette is inserted after the 3' terminator of the PsaB gene (5). The site-specific mutations on PsaA were made using the polymerase chain reaction (PCR) method with the *Platinum Pfx polymerase* (Invitrogen) and pIBC as a template. The unmethylated (mutation containing) DNA was selected by digestion with DpnI endonuclease (Promega). The mutated plasmids were checked by DNA sequencing and were used to transform the recipient strain, pWX. The transformants were selected and segregated for several generations on chloramphenicol supplemented BG11 plates under low light intensity ($2\text{-}3\ \mu\text{moles m}^{-2}\text{s}^{-1}$) at $30\ ^\circ\text{C}$ (12). The cells were also tested for growth on spectinomycin containing BGII plates to ensure that this resistance is no longer expressed. The genomic DNA was then extracted from these cells as previously described (13). The DNA fragment that contains the site-specific mutations was amplified by PCR and sequenced.

Cell growth and chlorophyll content. To measure growth rates of *Synechocystis* sp. PCC 6803 wild type and mutant strains, the cultures were grown in BG11 medium (14) to late exponential phase ($0.7\text{-}1.0\ \text{OD}_{730}$) at $30\ ^\circ\text{C}$. The cells were centrifuged at $4000\ \times\ g$ and washed twice by resuspension in BG11 medium. The 50ml-cultures were started with an initial concentration of $0.1\ \text{OD}_{730}$ and constant shaking at 140 rpm under low light ($5\text{-}10\ \mu\text{mol photons m}^{-2}\text{s}^{-1}$), normal light ($40\text{-}50\ \mu\text{mol photons m}^{-2}\text{s}^{-1}$) and high light ($90\text{-}100\ \mu\text{mol photons m}^{-2}\text{s}^{-1}$). For photoheterotrophic growth, the cultures were supplemented with 5mM glucose. The mutants were supplemented with 30mg/L chloramphenicol. Growth rates were monitored by absorbance measurements at 730nm (A_{730}) with a UV-160U spectrophotometer

(Shimadzu, Tokyo, Japan). Total chlorophyll content in the cells was performed by extractions with 100% methanol as previously described (15).

PSI trimer isolation. Cells were grown in large quantities in BG11 medium, in the presence of glucose (5mM) at normal light intensity to 1.0 OD₇₃₀. The cells were harvested and resuspended in SMN solution (0.4 mM sucrose, 10mM NaCl and 50 mM MOPS, pH 7.0). Thylakoid membrane extraction and isolation of PSI particles was performed according to previously published methods with minor alterations (16). Chlorophyll content determination in the membranes with 80% acetone was carried out as described previously (17). For isolation of PSI complexes the membranes (containing 6mg Chl) were incubated in SMN buffer with 10mM CaCl₂ for 0.5 hr, at room temperature in the dark, in order to promote trimerization. For solubilization, n-dodecyl- β -D-maltoside (DM) was added (1.5% final concentration) to the membranes, and the sample was incubated for 15 min in the dark on ice. The non-solubilized material was removed by centrifugation at 20,000 x g for 15 min and the photosynthetic complexes were separated with a 10 to 30% gradient of sucrose with 0.05% DM in 10mM MOPS, pH 7.0, by ultracentrifugation (160,000 x g) for 18 hrs at 4°C. The band containing the PSI trimers was collected, concentrated to 1mg Chl/ml and stored in -20°C.

77K Fluorescence emission spectra. Cell cultures were grown in the presence of 5mM glucose under light conditions of 40-50 $\mu\text{mol photons m}^{-2}\text{s}^{-1}$ and harvested at approximately 0.7 OD₇₃₀. Cells containing 5 μg of chlorophyll were diluted in 50ul water containing 50% (v/v) glycerol prior to freezing in liquid nitrogen. The low temperature fluorescence emission spectra were obtained by using a SLM 8000C spectrofluorometer as previously described (18), with the excitation wavelength set at 440nm, the excitation slit width at 4nm and the emission slit width at 2nm.

FTIR spectroscopy. Samples for FTIR were prepared by centrifugation (300000g for 60 min) of PS I trimers in Tris-HCl buffer (70mM; pH 7.0) containing 80 mM potassium ferrocyanide and 20 mM potassium ferricyanide. A small fraction of the resultant pellet was squeezed between two calcium fluoride windows and the thickness of the sample was adjusted to give an absorption of about 0.8 OD unit at the maximum around 1650 cm^{-1} with approximately half of this absorption being due to the amide I absorption and the other half

to the scissoring mode of water. Light-induced difference spectra were recorded on Nicolet 60SX and 860 FTIR spectrometers at a temperature of 5°C and at a resolution of 4 cm⁻¹ as previously reported (11).

HPLC analysis. Sample preparation (K. Redding, personal communication) was carried out in the dark on ice, whenever possible. PSI trimers (~100µg of Chl α) were treated with three volumes of de-gassed ethyl acetate. The sample was vortexed well and sonicated in an ice-water bath for 2 min. The upper organic phase was separated from the aqueous phase by centrifugation at 13000 rpm for 2min. The green organic phase was treated with de-gassed ethyl acetate again and the extraction was repeated. The ethyl acetate extracts were combined and filtered with a 0.4-µm Millex-FH filter. The sample was concentrated with a stream of nitrogen gas to a final volume of 50µl. Reverse-phase HPLC analysis was performed, according to Nakamura and Watanabe, 2001 (19), with some modifications. A Partisil ODS-3 column (250- 4.6 mm, 5µ) from Alltech was used for the separation. Samples were eluted with acetonitrile/ethanol/methanol/water (85:9:3:3) through the C-18 column at 1.5ml/min flow rate. Chl α and Chl α' were detected at 663nm with retention times ~6.5 and ~7.3 min respectively. To quantify peaks were collected separately, concentrated again with a nitrogen gas and and then reloaded on the column again.

ENDOR Spectroscopy. PSI trimers (~0.2mg Chl) were placed in standard 4mm Suprasil quartz EPR tubes and illuminated with a white 200 W lamp for ~10sec. The light was passed through a 20-cm water filter before it reached the sample. The PSI trimers were frozen at 77K while under illumination. ENDOR spectra of P700⁺ in samples were obtained by standard techniques on a Bruker ESP 300E EPR spectrophotometer equipped with a DICE ENDOR ESP 350 system and a Bruker ER4111 temperature controller at 120K (Mod. Freq. =12.5 kHz).

RESULTS

Physiological characterization of the mutants. In the single mutant PsaA Y731F the Tyr, which in wild type donates a hydrogen bond to the phytyl ester carbonyl oxygen of Chl α' , was replaced with a Phe. Mutant PsaA T739F has a Phe residue in place of the Thr at position 739. PsaA Y599L/S603G/T739Y is the triple mutant that has three residues mutated

to the homologous amino acids in PsaB. In the wild type, these positions are involved in a hydrogen bonding network to Chl α' (see Figure 2). The mutations were confirmed by sequencing the appropriate fragments of the genomic DNA extracted from the mutant strains. All mutants could grow photoautotrophically. Mutant PsaA Y731F does not show any differences in growth, compared to the wild type strain. However, PsaA T739F and PsaA Y599L/S603G/T739Y mutants show some differences in growth as well as in their chlorophyll content. Table 1 shows the doubling times and chlorophyll contents of the triple mutant and the wild type. The chlorophyll content, in this mutant is decreased and the doubling times are increased under all conditions. These data suggest an increased sensitivity in the mutant compared to the wild type. Although the total chlorophyll levels of the mutant decrease, the PSI to PSII ratio, as measured by 77K fluorescence, does not change. The ratio was determined by measuring the amplitude of the fluorescence emission in whole cells at 77K, on the basis of same chlorophyll content. The emission peak at 725 nm is due to PSI associated chlorophyll, whereas the emission peaks at 685 and 695 nm are derived mostly from PSII (Figure 3). According to these spectra, the PSI:PSII ratio remains the same as in the wild type.

P700⁺-P700 difference spectra. Vibrational spectroscopy is a technique used for obtaining bonding information of P700 with its surrounding protein environment (20). Bands at 1600-1800 cm⁻¹ region of the FTIR (P700⁺-P700) difference spectra, are due to vibrational modes from the C=O groups in chlorophyll. The neutral state of P700 contributes to the negative bands (-) and the positive bands (+) are associated with the oxidized state of the dimer. For the wild type, negative bands at ~1638 and 1698 cm⁻¹ (Figure 4) have been assigned to the 13¹ keto C=O vibrations for Chl α' and Chl α respectively (11). Upon conversion to P700⁺, these are represented by positive bands at ~1653 and ~1718 cm⁻¹. In the single mutant, PsaA T739F, the 1653(+)/1638(-) differential signal is reduced by ~50% compared to the wild type (Figure 4). This possibly suggests a rupture of the hydrogen bond to the 13¹ keto C=O of the Chl α' . Furthermore, a new negative band appears in mutant at 1676 cm⁻¹ and the positive band at 1687 cm⁻¹ increases, possibly related to the free 13¹ keto C=O of Chl α' . The spectrum obtained from the triple mutant PSI (has Thr mutated to a Tyr, the homologous amino acid in PsaB), demonstrates exactly the same differences at this

particular region of the spectrum. This means that the introduced Tyr does not form a hydrogen bond, even though this amino acid is able to do so. In addition, this mutant shows more differences in the 1720-1750 cm^{-1} region. According to (20), in the (P700⁺-P700) difference spectra of the wild type, signals at 1735(-)/1742(+) cm^{-1} and 1749(-)/1754(+) cm^{-1} have been assigned to vibrational modes of the C=O of the 13² carbomethoxy group of Chl α' and Chl α respectively. In the triple mutant difference spectra, a new signal appears at 1762 cm^{-1} and the 1735(-) cm^{-1} signal decreases significantly (Figure 4). As expected, mutants PsaA T739F and PsaA Y731F, do not show any perturbations at this spectral region. These data provide supporting evidence that the changes at this region are due the mutations of the Tyr and Ser, which hydrogen bond through a water molecule to the C=O bond of the 13² carbomethoxy group of Chl α' . The FTIR difference spectra of the PsaA Y731F mutant do not show any significant differences from the wild type. Since the vibrational modes of this C=O cannot be detected in the 1600-1800 cm^{-1} region, it is therefore concluded that rupture of the hydrogen bond to the phytyl ester carbonyl oxygen, does not cause any significant changes in the positioning of the dimer with respect to the protein surrounding it.

HPLC analysis. P700 is a dimer composed of Chl α and Chl α' . The nature of epimerization of Chl α to form Chl α' is still unknown. It has been suggested that the hydrogen bond to the 13¹-keto oxygen promotes epimerization at that position during the reaction center assembly (10). Therefore, the triple mutant, PsaA Y599L/S603G/T739Y, was analyzed by HPLC at 663nm (Figure 5). The PSI chlorophyll extractions were done with ethyl acetate, a procedure that minimizes post-extraction isomerizations of the chlorophyll (K. Redding, personal communication). In PSI of the wild type we see 1 Chl α' per 180 Chl α and in the mutant 1 Chl α' was detected per 220 Chl α . According to these results, although the amount of Chl α' is reduced in the mutant, the mutations of these three hydrogen bonding residues, do not prevent the Chl α' formation or incorporation in the redox center. PSI from single mutant PsaA T739F was also analyzed by HPLC and the Chl α' /Chl α levels were detected the same as in the wild type (data not shown).

ENDOR spectra of P700⁺. The ¹H-ENDOR spectra of P700⁺ provide information for the electronic structure of P700 (10). Based on experiments done with Chl α^{+} in organic solvents, PSI in single crystals or PSI isolated from mutants, the hyperfine constants (hfc's)

obtained in these spectra have been assigned to specific protons on P700 (21-23). The line pairs 1'/1 and 2'/2 in Figure 6, are assigned to the low spin carrying Chl α' . Line pairs 3'/3 and 5'/5 are assigned to the perpendicular and parallel hyperfine tensor components of the methyl protons at position 2 of the spin carrying Chl α . In a similar fashion, line pairs 4'/4 and 6'/6 belong to the methyl protons at position 7 and the splittings at 7'/7 and 8'/8 are due to the 12-methyl protons. Figure 6, shows the ENDOR spectra of the wild type and the triple mutant, PsaA Y599L/S603G/T739Y. The hfcs are also summarized on Table 2. According to these data, the perpendicular and parallel hyperfine tensors of the 12-methyl protons of Chl α , as well as the parallel hyperfine tensors of the 7-methyl protons, of the mutant are significantly lower than that of the wild type. The perpendicular and parallel hyperfine tensors of the 2-methyl protons increase slightly. Nevertheless, this increase does not compensate for the decrease observed in the hfcs of 7 and 12-methyl protons. This suggests that the electron spin density in P700⁺ is redistributed within the dimer. Similar results are demonstrated in the ENDOR spectrum of the single mutant PsaA T739F (Figure 7).

DISCUSSION

According to the crystal structure of *Synechococcus elongatus*, P700 is a heterodimer composed of Chl α and Chl α' , the 13² epimer of Chl α (2). The protein environment surrounds the heterodimer in a symmetric fashion except for the presence of a hydrogen bonding network between PsaA and Chl α' . The homologous residues in PsaB do not form these hydrogen bonds. It has been suggested that this asymmetry in protein-cofactor interaction might influence the biophysical properties of P700 (9, 10). In this study, we have used site-directed mutagenesis in PsaA of *Synechocystis* sp. PCC 6803, to disrupt these hydrogen bonds and study the effects on P700. Thr at position 739 of PsaA, is capable of donating a hydrogen bond to the 13¹-keto oxygen and to a water molecule, which donates a hydrogen bond to the 13² methyl ester oxygen of Chl α' as well. This residue was changed to Phe, which cannot hydrogen bond and has a similar chain structure with Tyr at the homologous position on PsaB. The water molecule also hydrogen bonds with Ser 603 and Tyr 599. In our triple mutant (PsaA Y599L/S603G/T739Y), the Tyr 599, Ser 603 and Thr 739 of PsaA were respectively mutated to Lys, Gly and Tyr, the amino acids at the

homologous positions in PsaB. These mutations make the interaction of P700 with the protein environment, more symmetric. Our third mutant (PsaA Y731F) involves Tyr at 731 of PsaA, which donates a hydrogen bond to the phytyl ester-carbonyl oxygen of Chl α' . In this mutant the hydrogen bond is disrupted by replacement of this tyrosine by Phe, the residue at the homologous position in PsaB.

All mutants can grow photoautotrophically. The triple mutant was investigated in more detail and has shown that in comparison to the wild type, it contains lower chlorophyll amounts. The PSI to PSII ratio, as demonstrated by the 77K fluorescence spectra of whole cells (Figure 3), remains the same in this mutant. Moreover, the decreased growth of this mutant under various light conditions, compared to the wild type suggests an increased sensitivity.

Bonding interaction of P700 with the protein. In this study, FTIR difference spectroscopy was used in order to study any changes in the bonding pattern of P700 and its protein environment. The (P700⁺-P700) difference spectra give information on the vibrational modes from the 13¹ keto C=O and the C=O of the 13² carbomethoxy group of both Chl α' and Chl α . The spectra obtained from PSI particles of the wild type (Figure 4) agree with previously published results (20). In these spectra, the differential signals at 1653(+)/1638(-) and 1718(+)/1698(-) are due to vibrations of the 13¹ keto C=O of Chl α' and Chl α respectively (positive signal associated with the oxidized state and negative with the neutral state of P700). The spectra obtained for the PsaA T739F mutant and the triple mutant, PsaA Y599L/S603G/T739Y, show differences in the 1700-1637 cm⁻¹ region of the spectrum, when compared to the wild type spectra. The differential signal 1653(+)/1638(-) in the mutants, is reduced by 50% compared to the wild type. Furthermore, a new negative band appears at 1676 cm⁻¹, possibly related to the free 13¹ keto C=O of Chl α' . This was expected since the Thr involved in a hydrogen bond with the 13¹ keto C=O of Chl α' , was changed to Phe, a residue of similar side chain structure, or Tyr (in the triple mutant), the residue at the homologous position in PsaB. Ideally, in the mutants, the signal 1653(+)/1638(-) should have been upshifted to 1718(+)/1698(-), where the 13¹ keto C=O signals of Chl α are observed. These results are given by both substitutions with Tyr (in the triple mutant) and Phe (in the single mutant). The latter, cannot hydrogen bond and

therefore, one cannot argue that they represent a remaining partial hydrogen bonding due to Tyr in the triple mutant. The remaining signal at 1653(+)/1638(-) can be a result of a change in the local dielectric constant or possibly a partial formation of a hydrogen bond with a newly inserted water molecule. Unlike the spectra of the single mutant (PsaA T739F), the FTIR difference spectra of the triple mutant also show differences in the 1754-1733 cm^{-1} region. This is a result of the two additional mutations of Tyr to Leu at position 599 and Ser to Gly at position 603. In the wild type, these amino acids are involved in a hydrogen bonding network involving a water molecule, which donates a hydrogen to the bridging oxygen of the 13^2 -carbomethoxy group of $\text{Chl}\alpha'$ (see Figure 2). Differential signals 1742(+)/1735(-) and 1754(+)/1749(-) are due to the C=O vibrations of the 13^2 - carbomethoxy group of $\text{Chl}\alpha'$ and $\text{Chl}\alpha$, respectively. In this mutant a new signal appears at 1762 cm^{-1} and the 1735(-) cm^{-1} signal decreases significantly, showing that the vibrational modes of the C=O of the 13^2 carbomethoxy group of $\text{Chl}\alpha'$ have been affected. More details about the FTIR analysis of this mutant will be presented elsewhere (M. Pantelidou, J. Bretton and P.R. Chitnis in preparation).

In the PsaA Y731F mutant, the Tyr at position 731 of PsaA was mutated to Phe, a residue of similar side chain structure that cannot hydrogen bond. According to Jordan et al., (2) this Tyr in the wild type PSI, forms a hydrogen bond with the phytyl ester carbonyl oxygen of $\text{Chl}\alpha'$. Unfortunately, the vibrational modes of this C=O bond cannot be detected in the FTIR difference spectra. Since the difference spectra obtained from this mutant, do not show any significant differences from the wild type, we can, therefore, conclude that this mutation did not cause any significant changes in the positioning of the $\text{Chl}\alpha/\text{Chl}\alpha'$ dimer with respect to the protein surrounding it.

Chla and Chla' content. It has been suggested that the hydrogen bond donated by Thr A739 to the 13^1 keto oxygen makes the 13^2 proton more acidic and promotes epimerization at this position, thus forming $\text{Chl}\alpha'$ (10). To determine if this theory is correct, HPLC was used to measure the $\text{Chl}\alpha'$ and $\text{Chl}\alpha$ levels in our triple mutant. The results (Figure 5) clearly demonstrate that $\text{Chl}\alpha'$ although lower, it is still present in PSI particles of the mutant and therefore its formation or incorporation of $\text{Chl}\alpha'$ is not inhibited. $\text{Chl}\alpha'$ and $\text{Chl}\alpha$

measurements were also performed for the single mutant, PsaA T739F. The ratio of Chl α' to Chl α in this mutant was the same as in the wild type (data not shown).

Electron spin distribution over P700⁺. The electronic structure of P700 has been extensively investigated by EPR and ENDOR (10). Based on comparisons with Chl α^{+} in organic solvents it has been proposed that the most of the electron spin density of P700⁺ (85%) is localized on Chl α of the heterodimer (21). FTIR results on the other hand, have concluded that the positive charge is more equally distributed with a 1:1 to 2:1 ratio favoring Chl α . FTIR spectroscopy measures the charge distribution, based on the upshifts of the C=O group vibrational frequencies upon oxidation of P700, and the amplitudes of the signals from the 13¹ keto group of Chl α and Chl α' (11, 20). However, the relations between charge distribution and signal upshift or signal amplitude has not yet been well defined. In addition, FTIR spectroscopy measures charge, which is not necessarily the same as spin distribution. For these reasons, we have used ENDOR for determining the electron spin density of P700 upon oxidation, in our triple mutant. The hfcs of specific protons of the spin carrying chlorophyll, Chl α , of P700 have been determined (21-23). Unfortunately, other than the two smallest hfcs in our ENDOR spectra (line pairs 1'/1 and 2'/2) no hfcs of Chl α' can be detected. In our ENDOR spectra of mutants PsaA T739F and PsaA Y599L/S603G/T739Y (Figure 6 and 7), splittings 7'/7 and 8'/8 are assigned to the perpendicular and parallel hyperfine tensor components of the Chl α 12-methyl protons. These hfcs, as well as the parallel hyperfine tensor components of the 7-methyl protons (6'/6) decrease significantly. The perpendicular and parallel hyperfine tensors of the 2-methyl protons do increase, however, this increase does not compensate for the decrease observed in the hfcs of 7 and 12-methyl protons. The rest of the hfcs do not change significantly. The results obtained from the ENDOR spectra suggest that the electron spin density in P700⁺ is redistributed within the dimer with a slight shift from Chl α towards the low spin carrying Chl α' .

Functional consequences of asymmetry. In summary, our data suggest that the hydrogen bonds of PsaA to the E ring of the Chl α' macrocycle affect the biophysical properties of P700. FTIR analysis of the single and triple mutant provides evidence that the bonding interaction of Chl α' is affected, suggesting a rupture of the hydrogen bond to the 13¹ keto oxygen of the chlorophyll. The triple mutant was further analyzed with HPLC and

ENDOR. The Chl α /Chl α' cofactor analysis by HPLC indicates that Chl α' although lower in the triple mutant, it is still present. However, the Chl α /Chl α' levels in the PsaA T739F mutant PSI, were the same as in the wild type. The ENDOR analysis of the electron spin density in both mutants, demonstrates that the mutation has caused electron spin density redistribution within P700⁺. The decrease of the 12-methyl and 7-methyl proton hfcs of the high spin carrying chlorophyll (Chl α), is interpreted as a shift towards Chl α' , the low spin carrying half of the dimer. This provides evidence that the hydrogen bonds of Chl α' affect the electronic structure of oxidized P700. The presence of the hydrogen bonding network on one half of the P700 dimer causes a shift of the electron spin density towards the other side. Our ENDOR spectra suggest that the mutations, which affected the hydrogen bonds of the low spin carrying chlorophyll and PsaA, caused a slight but significant electron spin shift from Chl α towards Chl α' .

REFERENCES

1. Chitnis P.R. (2001). *Annu. Rev. Plant Physiol. Plant Mol. Biol.*, 52, 593-626.
2. Jordan P., Fromme P., Witt H.T., Klukas O., Saenger W. and Krauß N. (2001). *Nature*, 411, 909-917.
3. Fromme P., Jordan P., Krauss N. (2001). *Biochim. Biophys. Acta*, 1507, 5-31.
4. Brettel K. and Leibl W. (2001). *Biochim. Biophys. Acta*, 1507, 100-114.
5. Xu W., Chitnis P., Valieva A., Est A., Pushkar Y.N., Krzystyniak B., Teutloff C., Zech S.G., Bittl R., Stehlik D., Zybailov B., Shen G. and Golbeck J.H. (2003). *J. Biol. Chem.*, 278, 27864-27875.
6. Putron S., Stevens D. R., Muhiuddin I. P., Evans M. C., Carter S., Rigby S. E. and Heathcote P. (2001). *Biochemistry*, 40, 2167-2175.
7. Boudreaux B., Macmillan F., Teutoll C., Rufat A., Gu F., Grimaldi S., Bittl R., Brettel K. and Redding K. (2001). *J. Biol. Chem.*, 276, 37299-37306.
8. Guergova-Kuras M., Boudreaux B., Joliot A., Joliot P. and Redding K. (2001). *PNAS*, 98, 4437-4442.
9. Golbeck J.H. (2003). *Annu. Rev. Biophys. Biomol. Struct.*, 32, 237-256.
10. Webber A.N. and Lubitz W. (2001). *Biochim. Biophys. Acta*, 1507, 61-79.

11. Breton J., Navedryk E. and Leibl W. (1999). *Biochemistry*, 38, 11585-11592.
12. Williams J.G.K. (1988). *Meth. enzymology*, 167, 766-778.
13. Smart L. B., Anderson S. L. and McIntosh L. (1991). *EMBO J.*, 10, 3289-3296.
14. Rippka R., Deruelles j., Waterbury J. B., Herdman M. and Stanier R. Y. (1979). *J. Gen. Microbiol.*, 111, 1-61.
15. MacKinney G. (1941). *J. Biol. Chem.*, 140, 315-322.
16. Sun J., Ke A., Jin P., Chitnis V. P. and Chitnis P. R. (1998). *Meth. Enzymol.*, 297, 124-139.
17. Arnon D. (1949). *Plant Physiol.*, 24, 1-14.
18. Shen G. Z. and Bryant D. A. (1995). *Photosynth. Res.*, 44, 41-53.
19. Nakamura A. and Watanabe T. (2001). *Anal. Sci.*, 17, 503-508.
20. Breton J. (2001). *Biochim Biophys Acta*, 1507, 180-193.
21. Kass H., Fromme P., Witt H. T. and Lubitz W. (2001). *J. Phys Chem.*, 105, 1225-1239
22. Käss H., Fromme P. and Lubitz W. (1996). *Chem. Phys. Lett.*, 257, 197-206.
23. Krabben L., Schlodder E., Jordan R., Carbonerra D., Giacometti G., Lee H., Webber A.N. and Lubitz W. (2000). *Biochemistry*, 39, 13012-13025.

FIGURE LEGENDS

- Figure 1. **Molecular structure of Chlorophyll α** (IUPAC numbering). Chl α' is the epimer at position 13².
- Figure 2. **Local protein environment of P700** (numbering is according to *Synechocystis* sp. PCC 6803). A. HisA676 and HisB651 are the coordinating ligands of P700. Putative hydrogen bonds between Chl α' , the water molecule and surrounding PsaA residues are shown by dotted lines. The respective residues on PsaB side are also shown; B. Closer view of the hydrogen bonds of PsaA Chl α' . The figures were drawn using the program *Swisspdbviewer* based on the coordinates of *Synechococcus elongatus*.
- Figure 3. **77K Fluorescence emission spectra of the wild type and the triple mutant PsaA-Y599L/S603G/T739Y**. Each spectrum was the average of three independent measurements. The excitation wavelength was 435 nm, which excites mostly chlorophyll. PSI and PSII emission maxima are shown with arrows.
- Figure 4. **Fourier transform infrared (FTIR) spectroscopy spectra**. The (P700⁺-P700) difference spectra are shown for the wild type (top), mutant PsaA Y731F (second from top), mutant PsaA T739F (third from top) and triple mutant PsaA Y599L/S603G/T739Y.
- Figure 5. **HPLC analysis of chlorophyll content (Chl α /Chl α') of wild type and the triple mutant**. The top row represents the HPLC traces (full scale = 1 AU) at 663nm of the injections of ethyl acetate extracts of PSI from wild type (left) and PsaA Y599L/S603G/T739Y (right). The Chl α /Chl α' fractions were collected and the Chl α' fraction (second minor peak after Chl α) was re-injected at a more sensitive setting. This is shown in the middle row (full scale = 0.02 AU). The large peak present in these spectra is a contamination of Chl α , due to tailing. Both peaks were purified and the Chl α fraction was added to the initial Chl α fraction (from the first row) and were re-injected. This is shown in the last row (full scale = 1.0 AU).
- Figure 6. **Electron nuclear double resonance (ENDOR) Spectra of P700⁺ of the wild type (upper) and the PsaA Y599L/S603G/T739Y mutant (lower)**. The splittings are shown with numbers and the reduction of the 12-methyl proton hfc's are indicated with dotted lines. The Larmor frequency of ¹H (not shown) is at 14.5 MHz.

(Conditions: temperature=120K, modulation frequency =12.5 kHz, modulation amplitude =2G, microwave power =20 mW, gain = 10^5 , time constant 81msec, 89 scans were summed).

Figure 7. **Electron nuclear double resonance (ENDOR) Spectra of P700⁺ of the wild type (upper) and the PsaA T739F mutant (lower).** The splittings are numbered and the reduction of the 12-methyl proton hfc's are indicated with dotted lines.

Table 1: Physiological characterization of the PsaA T739Y/S603G/Y599L mutant^α

Strains	Chlorophyll Content ($\mu\text{g}/\text{OD}_{730}/\text{ml}$)	Doubling Time (hours)				
		With Glucose			Without Glucose	
		Low Light ^β	Normal Light ^β	High Light ^β	Normal Light	High Light
Wild type	3.83±0.15	25.4±3.5	13.3±1.8	15.6±3.8	92.2±6.4	64.4±7.1
PsaA mutant T739Y/S603G/Y599L	2.36±0.18	39.4±6.1	20.9±1.2	21.6±4.0	148.8±7.5	103.2±9.0

^α Average of three independent measurements

^β Low, normal and high light conditions are 5-10, 40-50 and 90-100 $\mu\text{mol photons m}^{-2}\text{s}^{-1}$ respectively

Table 2: Proton hyperfine couplings in MHz of P700⁺ from the wild type and the mutants in *Synechocystis* sp. PCC 6803^a

Strains	PsaA Chl (1'/1)	PsaA Chl (2'/2)	A _⊥ (2) (3'/3)	A _∥ (2) (5'/5)	A _⊥ (7) (4'/4)	A _∥ (7) (6'/6)	A _⊥ (12) (7'/7)	A _∥ (12) (8'/8)
Wild type	0.89	1.79	2.48	3.59	3.26	4.32	5.26	6.14
PsaA T739Y/S603G/Y599L	0.86	1.77	2.65	3.69	3.24	4.16	5.02	5.94
PsaA T739F	0.88	1.80	2.55	3.76	3.28	4.19	5.02	5.87

^a The error for each measurement is ± 0.05 MHz

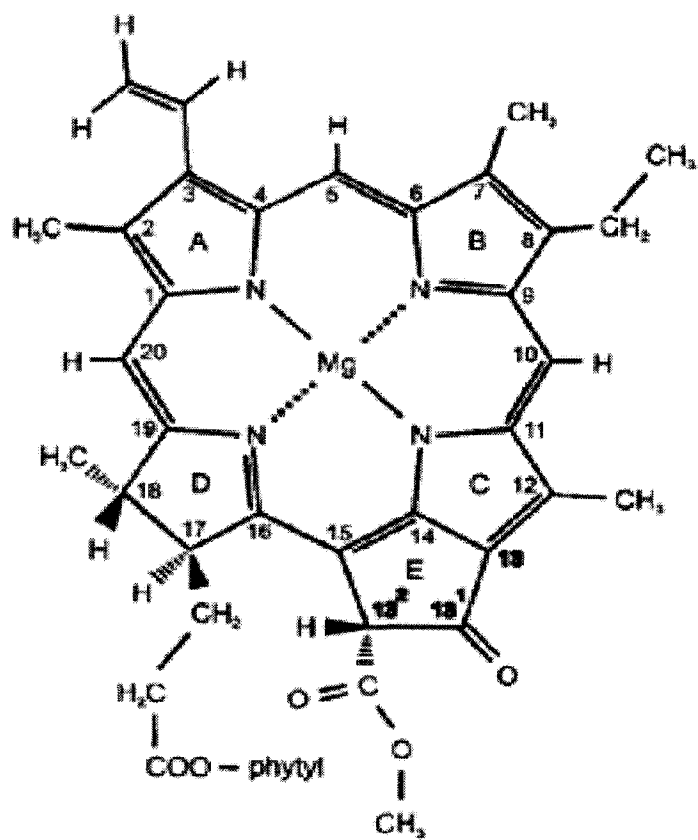


Figure 1

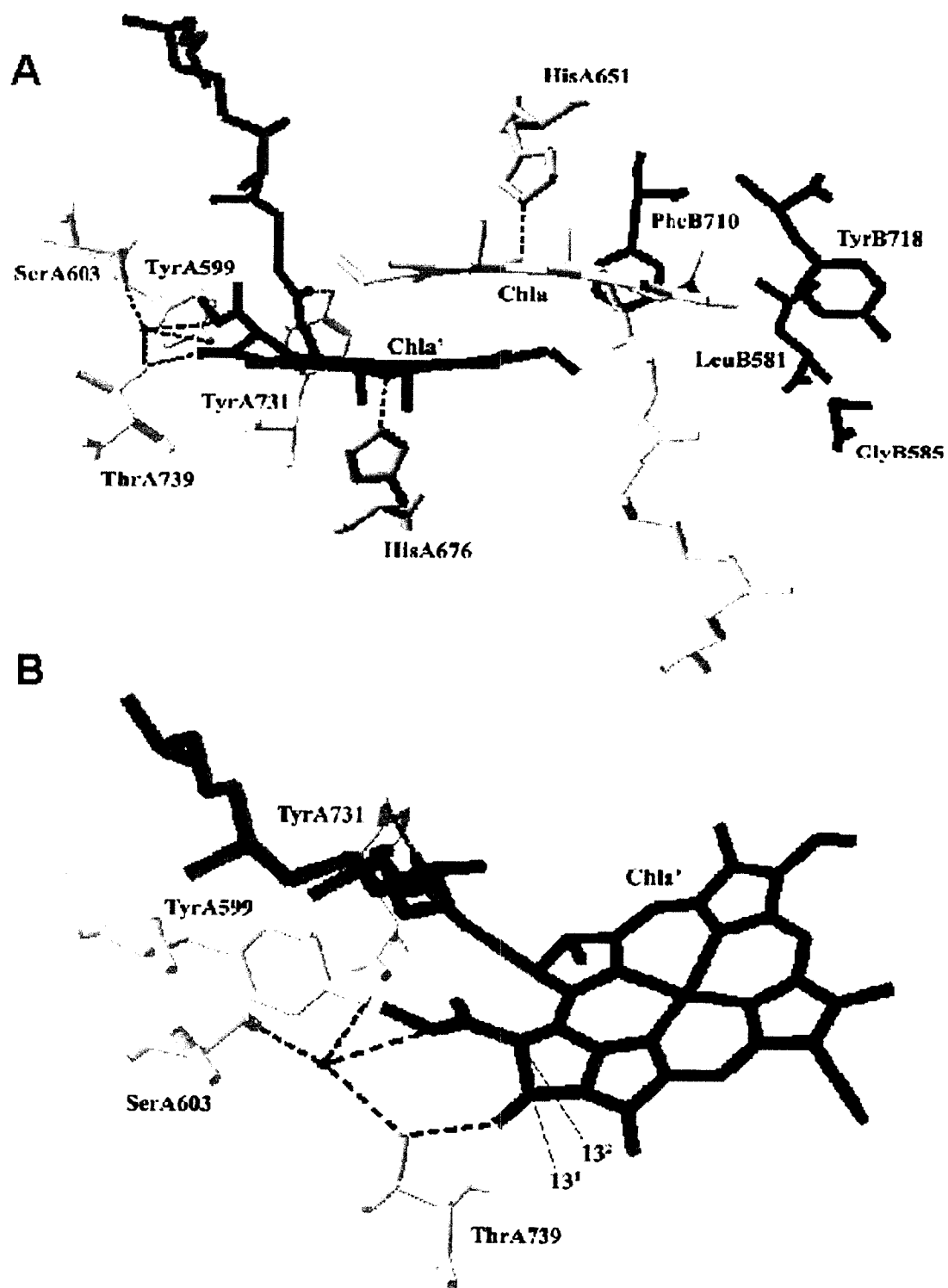


Figure 2

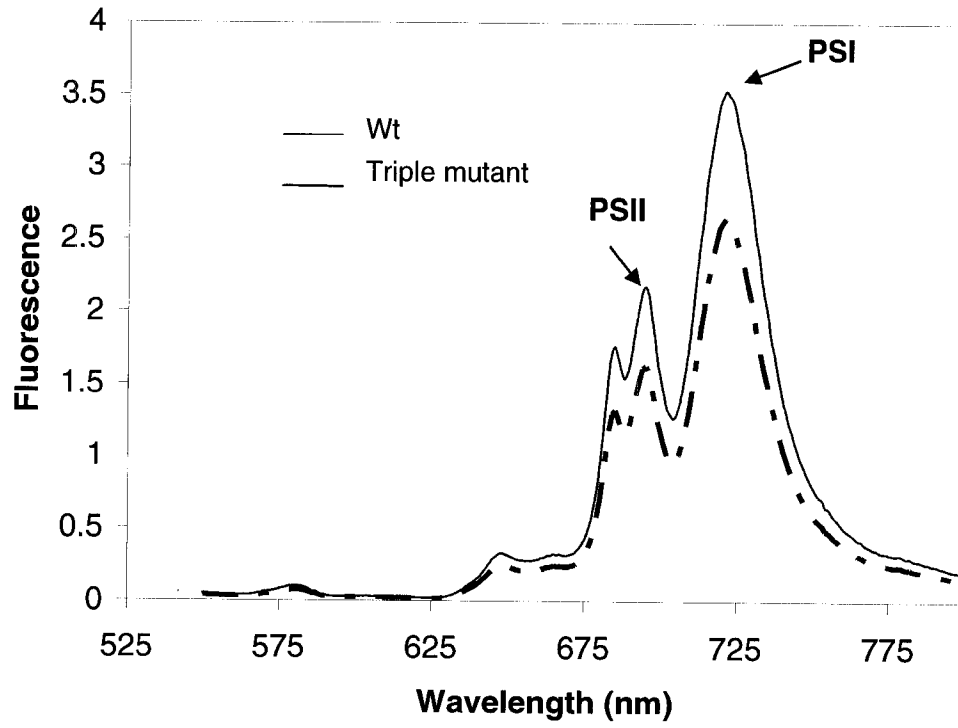


Figure 3

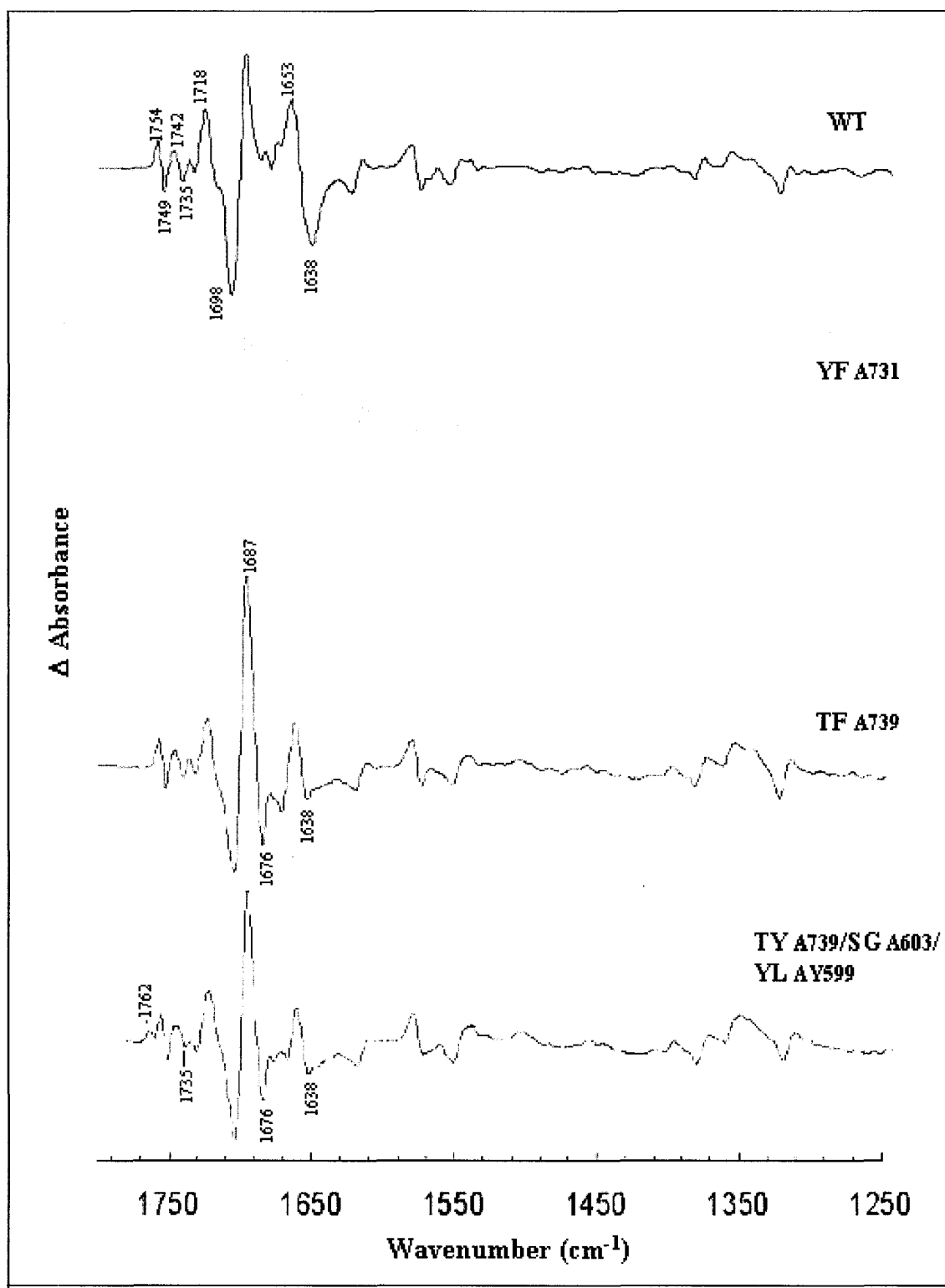


Figure 4

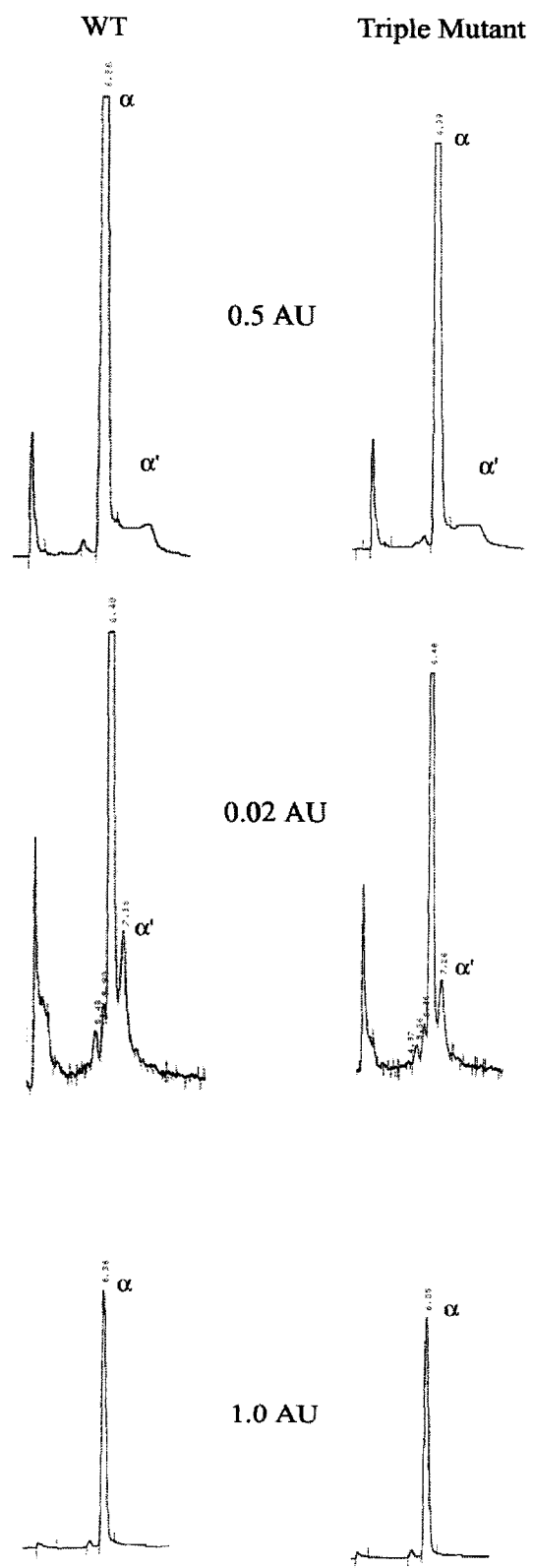


Figure 5

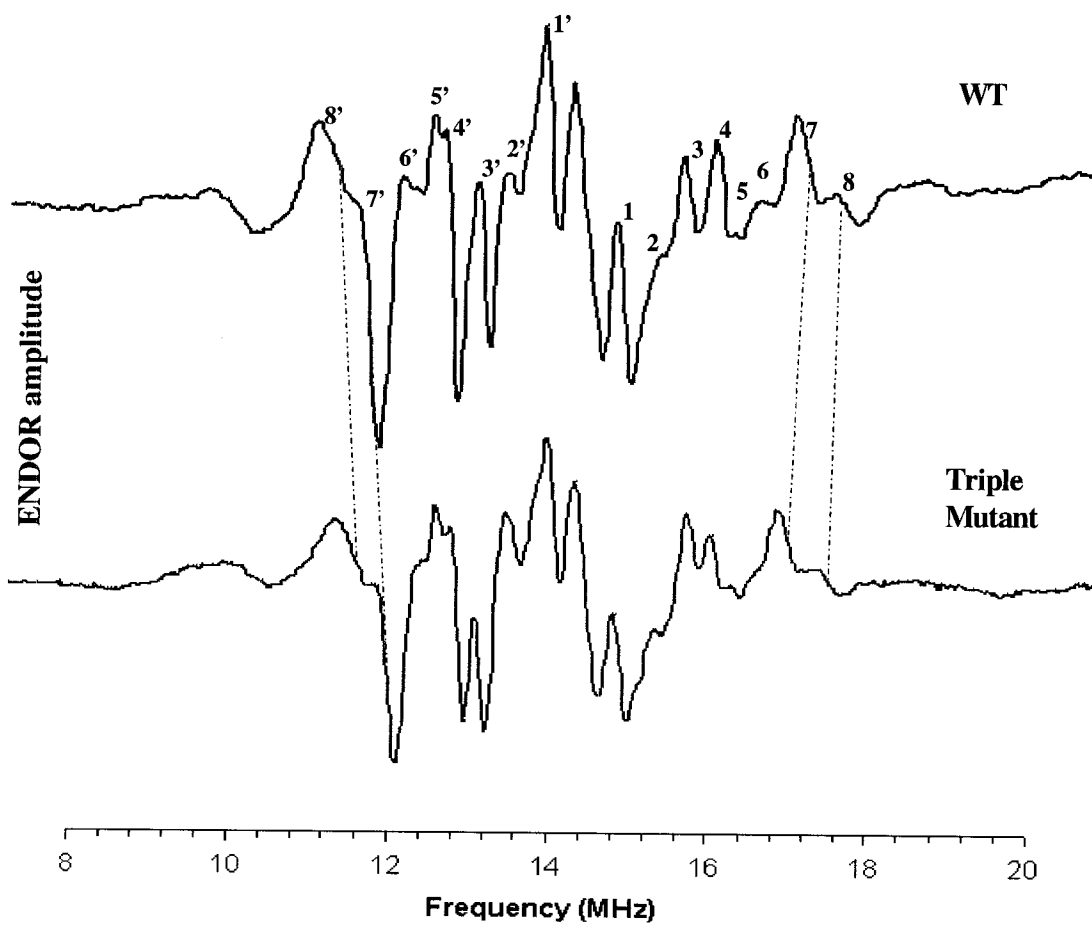


Figure 6

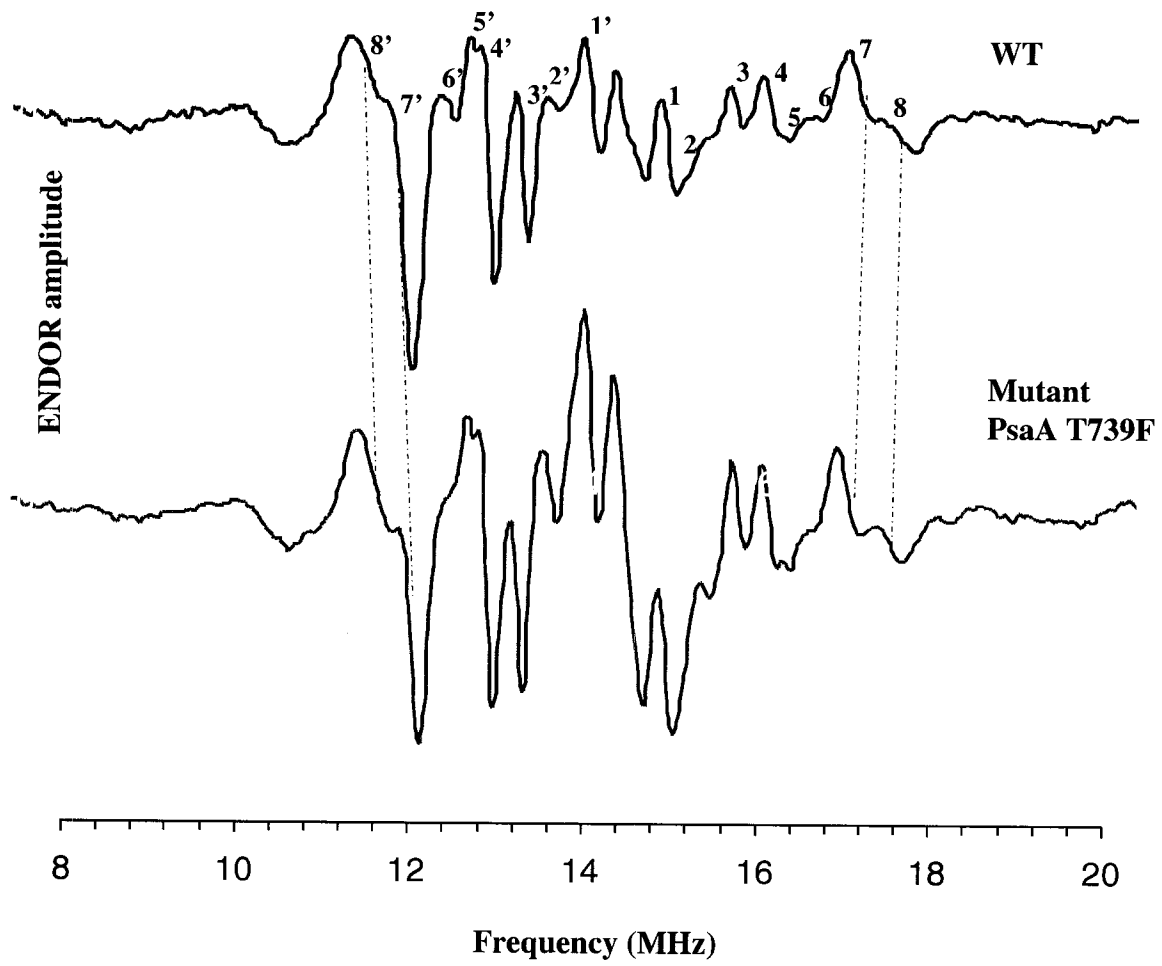


Figure 7

**CHAPTER 3. FTIR SPECTROSCOPY OF SYNECHOCYSTIS 6803 MUTANTS
AFFECTED ON THE HYDROGEN BONDS TO THE CARBONYL GROUPS OF
THE PsaA CHLOROPHYLL OF P700 SUPPORTS AN EXTENSIVE
DELOCALIZATION OF THE CHARGE IN P700^{+1*}**

A paper to be submitted to *Biochemistry*

Maria Pantelidou, Parag R. Chitnis, and Jacques Breton^{2**}

ABSTRACT

P700, the primary electron donor of photosystem I, is an asymmetric dimer made of one molecule of chlorophyll *a'* (P_A) and one of chlorophyll *a* (P_B). While the carbonyl groups of P_A are involved in hydrogen bonding interactions with several surrounding amino acid side chains and a water molecule, P_B does not engage hydrogen bonds with the protein. Light-induced FTIR difference spectroscopy of the photooxidation of P700 has been combined with site-directed mutagenesis in *Synechocystis* sp. PCC 6803 to investigate the influence of these hydrogen bonds on the structure of P700 and P700⁺. When the residue Thr A739 which donates a hydrogen bond to the 9-keto C=O group of P_A is changed to Phe, a differential signal at 1653(+)/1638(-) cm⁻¹ in the P700⁺/P700 FTIR difference spectrum upshifts by ~30-40 cm⁻¹, as expected for the rupture of the hydrogen bond or, at least, strong decrease of its strength. The same upshift is also observed in the FTIR spectrum of a triple mutant in which the residues involved in the three main hydrogen bonds to the 9-keto and 10a-carbomethoxy groups of P_A have been changed to the symmetry-related side chains present around P_B . In addition, the spectrum of the triple mutant shows a decrease of a differential signal around 1735 cm⁻¹ and the appearance of a new signal around 1760 cm⁻¹. This is consistent with the perturbation of a bound 10a-ester C=O group that becomes free in the triple mutant. All these observations support the assignment scheme proposed previously

¹ Part of this work was supported by a grant from US National Science Foundation (MCB 0078268)

² To whom correspondence should be addressed: Service de Bioénergétique, Bât. 532, CEA-Saclay, 91191 Gif-sur-Yvette Cedex, France. Tel: (331) 6908 2239. Fax: (331) 6908 8717. E-mail: cadara3@dsvidf.cea.fr.

for the carbonyls of P700 and P700⁺ (Breton, J. et al., 1999) and therefore reinforce our previous conclusions that the positive charge in P700⁺ is largely delocalized over P_A and P_B.

INTRODUCTION

The reaction center (RC) of photosystem I (PS I) is a large multisubunit integral membrane protein that uses light to drive electrons across the photosynthetic membrane of cyanobacteria, algae, and plants. Most of the cofactors involved in light collection and electron transfer processes are coordinated to the two main subunits, PsaA and PsaB, each containing 11 transmembrane α -helices that form the heterodimeric core of the RC. Light absorbed by an antenna pigment is rapidly trapped by a specialized dimer of excitonically coupled chlorophyll (Chl) molecules called P700 which is the primary electron donor of PS I. After excitation, an electron is ejected from the lowest excited state of P700 and is first passed onto a monomeric Chl. Subsequent charge stabilization is achieved by further electron transfer steps over a chain of acceptors. Owing to its prominent role, the structure of P700 in its neutral, triplet, and cationic states has been investigated in great detail using optical, vibrational, and magnetic resonance spectroscopic techniques leading to models for the organization of the pigments within the dimer and the distribution of charge and spin in the oxidized and triplet states of P700 (reviewed in ref. 1).

In the last two decades, X-ray crystallographic models of bacterial RC proteins have provided an invaluable source of information to complement the data obtained on their primary electron donors (P) by spectroscopy alone, notably when the resolution of the structures becomes sufficient to identify the amino acid side chains interacting with the pigments through hydrogen bonds to the carbonyl groups or axial ligation to the central Mg atoms of the bacteriochlorophyll (BChl) molecules. In this case, site-directed mutagenesis becomes a choice method to perturb selectively the pigment-protein interactions, therefore providing RCs with modified P, the structure and function of which can be probed by spectroscopy (reviewed in ref. 2). While X-ray crystallography provides key information on the geometry of the amino acid side chains acting as axial ligands or H-bond partners of the BChls in the ground state of P, it remains silent on several important aspects of the electronic structure of the special pair after charge separation occurs, such as the localization of the

triplet state in 3P or the hydrogen bonding status of the BChls and the charge distribution in P^+ . Among the spectroscopic tools that can bring specific information on the structure-function relationship in both native and genetically modified RCs, light-induced FTIR difference spectroscopy has emerged as a prominent technique (reviewed in refs 3-6). The complementary aspects of the spectroscopic and X-ray crystallographic approaches have been initially encountered in the field of purple photosynthetic bacteria. This combined approach is now striding along for the PS I and is also making progress in the case of PS II.

In the case of PS I, an initial structure at 4 Å resolution (7) showed P700 to be a dimer of Chl with a geometry similar to that of P in the RC of photosynthetic purple bacteria where His residues from the two homologous L and M polypeptides making up the core of the RC act as ligands to the Mg atom of the two BChl molecules of P. This observation led to an investigation of the $P700^+/P700$ FTIR difference spectra characterizing the photooxidation of P700 in a series of PS I mutants of *Chlamydomonas (C.) reinhardtii* in which each of the conserved pairs of His located symmetrically on the homologous PsaA and PsaB polypeptides is replaced by Gln. This study allowed an identification of the His axial ligand of each of the PsaA and PsaB Chl molecules of P700 (8). In the following, these Chls will be termed P_A and P_B in the ground state and P_A^+ and P_B^+ in the oxidized state. In a study of P700 photooxidation in the cyanobacterium *Synechocystis* sp. PCC 6803 (referred to in the following as *Synechocystis*) that combined global isotope labeling and a comparison of $P700^+/P700$ and $^3P700/P700$ FTIR difference spectra, it was possible for the first time to assign the 9-keto and 10a-ester C=O modes of the two Chls in P700 and $P700^+$ (9). Notably, it was concluded that both carbonyl groups of one Chl are free from interactions with the protein while the two carbonyl groups of the other Chl are engaged in hydrogen bonding interactions. An extreme downshift of 60 cm^{-1} was observed for the 9-keto C=O group of the latter Chl. The asymmetry in hydrogen bonding of the P700 Chls was found to remain in the $P700^+$ state and, upon assuming comparable extinction coefficient for the carbonyl groups of the two Chls, it was concluded that the positive charge in $P700^+$ is approximately equally shared between the two Chls. On the other hand, the triplet state in 3P700 was observed to be fully localized on the Chl that is engaged in strong bonding interactions with the protein.

When the first X-ray model of PS I from the cyanobacterium *Synechococcus* (*S.*) *elongatus* with a resolution (2.5 Å) sufficient to analyze the protein-cofactor interactions was reported (10), it became clear that P700 is indeed a very asymmetrical dimer (Figure 1). While P_B is a Chl *a* molecule with no hydrogen bonds to the nearby PsaB polypeptide, P_A is a Chl *a*' (epimer of Chl *a* at C₁₀) with both the 9-keto C=O and 10a-carbomethoxy groups forming hydrogen bonds with the PsaA polypeptide, either directly or through an intervening water molecule. An additional hydrogen bond between the PsaA polypeptide and the 7c-ester C=O of P_A was also described with no symmetrical interaction on the PsaB side. It should be stressed that the 7c-ester C=O group being out of conjugation to the Chl macrocycle is therefore not expected to contribute directly to a P700⁺/P700 FTIR difference spectrum (11). Finally, the His residues axial ligands of the two Chl molecules of P700 observed by X-ray crystallography turned out to be those assigned from the FTIR spectra (8).

Thus, the predictions from the FTIR studies (8,9) turned out to be in excellent agreement with the newest X-ray model (6,10). On the other hand, the conclusion on the delocalization of the positive charge in P700⁺ was at variance with the interpretation of a number of previous investigations using magnetic resonance techniques, notably some recent ENDOR studies on oriented PS I crystals and on *C. reinhardtii* bearing mutations on the His axial ligands to the P700 Chls, which had led to the conclusion that the spin in P700⁺ is essentially localized (≥ 85%) on P_B⁺ (1,12). A further discrepancy with the results from magnetic resonance spectroscopy was noticed for the localization of the triplet character in ³P700 which, at that time, was proposed to be on P_B from ADMR experiments (1,13,14) and on P_A from the FTIR study (6,9). The strong divergence between the conclusions derived from magnetic resonance spectroscopy and the FTIR experiments led Hastings et al. (15) to propose an alternative interpretation of the FTIR difference spectra with a completely different assignment for the 9-keto C=O of the P_A Chl, but that was more consistent with the interpretation of the magnetic resonance experiments. The later set of assignments were critically discussed in a subsequent investigation by FTIR spectroscopy of *Synechocystis* PS I preparations bearing mutations at the His axial ligand of the PsaB Chl (16). It was further shown in the latter study that the imidazole C₅-N_τ stretching mode of each of the two His axial ligands of the P700 Chls were similarly perturbed upon P700⁺ formation, an

observation supporting the proposal of extensive charge delocalization derived from our previous FTIR studies (6,9).

The 2.5 Å resolution model of P700 shows a complex array of hydrogen bonds in the vicinity of the 9-keto and 10a-ester C=O groups of P_A that also involves the water molecule H₂O-19 and several of the PsaA side chains. Notably, the amino acid residue Thr A743 (the equivalent residue is Thr A739 in both *Synechocystis* and *C. reinhardtii*; see Table I, for the correspondence with the *S. elongatus* numbering) is within hydrogen bonding distance to both the 9-keto C=O of P_A (Figure 1) and the H₂O-19 molecule (Figure 2, with numbering according to the sequence of *Synechocystis*). The X-ray model shows that the oxygen atom of H₂O-19, which is 3.2 Å away from the methoxy oxygen atom of the 10a-ester carbomethoxy group, is also within hydrogen bonding distance of Tyr A603 (2.7 Å), Ser A607 (2.9 Å) and, to a lesser extent, of Gly A739 (3.3 Å). All of these amino acid residues are highly conserved in *Synechocystis* and are numbered Tyr A599, Ser A603 and Gly A735, respectively (Table 1). Based on the X-ray structural model, several mutations at the residue Thr A739 were generated in *C. reinhardtii* and their effects were investigated with structural spectroscopy techniques (14,17). Although an initial report of the results of optical and magnetic resonance spectroscopy was presented as confirming the previous conclusions that the spin in P700⁺ and the triplet character in ³P700 were essentially localized on P_B (14), a later study that included FTIR difference spectroscopy of P700 photooxidation, led to a substantial change of opinion (17). It was notably proposed that the interpretation of previous optical measurements of P700 photooxidation was based on invalid assumptions concerning the coupling amongst the pigments. As a consequence, the conclusions from the ADMR measurements on the localization on P_B of the triplet in ³P700 had to be revised. Similarly, the ENDOR measurements on the new mutants indicated that the extent of electronic coupling amongst the two Chls in P700⁺ of wild type was larger than previously thought. On the other hand, the FTIR results on the mutants were taken to show the alteration of the hydrogen bond to the 9-keto carbonyl of P_A in the mutants. Although the absence of FTIR studies of isotopically labeled samples or of the triplet state of the mutants precluded a firm and direct assignment of the bands in the mutants, the FTIR data of Witt et al. (17) could be easily interpreted in the frame of the model previously put forward for the

assignment of the carbonyl bands in P700, P700⁺, and ³P700 (6,9). In contrast, a detailed FTIR study of another *C. reinhardtii* mutant at Thr A739 has been recently presented (18) as supporting the assignment scheme of Hastings et al. (15) for the 9-keto C=O group of P_A.

In the present study we report on the P700⁺/P700 FTIR difference spectrum of PS I trimers from *Synechocystis* in which the residue Thr A739 in hydrogen bonding interaction with the 9-keto C=O of P_A has been replaced with the non hydrogen bonding Phe side chain. The FTIR spectrum of this single mutant is compared to that of PS I bearing a set of three mutations that were devised to alter the hydrogen bonding pattern of the 9-keto and 10a-carbomethoxy groups of the PsaA Chl of P700 by making it similar to the environment of the symmetry-related PsaB Chl that exhibits no hydrogen bonding interaction with the protein (Figure 2).

EXPERIMENTAL PROCEDURES

Site-directed mutagenesis. Site-specific mutations in *psaA* gene were performed using pIBC as the donor plasmid and pWX as the recipient *Synechocystis* strain, as described in (19). Strain pWX lacks a part of *psaA* and the whole *psaB* gene. Plasmid pIBC consists most of *psaA* gene, *psaB* gene and its 760-bp downstream region incorporated into the pBluescript II KS vector. A chloramphenicol resistance cassette gene is located after the 3' terminator of the *psaB* gene. PCR mutagenesis was performed using the *Platinum Pfx Polymerase* (Invitrogen) and pIBC as a template. The mutation containing DNA was selected by digestion with *DpnI* endonuclease (Promega). The mutated plasmids were checked by sequencing and were used to transform the recipient strain, pWX. The transformants were selected and segregated for several generations on chloramphenicol supplemented BG-11 plates under low light intensity (2-3 $\mu\text{moles m}^{-2}\text{s}^{-1}$) at 30 °C. The fragment containing the site-specific mutations was amplified from genomic DNA by PCR and was sequenced to confirm the presence of the desired mutations. In the single mutant, the Thr PsaA 739 (Thr A739) is replaced by Phe while in the triple mutant Tyr A599, Ser A603, and Thr A739 are mutated to Leu, Gly, and Tyr, respectively.

Cell growth and PS I complex isolation. The *Synechocystis* wild type and mutant strains, were grown in BG-11 medium at 30 °C. The cultures were grown in large bottles

with aeration, under light intensity of 40-50 $\mu\text{mol photons m}^{-2}\text{s}^{-1}$. The mutants were supplemented with 30mg/L chloramphenicol and all strains were grown in the presence of glucose (5mM). For global ^{15}N labeling of cells, the cultures were grown in ^{15}N labeled media. BG-11 was supplemented with $\text{Na}^{15}\text{NO}_3$ (from H^{15}NO_3 purchased from Cambridge Isotope Laboratories). Growth was monitored by absorbance measurements at 730 nm (A_{730}) with a UV-160U spectrophotometer (Shimadzu). The cells were harvested at mid to late exponential growth (1.0 OD_{730}) with centrifugation at 4000g. Thylakoid membrane extraction and isolation of PS I trimers was performed according to previously published methods with minor alterations (20). PS I complexes were concentrated to 1mg Chl/ml and stored at -60°C .

FTIR measurements. Samples for FTIR were prepared by centrifugation ($300000 \times g$ for 60 min) of PS I trimers in Tris-HCl buffer (70mM; pH 7.0) containing 80 mM potassium ferrocyanide and 20 mM potassium ferricyanide. A small fraction of the resultant pellet was squeezed between two calcium fluoride windows and the thickness of the sample was adjusted to give an absorption of about 0.8 OD unit at the maximum around 1650 cm^{-1} with approximately half of this absorption being due to the amide I absorption and the other half to the scissoring mode of water. Light-induced difference spectra were recorded on Nicolet 60SX and 860 FTIR spectrometers at a temperature of 5°C and at a resolution of 4 cm^{-1} as previously reported (9,16).

RESULTS

P700⁺/P700 FTIR spectrum of the T(A739)F single mutant. Figure 3 shows a comparison of the light-induced P700⁺/P700 FTIR difference spectra of a wild type control (a) and of the T(A739)F mutant (b). The two spectra have been normalized by minimizing the residuals over the whole frequency range between 1000 and 5000 cm^{-1} (not shown). The wild type minus mutant double-difference spectrum is shown in figure 3c. The largest impact of the mutation on the P700⁺/P700 FTIR spectrum occurs in the spectral range characteristic of the 9-keto C=O of the Chls of P700 and P700⁺ between 1720 and 1635 cm^{-1} . The $1653(+)/1638(-) \text{ cm}^{-1}$ differential signal in the spectrum of wild type (Fig. 3a) is replaced by another one of much reduced amplitude and mostly positive at $1651(+)/1642(-) \text{ cm}^{-1}$ in the

spectrum of the mutant (Figure 3b). This is accompanied by the development of a large negative band at 1676 cm^{-1} and a positive one at 1688 cm^{-1} in the mutant that overlaps with a preexisting positive band at 1687 cm^{-1} in the wild type. Together these changes contribute the two large differential signals of comparable amplitudes but of opposite signs at $1689(-)/1676(+)$ and $1660(+)/1637(-)\text{ cm}^{-1}$ in the double-difference spectrum (Figure 3c). The amplitude of the $1718/1698\text{ cm}^{-1}$ signal in the spectrum of the control is reduced by 15-20% in the mutant.

Above 1725 cm^{-1} , very little difference is observed between the spectrum of wild type (Figure 3a) and that of the T(A739)F single mutant (Figure 3b) except for a $\sim 1\text{ cm}^{-1}$ upshift upon mutation of the small differential signal at $1735(-)/1730(+)\text{ cm}^{-1}$. This upshift is responsible for the small negative band at 1733 cm^{-1} in the double-difference spectrum (Figure 3c). On the other hand, a $2\text{-}3\text{ cm}^{-1}$ downshift of the macrocycle C=C marker mode of 5-coordinated Chl at 1608 cm^{-1} (21) is amongst the other significant perturbations which can be identified upon comparing the $P700^+/P700$ FTIR spectra of wild type and of the T(A739)F mutant. Similarly, the coupled C-C, C-H, and C-N modes of the Chl macrocycle absorbing between 1400 and 1250 cm^{-1} are also affected both in amplitude and in frequency by the mutation.

P700⁺/P700 FTIR spectrum of the triple mutant. Figure 4 shows a comparison of the light-induced $P700^+/P700$ FTIR difference spectra of the wild type control (a) and of triple mutant (b) together with the corresponding double-difference spectrum wild type minus triple mutant (c). In the frequency range below 1725 cm^{-1} of the $P700^+/P700$ FTIR spectra most of the changes which are induced by the triple mutation (Figure 4b) were also observed in the spectrum of the T(A739)F single mutant (Figure 3b). The double-difference spectrum (Figure 4c), which is also very comparable to that calculated for the single mutant (Figure 3c), exhibits two large differential signals of nearly equal amplitudes but of opposite signs at $1690(-)/1676(+)$ and $1657(+)/1637(-)\text{ cm}^{-1}$. Furthermore, the spectrum of the triple mutant (Figure 4b) also exhibits a downshift of the macrocycle C=C marker mode of 5-coordinated Chl at 1608 cm^{-1} and a perturbation of the coupled C-C, C-H, and C-N modes of the Chl macrocycle in the $1400\text{-}1250\text{ cm}^{-1}$ frequency range as previously observed for the

T(A739)F single mutant (Figure 3b). The amplitude of the 1718/1698 cm^{-1} signal in the spectrum of the control is also reduced by 15-20% in the triple mutant.

In the triple mutant, a significant alteration of the P700⁺/P700 FTIR spectrum is detected in the frequency range typical of the 10a-ester C=O above 1725 cm^{-1} . Upon mutation, a new positive band appears at 1762 cm^{-1} while the amplitude of the small differential signal at 1735(-)/1730(+) cm^{-1} is strongly decreased (Figure 4b). The 1742 (+)/1735(-) cm^{-1} differential signal of wild type is reduced in amplitude in the mutant spectrum. On the other hand, the differential signal at 1754(+)/1749(-) cm^{-1} , previously assigned to the free 10a-ester C=O of P_B⁺/P_B (9), is not affected by the mutation.

Effect of ¹⁵N global labeling on the P700⁺/P700 FTIR spectrum of the triple mutant.

The 1651(+)/1642(-) cm^{-1} signal that remains in the spectrum of the single and triple mutants (Figures 4b and 5b) could originate from protein amide I C=O modes or from the 9-keto C=O vibration of a P700 Chl in hydrogen bonding interaction with the OH group of a water molecule (or of the Tyr introduced at the PsaA 739 site in the triple mutant). In order to help discriminate between these two possibilities, global ¹⁵N labeling was performed on the triple mutant. In figure 5, the P700⁺/P700 FTIR spectrum of the unlabeled sample of the triple mutant (Figure 5a) is compared to that of the uniformly ¹⁵N labeled sample (Figure 5b) and to the unlabeled minus ¹⁵N labeled double-difference spectrum (Figure 5c). The bands around 1550 cm^{-1} in the spectral range characteristic of the combined C-N stretching (40%) and N-H bending (60%) vibrations of the amide II mode are strongly affected. Notably, a differential signal at 1563(+)/1556(-) cm^{-1} exhibits upon labeling the same 14-15 cm^{-1} downshift characteristic of the amide II mode that is observed for this band in the abs spectrum of the labeled sample (not shown). Similar changes have been previously reported for the P700⁺/P700 FTIR spectrum of uniformly ¹⁵N labeled wild type samples (9,16). The coupled C-C, C-H, and C-N modes of the Chl macrocycle absorbing between 1400 and 1250 cm^{-1} are also affected by the labeling. Very clear downshifts of many bands are also observed in the frequency range of the amide A band around 3300 cm^{-1} corresponding to the N-H stretching modes of proteins (not shown).

In order to visualize the small frequency shifts induced by the ¹⁵N labeling on the amide I bands, the spectra previously shown in figure 5 are presented in the spectral range

1730-1630 cm^{-1} (Figure 6). Upon comparing the P700⁺/P700 FTIR spectrum of the unlabeled and uniformly ¹⁵N-labeled samples, two main effects are detected. Firstly, a small shift ($< 1 \text{ cm}^{-1}$) of the large differential signal at 1698 (-)/1688(+) cm^{-1} in the P700⁺/P700 FTIR spectrum of the unlabeled samples gives rise to a band centered at 1691 cm^{-1} in the double-difference spectrum (Figure 6c). Secondly, a relatively larger perturbation is observed for the differential signal at 1651(+)/1642(-) cm^{-1} in the spectrum of the unlabeled sample which downshifts by 1-2 cm^{-1} upon ¹⁵N labeling. The latter effect, which gives rise to the 1654/1648 cm^{-1} differential signal in the double-difference spectrum (Figure 6c), is more characteristic of a protein amide I mode than of a 9-keto Chl C=O mode (22).

DISCUSSION

Comparison with the P700⁺/P700 FTIR Spectra of Other Mutants at Thr PsaA739.

Although the present P700⁺/P700 FTIR spectroscopic study is the first report of mutants at the Thr A739 site in the cyanobacterium *Synechocystis*, two previous studies have reported FTIR spectra of mutants at the same site in the algae *C. reinhardtii*. Notably, this key Thr residue has been replaced with Tyr, His, and Val (17) and by Ala (18). In all cases, the reported P700⁺/P700 FTIR spectra show a strong reduction of the amplitude of the differential signal centered around 1645 cm^{-1} in wild type together with the appearance of a new differential signal centered at higher frequency in the spectrum of the mutants. This is closely comparable to what is observed in the present study where the 1653(+)/1638(-) cm^{-1} differential signal in the spectrum of wild type is replaced by a differential signal negative at 1676 cm^{-1} and positive at 1688 cm^{-1} after mutation (Figures 3 and 4).

In the study by Witt et al. (14), it was further observed that the frequency of the new negative band appearing in the spectra of the mutants was dependant upon the nature of the residue introduced at the mutated site, suggesting that it was determined by the possibility of the new residue to engage in hydrogen bonding interactions with the 9-keto carbonyl of P_A. This negative band was found at 1657, 1669, or 1672 cm^{-1} upon replacing Thr by Tyr, His, or Val, respectively. The latter frequency was also observed for the negative band in the study by Wang et al. (18), where Ala was introduced at the same position.

Shifts and amplitude changes of the C=O ester bands of the Chls of P700 observed above 1725 cm^{-1} have been described upon T(A739)A mutation, leading to band assignments (18). While the assignments of the two differential signals found at higher frequency are the same as those previously proposed on the basis of the comparison of the P700⁺/P700 and ³P700/P700 FTIR spectra (9), the small signal around 1730 cm^{-1} was assigned to the 7c-ester C=O of P_A. It should be noticed that the perturbation of these C=O ester bands described for the Thr to Ala mutation in *C. reinhardtii* (18) has no counterparts in the case of the T(A739)F single mutant in *Synechocystis* investigated here as only a $\sim 1\text{ cm}^{-1}$ upshift of the small differential signal at $1735(-)/1730(+)\text{ cm}^{-1}$ is observed upon mutation (Figure 3a,b). Further studies will be required to find out whether this difference is primarily due to the different species involved or is related to the nature of the residue introduced at the Thr A739 site.

Effect of Mutations at Thr A739 on the 9-keto C=O Vibration of the PsaA Chl of P700. By combining global isotope labeling and a comparison of P700⁺/P700 and ³P700/P700 FTIR difference spectra, the 9-keto and 10a-ester C=O modes of the two Chls in P700 and P700⁺ were assigned (9). When these assignments could be correlated with the high-resolution structure of PS I (10), it became possible to identify the 9-keto and 10a-ester C=O modes of P_A, P_A⁺, P_B, and P_B⁺ (6). Notably, a differential signal at $1656(+)/1637(-)\text{ cm}^{-1}$ in the P700⁺/P700 spectrum of wild type *Synechocystis* at 90 K was assigned to the upshift upon photooxidation of the 9-keto mode of P_A in strong hydrogen bonding interaction with the OH group of Thr A739 (6,9).

Therefore, the upshift by $\sim 30\text{-}40\text{ cm}^{-1}$ of the $1657\text{-}1660(+)/1637(-)\text{ cm}^{-1}$ differential signal observed for both the single T(A739)F mutant and the triple mutant (Figures 3c and 4c) when the Thr residue in hydrogen bonding interaction with the 9-keto C=O group of P_A is perturbed fits well within our previously proposed assignment scheme (6,9). The same model has been used to rationalize the effect of the mutations at Thr A739 in *C. reinhardtii* although the possibility that the observed spectral changes around $1630\text{-}1660\text{ cm}^{-1}$ could be obscured by absorption changes of the amide I protein band was not considered (17). On the other hand, a very different assignment scheme has been used to explain the equivalent changes observed when the Thr residue was mutated to Ala (18). This point will be discussed in a subsequent section.

It is worth noting that only a fraction of the differential signal centered around 1645 cm^{-1} upshifts upon T(A739) mutations (Figures 3 and 4) leaving a differential signal at $1651(+)/1642(-)\text{ cm}^{-1}$. A comparable feature is also present in the T(A739)A mutant in *C. reinhardtii* (18). These remaining signals could have different origins. It could represent a side chain contribution or the amide I signature of a protein conformational and/or electrostatic change. Alternatively, it could also correspond to the upshift upon P700 photooxidation of the 9-keto C=O carbonyl group of a fraction of P_A that would remain in hydrogen bonding interaction with the OH group of a water molecule present in the mutated cavity (or with the OH side chain of the Tyr introduced at the PsaA 739 site in the triple mutant). In order to test between these possibilities, global ^{15}N labeling of the triple mutant was used. For isolated Chl it has been demonstrated that the 9-keto C=O vibration was essentially insensitive to the labeling of the centrally located nitrogen atoms (9). On the other hand, the coupling between the C=O and N-H modes within the peptide bond leads to a small downshift ($1\text{-}3\text{ cm}^{-1}$) of the amide I mode upon ^{15}N labeling (22). Therefore, the $\sim 1\text{-}2\text{ cm}^{-1}$ downshift upon global ^{15}N labeling of the $1651(+)/1642(-)\text{ cm}^{-1}$ differential signal in the $P700^+/P700$ FTIR spectrum of the triple mutant (Fig. 6) preferentially indicates a protein conformational change rather than a contribution from the 9-keto C=O group of a sub-population of P_A . This conclusion reinforces our earlier observation (16) that it was somewhat hazardous to assign the differential signal centered around 1645 cm^{-1} in the $P700^+/P700$ FTIR spectrum of wild type to the 9-keto C=O of P_A solely on the basis of the effect of mutations (17). It is interesting to note that global ^{15}N labeling also elicits a small effect on the large $P700^+/P700$ bands located around $1680\text{-}1690\text{ cm}^{-1}$ (Figure 5). Comparable effects have been detected previously for wild-type (9). It is therefore likely that the positive band at 1688 cm^{-1} in $P700^+/P700$ FTIR spectra of both the mutants and the wild type contains some contributions from protein amide I modes. This proposal appears highly probable in view of the existence of a sizeable contribution from amide II modes (Figure 5). Additional contributions from protein modes that are sensitive to photooxidation of P700 and that differ between wild type and mutants are probably responsible for the differences seen around $1660\text{-}1670\text{ cm}^{-1}$ in the $P700^+/P700$ FTIR difference spectra of both the wild type and the mutants (Figures 3 and 4).

When comparing the P700⁺/P700 FTIR spectra of the single T(A739)F mutant (Figure 3b) and of the triple mutant (Figure 4b), the bands assigned to the P_A⁺/P_A vibrations of the 9-keto C=O group are found at identical frequencies at 1688/1676 cm⁻¹ in both mutants. Similarly, when the hydrogen bonding Thr residue A739 in *C. reinhardtii* is replaced by the non hydrogen bonding residues Val (17) or Ala (18), the P_A⁺/P_A 9-keto C=O vibrations are observed at 1688/1672 cm⁻¹. The corresponding frequencies for the bands assigned to P_B⁺/P_B 9-keto C=O vibrations are 1718/1698 cm⁻¹. For the 9-keto C=O group of Chl⁺/Chl in tetrahydrofuran, the corresponding values are 1718/1693 cm⁻¹ (11). The ~20-30 cm⁻¹ frequency downshift observed for the P_A⁺/P_A 9-keto C=O vibrations in the mutants compared to P_B⁺/P_B or to Chl⁺/Chl in solution suggests that the 9-keto C=O group of P_A and P_A⁺ is in hydrogen bonding interaction with a water molecule in the T(A739)F mutant of *Synechocystis* and the T(A739)V and T(A739)A mutants of *C. reinhardtii*. In the case of the triple mutant of *Synechocystis*, it is also possible that the hydrogen bond donor is the OH side chain of the introduced Tyr residue.

Finally, for the triple mutant, the observation that the mutations introduced at the two sites in addition to Thr A739 have no effect on the 9-keto C=O mode of P_A is consistent with the X-ray model that shows Thr A739 as the only residue in hydrogen bonding interaction with the 9-keto C=O mode of P_A (10). Introducing other amino acid side chains at the Thr A739 site will be necessary to explore in more details the effect of the strength of hydrogen bonds and the polarity of the local environment on the IR frequency of the 9-keto C=O mode in P_A and P_A⁺ and to compare it to the corresponding frequencies of 1698 and 1718 cm⁻¹ for P_B and P_B⁺, respectively.

Effect of the Triple Mutation on the 10a-ester C=O Vibrations of the PsaA Chl of P700. The observation that neither the single T(A739)F mutation nor the triple mutation perturbs the 1754(+)/1749(-) cm⁻¹ differential signal present in the spectrum of wild type (Figure 3b) provides further support to our previous assignment of this band to the 10a-ester C=O group of P_B that is free from hydrogen bonding interaction (6,9). The T(A739)F mutation has very little impact on the P700⁺/P700 FTIR absorption changes assigned to the C=O ester vibrations of the Chl of P700 (Figure 3). This is taken to indicate that the water molecule H₂O-19, which is held by several residues, including Thr A739, and is proposed to

be the hydrogen bond donor to the bridging oxygen of the 10a-carbomethoxy group of P_A , is probably still present in the single T(A739)F mutant. It is possible that the minute upshift upon the T(A739)F mutation of the small differential signal at 1735(-)/1730(+) cm^{-1} in the $P700^+/P700$ spectrum of wild type (Figure 3) results from a minor displacement of H_2O -19. On the other hand, the spectrum of the triple mutant is significantly modified in this frequency range. Notably, a complex set of two negative bands at 1735 and 1726 cm^{-1} with a positive band located in between at 1730 cm^{-1} in the wild type spectrum is strongly affected while a new positive band appears at 1762 cm^{-1} in the triple mutant (Figure 4). These observations clearly show that a perturbed 10a-ester C=O group of P_A absorbing at a frequency lower than that of an unbound Chl 10a-ester C=O group, becomes free of interaction when Tyr A599, Ser A603, and Thr A739 are simultaneously replaced by their PsaB homologues Leu, Gly, and Tyr, respectively. This suggests that in the triple mutant, the H_2O -19 water is either no longer present in the site or, at least, is interacting much less with the 10a-carbomethoxy group of P_A . Previously, a 1740(+)/1733(-) cm^{-1} differential signal in the $P700^+/P700$ FTIR difference spectrum of *Synechocystis* at 90 K was assigned to the upshift upon photooxidation of the 10a-ester C=O group of P_A (6,9). Recently the same assignment scheme has also been favored in *C. reinhardtii* at ambient temperature (18). At first sight, the frequency upshift of a 10a-ester C=O group upon removal of the hydrogen bonds to water H_2O -19 observed in the present study also appears to support our previous assignment (6,9).

However, the precise assignment of the set of bands observed in the frequency range 1725 to 1745 cm^{-1} still appears problematic, notably in view of the complex hydrogen bond network involving H_2O -19 and of the very peculiar nature and geometry of the hydrogen bond between this water molecule and the bridging oxygen of the 10a-carbomethoxy group of P_A (Figure 2). One difficulty arises from the comparison of the FTIR spectra of the single T(A739)F mutant (Figure 3b) and of the triple mutant (Figure 4b). The two additional mutations, S(A603)G and Y(A599)L, seem to induce primarily a decrease of amplitude of a positive band present at 1731 cm^{-1} in the spectrum of the single mutant and the appearance of a band at 1762 cm^{-1} in the spectrum of the triple mutant. Our previous assignment of the 10a-ester C=O group of P_A (6,9) would have been more consistent with the disappearance or

the perturbation of the wild type 1742(+)/1735(-) cm^{-1} differential signal and the appearance of a differential signal at higher frequency in the spectrum of the triple mutant. One possibility to explain this behavior would be to consider that the response of the 10a-carbomethoxy group to P700⁺ formation is to change its extent of conjugation to ring V, e.g., by changing its orientation with respect to the plane of the Chl macrocycle, and that the interaction with water H₂O-19 modulates this conjugation.

Another difficulty arises from the observation of the small 1730(+)/1726(-) cm^{-1} differential signal in the P700⁺/P700 FTIR difference spectrum of wild type *Synechocystis*. This third set of bands in the region of absorption of the C=O ester vibrations, which is barely noticeable in the 90 K spectra (9), was first ascribed to an unspecified 10a-ester C=O vibration of P700 on the basis of selective isotope labeling (23). A similar feature of small amplitude at 1731(+)/1728(-) cm^{-1} was also observed in the room temperature P700⁺/P700 FTIR difference spectrum of *C. reinhardtii* at 2 cm^{-1} resolution (15) and was recently assigned to the 7c-ester C=O of the PsaA Chl of P700 (18). The absence of significant perturbation of the P700⁺/P700 FTIR spectrum in the frequency range of the Chl ester C=O vibrations in the mutant Y(A731)F (H. Tang; W. Xu, M. P., P. C., and J. B., unpublished results), where the hydrogen bonding interaction with the 7c-ester C=O of P_A in wild type (Figure 2) should be disrupted, shows that such an assignment cannot be made for the equivalent 1730(+)/1726(-) cm^{-1} differential signal in *Synechocystis*.

Effect of the Mutations on the Conformation of the Macrocycle of the P700 Chls. One interesting observation for the P700⁺/P700 FTIR spectra of both the single T(A739)F and the triple mutants is the 2-3 cm^{-1} downshift of the macrocycle C=C marker mode of 5-coordinated Chl at 1608 cm^{-1} (21) compared to wild type. Similar perturbations of these modes have also been noticed in the spectrum of the T(A739)A mutant in *C. reinhardtii* (18). The spectral features assigned to the coupled C-C, C-H, and C-N modes of the Chl macrocycle absorbing between 1400 and 1250 cm^{-1} are also strongly affected by the mutations at the Thr A739 site (Figures 3 and 4). This shows that mutations at Thr A739 have a large impact on the conformation of the Chl ring of P700. Much smaller perturbations of these modes are observed in the mutants on the His axial ligand to P_B (16). It is therefore probable that the strong hydrogen bond between Thr A739 and the 9-keto C=O group of P_A

is responsible for a strain of the Chl macrocycle and that the weakening of this hydrogen bond releases the strain. However, it is noticeable that the conformational change of the macrocycle induced by the T(A739)F mutation has only very little impact on the geometry and hydrogen bonding status of the 10a-ester C=O group of the Chls of P700.

Discussion of the Assignment Scheme of Hastings et al. The assignment scheme for the 9-keto and 10a-ester C=O carbonyls of P700 used in the present study has been originally developed on the basis of a comparison of the P700⁺/P700 and ³P700/P700 FTIR spectra that showed clearly that the 9-keto C=O group of one of the Chl of P700 in *Synechocystis* absorbs at 1637 cm⁻¹ at 90 K (9). The major functional outcome from these FTIR studies was that after photooxidation, the positive charge was essentially delocalized over the two Chl molecules in P700⁺ with a distribution ranging between 1:1 and 2:1 in favor of P_B⁺. In addition, the triplet state in ³P700 was found to be fully localized on P_B (6,9). Both of these conclusions were at variance with those derived from magnetic resonance studies of P700⁺ and ³P700 in wild type and mutant samples which were interpreted to show that both the spin in P700⁺ and the triplet character in ³P700 were essentially localized on P_B (1). This large discrepancy between the interpretation of the results of FTIR and magnetic resonance experiments led Hastings et al. (15) to propose an alternative assignment of bands for the 9-keto C=O groups of the P700 Chls in the P700⁺/P700 FTIR difference spectra of *C. reinhardtii*. The essential difference between the assignments proposed by Hastings et al. (15) and ours (6,9,16) deals with the frequency of the bands of the 9-keto C=O group of P_A in P700 and P700⁺. In the neutral state this C=O group is proposed to absorb at 1697 cm⁻¹ (15) or at 1637 cm⁻¹ (6,9) while in P700⁺ it is found at 1687 cm⁻¹ (15) or at 1656 cm⁻¹ (6,9).

Thus, in the assignment scheme of Hastings et al. (15), the 9-keto C=O group of P_A absorbs at a high frequency (1697 cm⁻¹) characteristic of a carbonyl group in an apolar environment and with no hydrogen bonding interactions. Moreover, the 9-keto C=O group of this Chl is proposed to downshift by 10 cm⁻¹ upon P700⁺ formation. Such a downshift upon cation formation of the frequency of a C=O group conjugated to the ring V of Chl would be unprecedented. The formation of the cation state of BChl (24) or Chl (11) in solution is always accompanied by an upshift of the frequency of the 9-keto and 10a-ester C=O vibrations. Similarly, P⁺ formation in purple bacteria (25), green bacteria (25-27),

heliobacteria (25,28), as well as generation of $P680^+$ in PS II (29,30), is characterized by an upshift of the frequency of the 9-keto and 10a-ester C=O vibrations. Even in the assignment scheme of Hasting et al. (15), the vibrations of the 9-keto C=O group of P_B and of the 10a-ester of both P_A and P_B upshift upon $P700^+$ formation. In order to explain such an unusual behavior of the 9-keto C=O group of P_A , one would probably have to invoke the establishment of an unusually strong hydrogen bond to this group in $P700^+$.

In a more recent study, essentially the same assignment scheme was used to interpret the effect of replacing the Thr A739 residue in hydrogen bonding interaction with the 9-keto C=O group of P_A by an Ala residue in *C. reinhardtii* (18). The impact of the T(A739)A mutation on the bands assigned by Wang et al. (18) to the 9-keto C=O vibration of P_A and P_A^+ is actually very modest as this vibrational mode is proposed to upshift upon mutation by only 4 cm^{-1} from 1695 to 1699 cm^{-1} in P_A and by 2 cm^{-1} from 1686 to 1688 cm^{-1} in P_A^+ (18). A comparison with the corresponding assignments proposed in the present work for wild type and the T(A739)F mutant in *Synechocystis* is given in Table 2. Taking the assignments in Wang et al. (18) at face value, the straightforward interpretation of the 9-keto C=O frequencies proposed for P_A and P_A^+ by Wang et al. (18) would be to consider that this carbonyl groups of P_A is free from bonding interactions in both wild type and mutant and that an unusually strong hydrogen bond to the 9-keto C=O group is present in P_A^+ and is essentially unchanged upon mutation. Such assignments are difficult to reconcile with the presence of the hydrogen bond to the 9-keto C=O group of P_A in the structural model of $P700$ (10). The data in Table 2 can be compared to the other example of the effect of mutations affecting the hydrogen bonding of the 9-keto C=O groups of the primary electron donor on the P^+/P FTIR difference spectra. When the non hydrogen bonding Leu residues M160 and L131 located near the 9-keto C=O groups of P in *Rhodobacter sphaeroides* are replaced by His side chains, the frequency downshift for the bands assigned to the 9-keto C=O groups in the P_L^+/P_L and P_M^+/P_M transitions were found to vary in the range of 20 to 35 cm^{-1} (31). The latter range of values for the mutation-induced frequency shifts is much closer to the 30 - 40 cm^{-1} range corresponding to the assignment scheme reported in the present study (Table 2) than to the 2 - 4 cm^{-1} range proposed by Wang et al. (18). The effect of the T(A739)A mutation in *C. reinhardtii* on the 9-keto C=O vibration of P_B and P_B^+ and on the 10a-ester

C=O modes are either absent or very minor and the corresponding bands keep the same assignments as proposed previously (6,9,18).

The wild type minus T(A739)F mutant double-difference spectrum in *Synechocystis* is dominated by two differential signals of opposite signs at 1660(+)/1637(-) cm^{-1} and 1689(-)/1676(+) cm^{-1} (Figure 3c) which have been assigned in the present work to the 9-keto C=O vibrations of P_A^+/P_A in wild type and mutant. A set of two closely comparable features at 1660(+)/1636(-) cm^{-1} and 1690(-)/1672(+) cm^{-1} also dominates the equivalent double-difference spectrum for the T(A739)A mutation in *C. reinhardtii* (18) and therefore the assignment should be the same for these comparable mutations in the two species. Rather, in the assignment scheme of Hastings and coworkers (15,18), the differential signal at 1654(+)/1637(-) cm^{-1} in the $\text{P700}^+/\text{P700}$ FTIR difference spectrum of wild type is proposed to arise from the imidazole $\text{C}_4=\text{C}_5$ mode from the His axial ligands to the Mg atom of the P700 Chls. The frequency of 1637 cm^{-1} for a $\text{C}_4=\text{C}_5$ imidazole mode coordinated to the Mg atom at N_τ and protonated at N_δ (16) is difficult to reconcile with the usual frequency range of 1606-1593 cm^{-1} established for this mode in 4-methylimidazole (32). Furthermore, the $\text{P700}^+/\text{P700}$ FTIR difference spectrum of *Synechocystis* isotope-edited with uniformly ^{13}C -labeled His has revealed a small band at 1612 cm^{-1} with an amplitude and a position adequate to be identified with the $\text{C}_4=\text{C}_5$ mode from the His axial ligands of P700 (16,32). Therefore, the proposed assignment of the differential signal at 1654(+)/1637(-) cm^{-1} to an imidazole $\text{C}_4=\text{C}_5$ mode (15,18) is incompatible with the present observations. Relevant to this point, in a very recent publication from the group of Hastings (33), the authors have dismissed their previous assignment. Note, however, that they do not provide an alternative assignment for the large differential signal at 1654(+)/1637(-) cm^{-1} in their $\text{P700}^+/\text{P700}$ FTIR difference spectrum of wild type *C. reinhardtii*.

Implications of the FTIR Results for Charge Distribution in P700^+ . The distribution of the positive charge over the two Chls of P700^+ is an important parameter related to the $\text{P700}^+/\text{P700}$ mid-point redox potential, to the charge transfer properties, and, possibly, to the directionality of PS I electron transfer reactions. Besides FTIR difference spectroscopy, ENDOR is the most prominent technique that has been extensively used to address the question of the electronic structure of P700^+ (1,34,35). From the most detailed studies (1), it

has been concluded that P_B carries all or most of the spin density in $P700^+$ while P_A carries no or little (0 to 15%) spin density. Possible explanations for the stringent discrepancy between the rather symmetrical charge distribution in $P700^+$ derived from FTIR spectroscopy and the highly anisotropic distribution of spin density determined by ENDOR have been discussed previously (16). Notably, it was stressed that the conclusion from ENDOR is based essentially on the comparison of the sum of the assigned proton hfcs of three methyl groups of P_A^+ with those in isolated Chl a^+ (12) although the authors of the magnetic resonance studies have provided various reasons why such comparison could be unreliable in the case of $P700^+$ (1,12,17). It has been further proposed that the small amount of electron spin density located on the three assigned methyl groups of P_A^+ , which are not conjugated to the Chl macrocycle, may not be directly related to the average distribution of the unpaired electron between P_A^+ and P_B^+ (16). More recently, semiempirical quantum chemical calculations have been taken to indicate that, owing to spin polarization effects, the spin asymmetry in $P700^+$ could be significantly larger than the charge asymmetry (36).

In the FTIR experiments, the charge density distribution between P_A^+ and P_B^+ has been assessed by the relative amplitudes of the differential signals assigned to the change of bond order of the 9-keto and 10a-ester C=O groups of the two Chls of $P700$ upon photooxidation (6,9). Upon assuming that the extinction coefficients for these groups were comparable for the P_A^+/P_A and P_B^+/P_B transitions, it was concluded that the charge density distribution between P_A^+ and P_B^+ was in the range 1:1 to 2:1 in favor of P_B . This conclusion of a rather symmetrical charge distribution in $P700^+$ has been further supported by an independent FTIR measurement of the relative perturbation of the imidazole $C_5-N\tau$ stretching mode of the His axial ligand of P_A and P_B (16).

In the present study of the Thr A739 mutants, the wild type minus mutant double-difference spectra (Figures 3c and 4c and Table 2) show that the 30-40 cm^{-1} frequency upshift upon mutation of the differential signal assigned to the 9-keto C=O group of P_A^+/P_A affects only marginally the amplitude of this differential signal. The peak to peak amplitude of the P_A^+/P_A differential signal increases by ~5% and ~25% in the triple mutant and the T(A739)F single mutant, respectively. A comparable observation is also valid for the T(A739)A mutation in *C. reinhardtii* (18), provided our assignment scheme is used. In the

spectra of all these mutants, a small decrease by 15-20% of the peak to peak amplitude of the differential signal assigned to the 9-keto C=O group of P_B^+/P_B can be noticed relative to the spectrum of wild type. This may indicate a slight redistribution of the positive charge toward P_A^+ upon Thr A739 mutation. It should also be pointed out that, even after this small mutation-induced redistribution of charge has occurred, the amplitude of the P_A^+/P_A differential signal remains close or somewhat smaller than that of the P_B^+/P_B differential signal. Hence, it can be concluded that the strong hydrogen bond to the 9-keto C=O group of P_A modulates only marginally the distribution of charge in $P700^+$.

In conclusion, the effect of mutations at the Thr A739 site on the $P700^+/P700$ FTIR difference spectra in *Synechocystis* reported here is consistent with the band assignment scheme previously used to interpret the spectra (6,9,16). This observation is strengthened by the results of previous FTIR studies of other mutants at the same site in *C. reinhardtii* by Witt et al. (17) and Wang et al. (18), although in the latter case a very different assignment scheme was used. Therefore, the results derived from the present FTIR study reinforce the view of a strong delocalization of the positive charge over the two Chl molecules in $P700^+$.

ACKNOWLEDGMENTS

The authors thank E. Nábedyk, W. Leibl, H. Tang, and W. Xu for stimulating discussions.

REFERENCES

1. Weber, A. N., and Lubitz, W. (2001). *Biochim. Biophys. Acta*, 1507, 61-79.
2. Hoff, A. J., and Deisenhofer, J. (1997). *Phys. Reports*, 287, 1-247.
3. Mäntele, W. (1993), in *The Photosynthetic Reaction Center* (Deisenhofer, J., and Norris, J. R., Eds), Vol. II, pp 239-283. Academic Press, San Diego.
4. Nábedyk, E. (1996), in *Infrared Spectroscopy of Biomolecules* (Mantsch, H. H., and Chapman, D., Eds), pp 39-81, Wiley-Liss, New York.
5. Breton, J., and Nábedyk, E. (1996). *Biochim. Biophys. Acta*, 1275, 84-90.
6. Breton, J. (2001). *Biochim. Biophys. Acta*, 1507, 180-193.

7. Krauß, N., Schubert, W.-D., Klukas, O. P., Fromme, P., Witt, H. T., and Saenger, W. (1996). *Nature Struct. Biol.*, *3*, 965-973.
8. Redding, K., MacMillan, F., Leibl, W., Brettel, K., Hanley, J., Rutherford, A. W., Breton, J., and Rochaix, J.-D. (1998). *EMBO J.*, *17*, 50-60.
9. Breton, J., Nabdryk, E., and Leibl, W. (1999). *Biochemistry*, *38*, 11585-11592.
10. Jordan, P., Fromme, P., Witt, H. T., Klukas, O., Saenger, W., and Krauß, N. (2001). *Nature*, *411*, 909-917.
11. Nabdryk, E., Leonhard, M., Mäntele, W., and Breton, J. (1990). *Biochemistry*, *3242-3247*.
12. Käss, H., Fromme, P., Witt, H. T., and Lubitz, W. (2001). *J. Phys. Chem. B*, *1* 1225-1239.
13. Krabben, L., Schlodder, E., Jordan, R., Carbonera, D., Giacometti, G., Lee, H., Weber, A. N., and Lubitz, W. (2000). *Biochemistry*, *39*, 13012-13025.
14. Witt, H., Schlodder, E., Teutloff, C., Bordignon, E., Carbonera, D., Niklas, J., and Lubitz, W. (2001), in *PS2001 Proceedings 12th Int. Congr. Photosynthesis*, S6-011, CSIRSO Publishing, Collingwood, Victoria, Australia.
15. Hastings, G., Ramesh, V. M., Wang, R., Sivakumar, V., and Weber, A. (2001). *Biochemistry*, *40*, 12943-12949.
16. Breton, J., Xu, W., Diner, B. A., and Chitnis, P. (2002). *Biochemistry*, *41*, 11200-11210.
17. Witt, H., Schlodder, E., Teutloff, C., Niklas, J., Bordignon, E., Carbonera, D., Kohler, S., Labahn, A., and Lubitz, W. (2002). *Biochemistry*, *41*, 8557-8569.
18. Wang, R., Sivakumar, V., Li, Y., Redding, K., and Hastings, G. (2003). *Biochemistry*, *42*, 9889-9897.
19. Xu, W., Chitnis, P., Valieva, A., van der Est, A., Pushkar, Y. N., Krzystyniak, B., Teutloff, C., Zech S. G., Bittl, R., Stehlik, D., Zybailov, B., Shen, G., and Golbeck, J.H. (2003). *J. Biol. Chem.*, *278*, 27864-27875.
20. Sun, J., Ke, A., Jin, P., Chitnis, V. P., and Chitnis, P. R. (1998). *Meth. Enzymol.*, *297*, 124-139.
21. Fujiwara, M., and Tasumi, M. (1986). *J. Phys. Chem.*, *90*, 5646-5650.

22. Noguchi, T., and Sugiura, M. (2003). *Biochemistry*, 42, 6035-6042.
23. Kim, S., and Barry, B. A. (2000). *J. Am. Chem. Soc.*, 122, 4980-4981.
24. Mäntele, W., Wollenweber, A. M., Nabedryk, E., and Breton, J., (1988).. *Proc. Natl. Acad. Sci. U.S.A.*, 85, 8468-8472.
25. Nabedryk, E., Leibl, W., and Breton, J. (1996). *Photosynth. Res.*, 48, 301-308.
26. Noguchi, T., Kusumoto, N., Inoue, Y., and Sakurai, H. (1996). *Biochemistry*, 35, 15428-15435.
27. Mezzetti, A., Seo, D., Leibl, W., Sakurai, H., and Breton, J. (2003). *Photosynth. Res.*, 75, 161-169.
28. Noguchi, T., Fukami, Y., Oh-oka, H., and Inoue, Y. (1997). *Biochemistry*, 36, 12329-12336.
29. Breton, J., Hienerwadel, R., and Nabedryk, E. (1997), in *Spectroscopy of Biological Molecules: Modern Trends* (Carmona, P., Navarro, R., and Hernanz, A., Eds), pp 101-102, Kluwer, Dordrecht, The Netherlands.
30. Noguchi, T., Tomo, T., and Inoue, Y. (1998). *Biochemistry*, 37, 13164–13625.
31. Nabedryk, E., Allen, J. P., Taguchi, A. K. W., Williams, J. C., Woodbury, N. W., and Breton, J. (1993). *Biochemistry*, 32, 13879-13885.
32. Hasegawa, K., Ono, T., and Noguchi, T. (2002). *J. Phys. Chem. A*, 106, 3377-3390.
33. Wang, R., Sivakumar, V., Johnson, T. W., and Hastings, G. (2004). *Biophys. J.*, 86, 1061-1073.
34. Deligiannakis, Y., and Rutherford, A. W. (2001). *Biochim. Biophys. Acta*, 1507, 226-246.
35. Rigby, S. E. J., Evans, M. C. W., and Heathcote, P. (2001). *Biochim. Biophys. Acta*, 1507, 247-259.
36. Plato, M., Krauß, N., Fromme, P., and Lubitz, W. (2003). *Chem. Phys.*, 294, 483-499.

FIGURE LEGENDS

Figure 1. **Molecular structure of Chlorophyll α** (S.I numbering). P_A is the epimer at position C10.

Figure 2. **Structural model of P700, the primary electron donor of photosystem I.** (A) General view along the pseudo- C_2 symmetry axis showing the organization of the dimer of chlorophyll a (P_B) and chlorophyll a' (P_A) with their central Mg atoms coordinated to the side chains of His B651 and His A676, respectively. Also shown are the amino acid residues located in the close vicinity of water H_2O -19 and of the carbonyl groups of P700. Note the residues engaged in putative hydrogen bonds with the carbonyls of P_A and the symmetry-related side chains that appear free from hydrogen bonding interactions with P_B . (B) A different view of the region surrounding the 9-keto and 10a-ester carbonyls of P_A .

Figure 3. **Light-induced $P700^+/P700$ FTIR difference spectrum of PS I complexes from *Synechocystis* sp. PCC 6803 at 5°C.** (a) wild type PS I, (b) mutant T(A739)F. (c) Double-difference spectrum, wild type minus T(A739)F mutant. Each division on the vertical scale corresponds to 5×10^{-4} absorbance unit. About 100000 interferograms added. The frequency of the bands is given $\pm 1 \text{ cm}^{-1}$.

Figure 4. **Light-induced $P700^+/P700$ FTIR difference spectrum of PS I complexes from *Synechocystis* at 5°C.** (a) wild type PS I, (b) a triple mutant containing the T(A739)Y, S(A603)G, and Y(A599)L changes. (c) Double-difference spectrum, wild type minus triple mutant. Each division on the vertical scale corresponds to 5×10^{-4} absorbance unit.

Figure 5. **Light-induced $P700^+/P700$ FTIR difference spectrum of PS I complexes from the triple mutant *Synechocystis* at 5°C.** (a) unlabeled PS I, (b) ^{15}N -labeled PS I. (c) Double-difference spectrum, unlabeled-*minus*- ^{15}N -labeled. Each division on the vertical scale corresponds to 4×10^{-4} absorbance unit.

Figure 6. **Expended view of the spectra of PS I complexes from the triple mutant shown in figure 4.** The traces for unlabeled (continuous line) and ^{15}N -labeled (dotted line) PS I are overlaid in the top part of the figure. The double-difference spectrum, unlabeled-*minus*- ^{15}N -labeled is shown as the bottom trace.

Table 1. Hydrogen Bonding Residues of PsaA (and Homoloques in PsaB) in
Synechococcus elongatus and *Synechocystis* sp. PCC6803*

<i>S. elongatus</i>		<i>Synechocystis</i>	
Tyr A603	Leu B590	Tyr A599	Leu B581
Ser A607	Gly B594	Ser A603	Gly B585
Thr A743	Tyr B727	Thr A739	Tyr B718

*Based on the 2.5 Å crystal structure of PS I in *S. elongatus* by Jordan et al. (9).

Table 2. Approximate Frequencies (cm^{-1}) of the P700⁺/P700 Bands Assigned to the 9-keto C=O Carbonyls of P_A and P_B in Wild Type and Thr A739 Mutants by Wang et al., (18) and in this Work

	Wang et al., (18)		This work	
	WT	T(A739)A	WT	T(A739)F
P _A	1695	1699	1637	1676
P _A ⁺	1686	1688	1660	1689
P _B	1704	1704	1698	1698
P _B ⁺	1716	1713	1718	1717

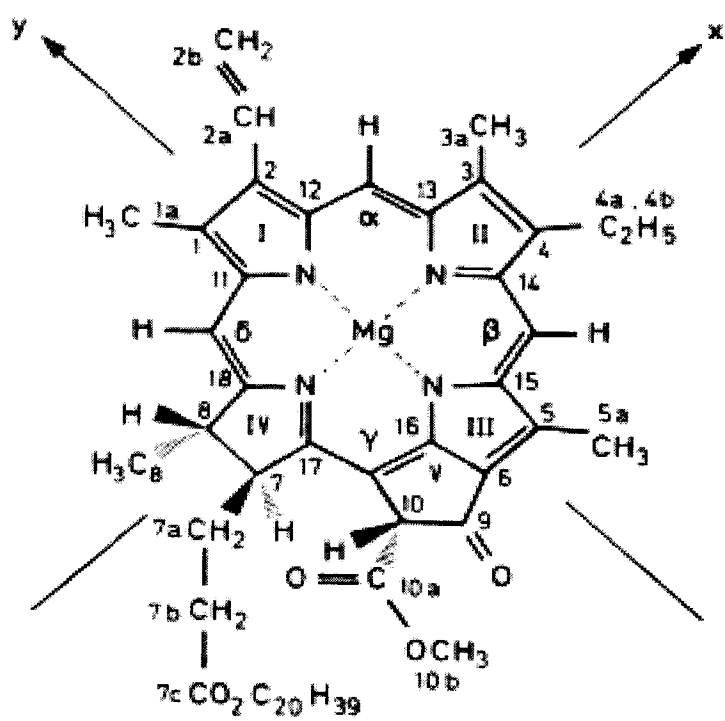


Figure 1

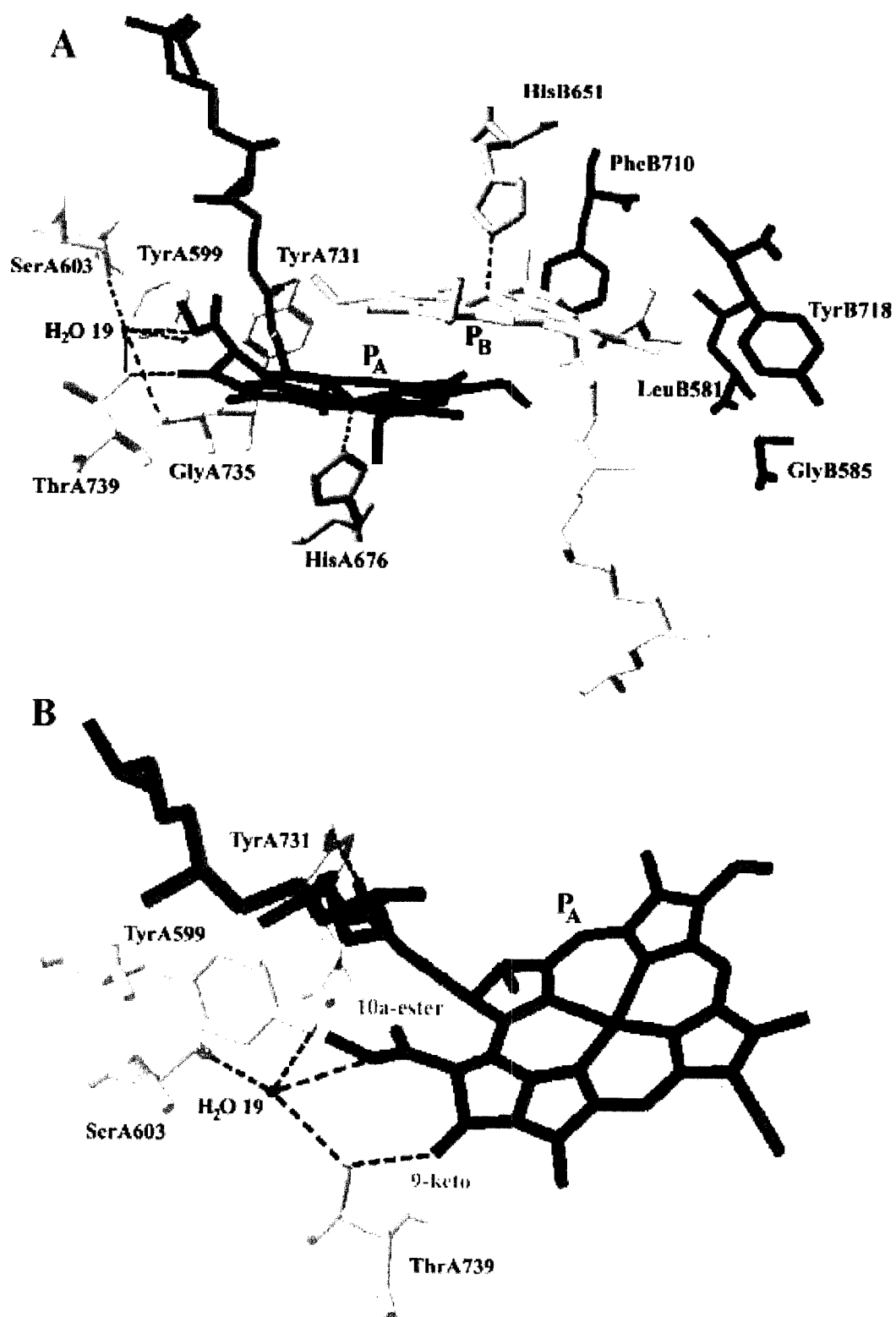


Figure 2

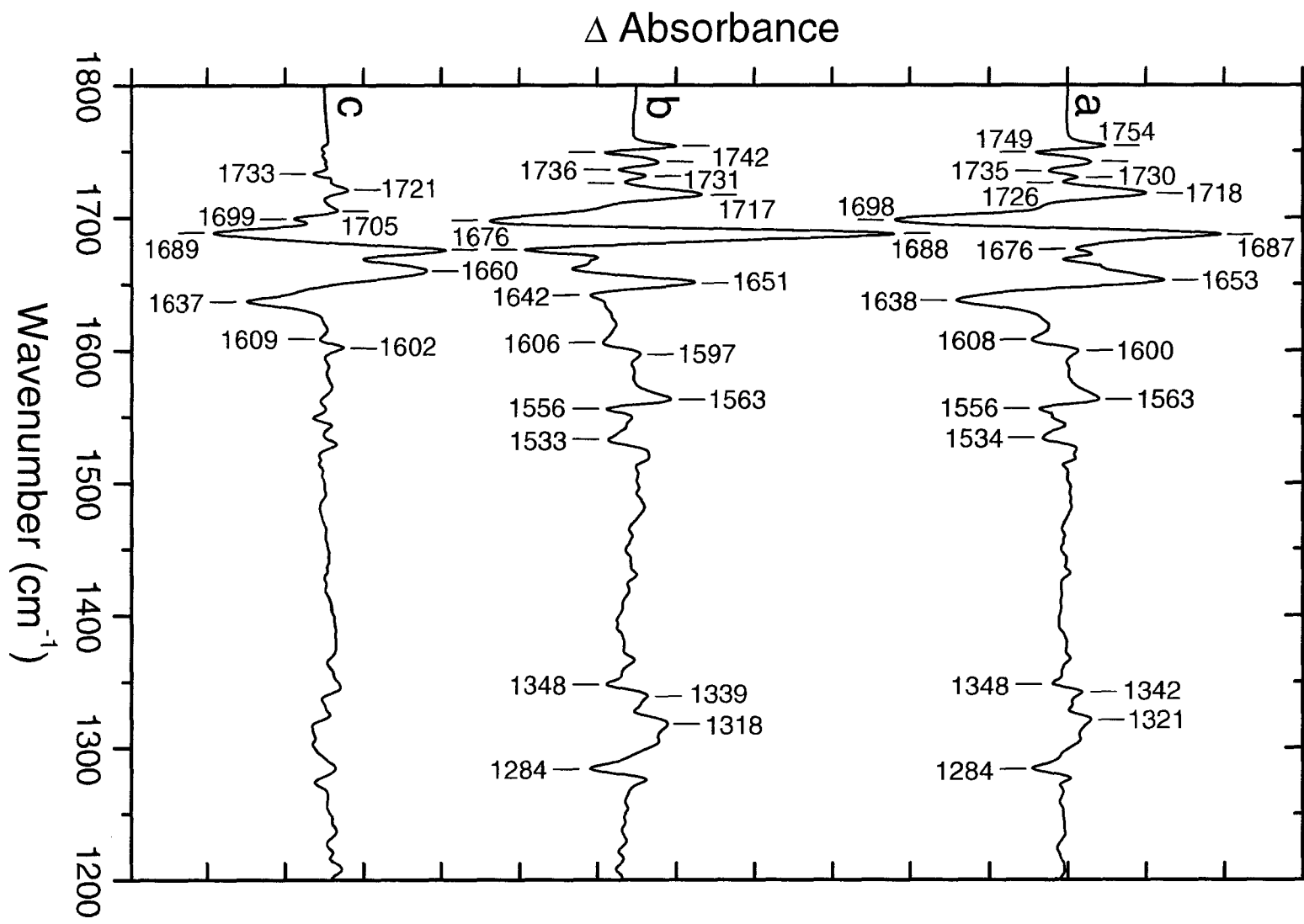


Figure 3

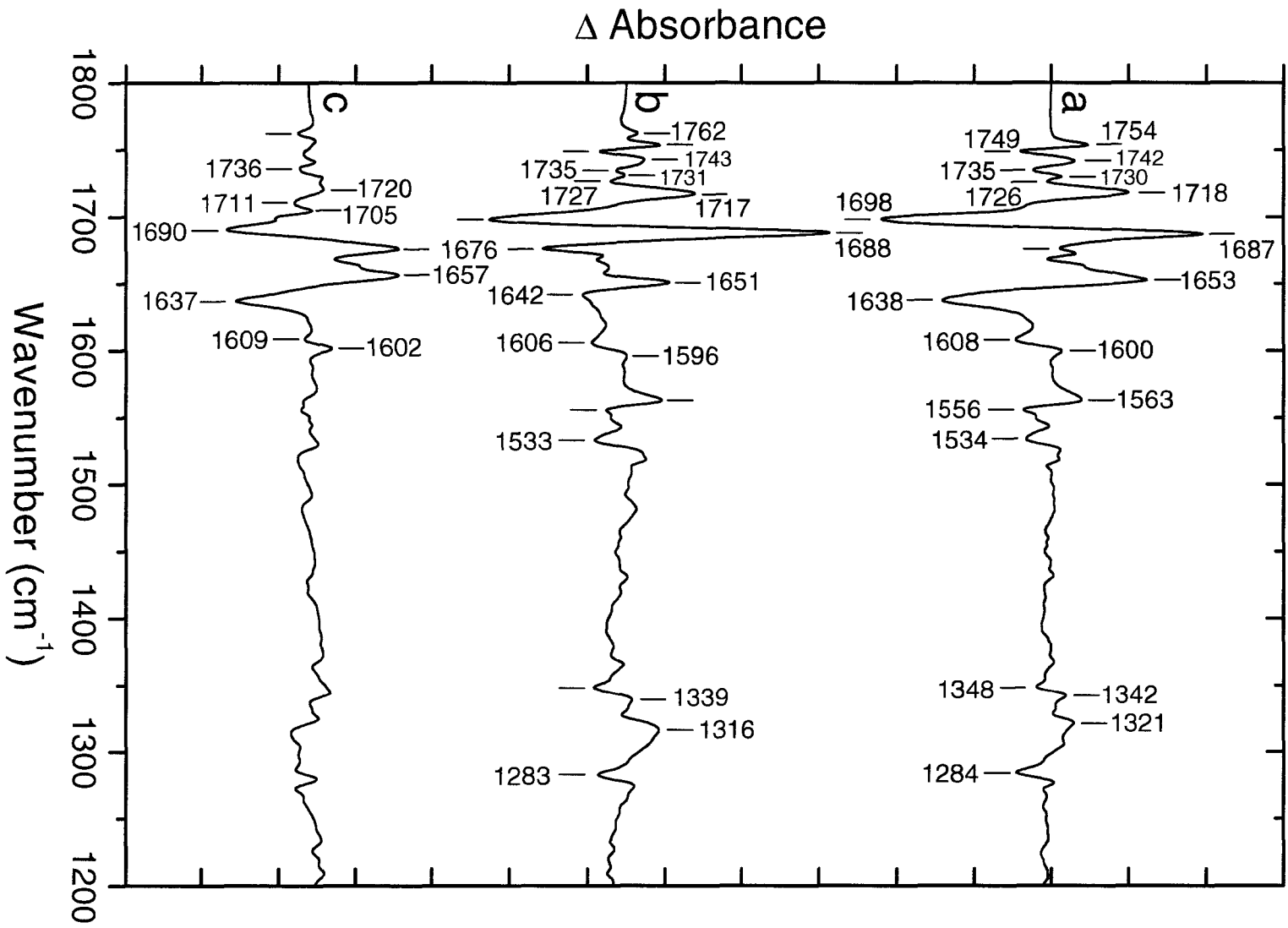


Figure 4

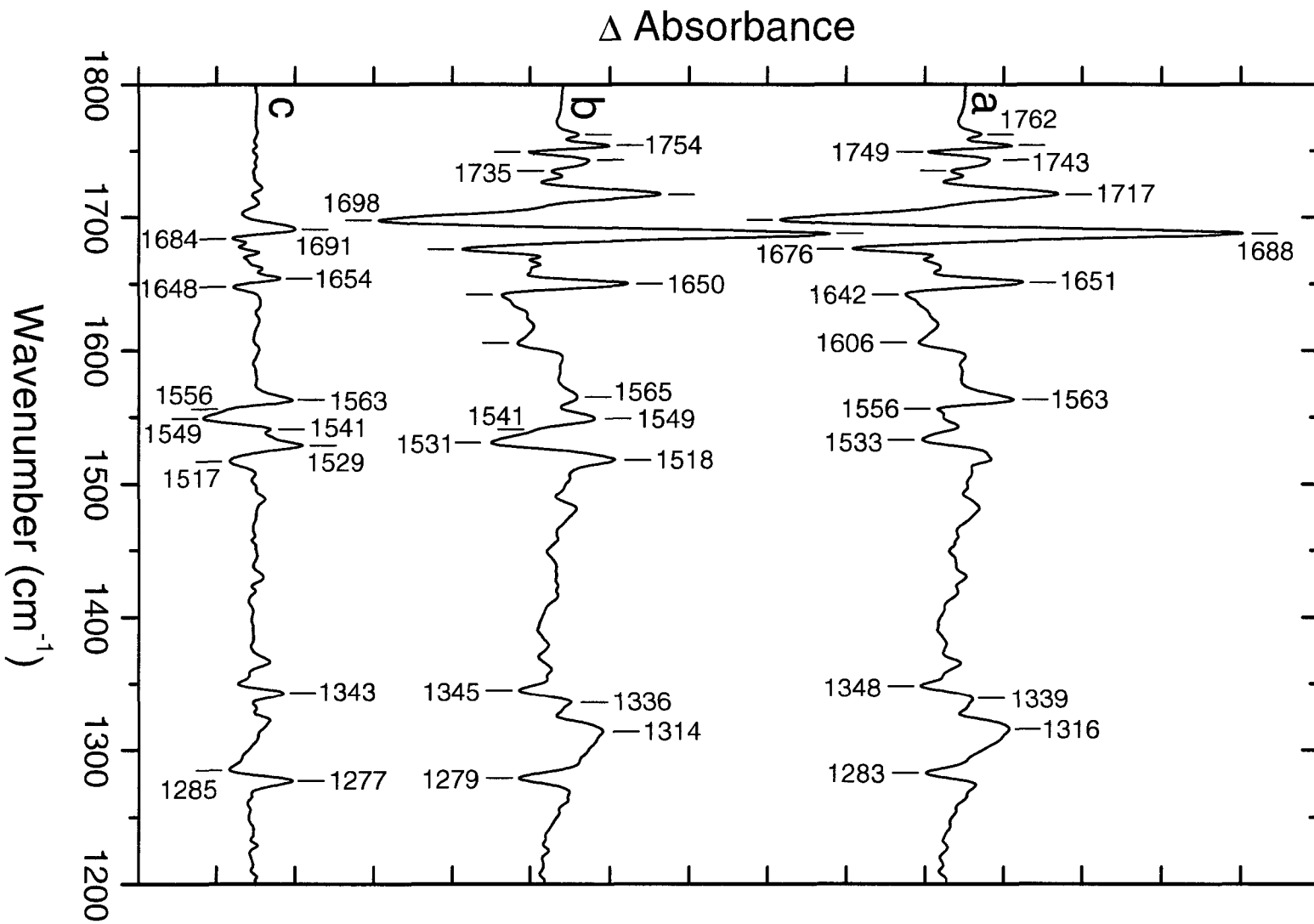


Figure 5

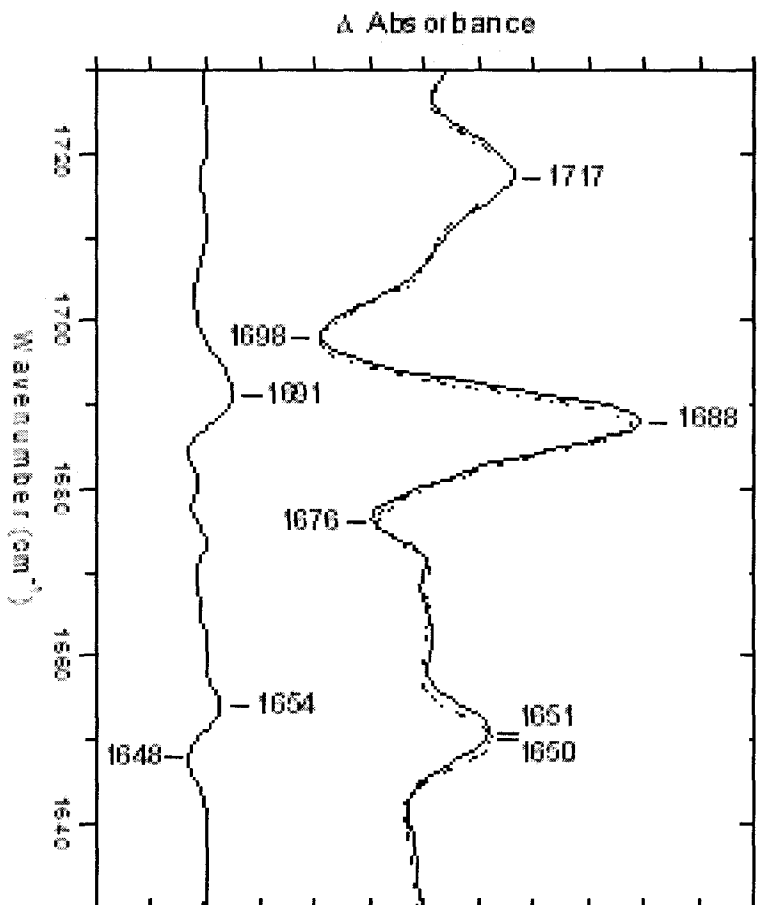


Figure 6

**CHAPTER 4. SITE-DIRECTED MUTAGENESIS OF AMINO ACIDS IN PsaB
SURROUNDING THE PRIMARY ELECTRON DONOR
OF PHOTOSYSTEM I^{1*}**

A paper to be submitted to *Biochemistry*

Maria Pantelidou, Tanya Konovarova, Kevin Redding, Jacques Breton, Parag R. Chitnis^{2**}

ABSTRACT

P700, the primary electron donor of photosystem I (PSI), is a chlorophyll heterodimer composed of chlorophyll α (Chl α) and chlorophyll α' (Chl α'), the epimer at the 13² position. Chl α' is hydrogen bonded to several amino acids of PsaA. These hydrogen bonds are not present in the PsaB half of the dimer, and the homologous positions in PsaB are occupied by different amino acids. We used site-directed mutagenesis in *Synechocystis* sp. PCC 6803 to study the effects of the absence of the hydrogen bonds of P700 with PsaB, by mutating the residues in PsaB with the respective homologues in PsaA. All mutants could grow photoautotrophically. Fourier transform infrared (FTIR) spectroscopy was used to study the protein-cofactor interactions in PSI of the mutants. The (P700⁺-P700) difference spectra of our double (PsaB L581Y/G585S) and triple mutant (PsaB L581Y/G585S/Y718T), suggested an insertion of a hydrogen bond to the 13¹-keto C=O of Chl α , with the other side of the dimer (Chl α') still hydrogen bonding to PsaA. The electronic structure of P700⁺ in our mutants was studied by electron nuclear double resonance (ENDOR) spectroscopy. In this study, the hfcs of the methyl protons at positions 2, 7 and particularly 12 of the double mutant Chl α were increased, revealing an even more asymmetric electron spin distribution, with a shift towards B side Chl α . However, the ENDOR spectra of the triple mutant, which has the additional Tyr718 to Thr mutation, showed only a slight increase in hfcs of the methyl protons at positions 2 and 7 and those assigned to position 12, were unchanged. An

¹ This work was supported by a grant from US National Science Foundation (MCB 0078268)

² To whom correspondence should be addressed. Tel: 703-292-7132; Fax: 703-292-9061; Email: pchitnis@nsf.gov

introduction of a hydrogen bond at this site, observed by FTIR, is expected to stabilize the ground state and thus decrease the electron spin density above Chl α . ENDOR spectroscopy, however, gives the opposite result. We therefore conclude that other factors, such as the induced polarity of the environment, also influence the electron spin localization in the heterodimer of our mutants.

INTRODUCTION

Cyanobacteria, algae and green plants, utilize two reaction centers, photosystem I (PSI) and photosystem II (PSII). In PSI, an electron is transferred from plastocyanin on the luminal side of the thylakoid membrane, to ferredoxin on the stromal side (1). The X-ray crystallography of PSI in cyanobacteria has given a great deal of information about its structure (2). It is composed of 12 subunits (Psa A, B, C, D, E, F, I, J, K, L, M and X), 96 chlorophyll α molecules, 22 beta-carotenes, two phylloquinones and three iron-sulfur clusters. The two largest subunits, PsaA and PsaB, are related by a pseudo-C2 symmetrical axis. The five carboxy-terminal helices of PsaA and PsaB subunits form two semicircles and symmetrically engulf the cofactors of the electron transfer chain (ETC) cofactors (3). These cofactors consist of a) the primary electron donor of PSI, which is a chlorophyll pair called P700, b) the primary acceptor A₀ (another chlorophyll pair), c) a phylloquinone pair and d) the three [Fe₄S₄] clusters. According to the crystal structure, another chlorophyll pair is present between P700 and A₀ but its participation in the electron transfer is not certain (3). The electron transfer process starts when the antenna chlorophylls of PSI harvest the energy from photons and transfer it to P700. P700 is first excited to P700* and then becomes oxidized (P700⁺) upon electron transfer to A₀. The electron is then transferred to the phylloquinone and then to three iron-sulfur clusters F_X, F_A and F_B. Finally, after reduction of ferredoxin, the electron reaches NADP⁺ reductase at the stromal (cytoplasmic) side of the membrane. P700⁺ goes back to its ground state by uptaking an electron from plastocyanin (1).

P700, A₀, and the two phylloquinones are pairs forming two structurally symmetric branches, A and B. These branches are related by the same pseudo-C2 symmetry, and interact with PsaA and PsaB symmetrically (1). The issue of directionality of electrons along

one or both the two branches of the ETC, has been under investigation in the past years (4 for rev.). Electron paramagnetic resonance (EPR) and electron nuclear double resonance (ENDOR) spectroscopy studies on point mutants of the phylloquinone pockets argue that the electron transfer chain is unidirectional, primarily along PsaA (5-7). Optical studies on the reoxidation of phylloquinone support that both branches are involved in electron transfer but A branch is mostly active (8). P700, the primary electron donor of PSI, can possibly have a great contribution in the directionality of electron flow. This chlorophyll dimer is characterized by an asymmetry in both its structure and the interaction to its environment.

According to Jordan et al. (2), the two chlorophylls molecules forming P700 are positioned perpendicular to the membrane plane and parallel to each other with an interplanar distance of about 3.6Å. The chlorin planes overlap only at the A and B rings, and they are both coordinated through their Mg²⁺ ions to histidine (His) residues on PsaA and PsaB (2). Both chlorophylls are chlorophyll α molecules (Chl α), but the one coordinated by PsaA (called Chl α') is the C13² epimer of Chl α (Figure 1). PsaB, on the other hand, coordinates Chl α , the other half of P700 (Chl α' and Chl α will be used to distinguish the two chlorophyll molecules). Subunits PsaA and PsaB interact with Chl α' and Chl α , respectively, in a similar way, except for the presence of a hydrogen bonding network on A side. As shown in Figure 2, Thr at PsaA 739 (numbering will be according to *Synechocystis*), is capable of donating a hydrogen bond to the 13¹ keto oxygen the Chl α' and to a water molecule. This water molecule forms a hydrogen bond to the bridging oxygen of the 13² carbomethoxy group of Chl α' . It also hydrogen bonds with the following surrounding residues: Ser A603, Tyr A599 and Gly A735. The Tyr A731 is also within hydrogen bond distance with the phytyl ester-carbonyl oxygen of Chl α' . The homologous positions on PsaB are occupied by different amino acids that do not form hydrogen bonds with Chl α (see Figure 2). The hydrogen bonds are thought to stabilize the ground state and thus increase the redox potential of P700/P700⁺ (9). The absence of this bonding pattern between Chl α and PsaB, results in a significant asymmetry in the environment of P700. The interaction of P700 with the surrounding environment affects the dimer's biophysical properties.

P700 could play a key role in the directionality of electron transfer along the two branches of the ETC and therefore the electronic structure of P700 has been studied

extensively in the past years. Fourier transform infrared (FTIR) difference spectroscopy, measures a more equally distributed positive charge over the two chlorophylls of P700⁺ with ratios of 1:1 or 2:1, favoring B-side Chl α (11). However, ENDOR and EPR studies, have shown that the electron spin distribution over P700⁺, is asymmetrical, favoring the PsaB coordinated chlorophyll (Chl α) by ratios \geq 4:1 (10 for rev.). In this study, we investigated whether the asymmetry in the P700-protein interaction, affects the biophysical properties of P700. Site-directed mutagenesis was used in order to mutate PsaB amino acids in *Synechocystis* sp. PCC 6803, to the respective hydrogen bonding residues of PsaA. The mutants generated are: PsaB L581Y/G585S/Y718T triple mutant, PsaB L581Y/G585S double mutant and the single mutant, PsaB F710Y (see Figure 2). The changes in protein-cofactor interactions in PSI were studied by FTIR difference spectroscopy. The electronic structure of the P700⁺ in the triple mutant was also investigated by ENDOR spectroscopy.

EXPERIMENTAL PROCEDURES

Site-directed mutagenesis. The donor plasmid pGEM-3C+ was used for creating mutations. This plasmid contains the C-terminal region of the *psaB* gene, resistance genes for chloramphenicol and ampicillin, and a 760 bp region down stream of the *psaB* gene (5). The site-specific mutations on PsaB were made using the polymerase chain reaction (PCR) method with the *Platinum Pfx polymerase* (Invitrogen) and pGEM-3C+ as a template. The mutagenic primers used are listed in Table 1. The unmethylated (mutation-containing) DNA was selected by digestion with DpnI endonuclease (Promega). The mutated plasmids were checked by DNA sequencing and were used to transform the recipient strain, PCRT Δ B. In this strain, an 1176-bp region of the *psaB* gene (corresponding to the C-terminal half of the protein) is replaced by the kanamycin-resistance cassette. The transformants were selected and segregated for several generations on chloramphenicol supplemented BG11 plates under low light intensity (2-3 $\mu\text{moles m}^{-2}\text{s}^{-1}$) at 30 °C (12). The cells were also tested for growth on Kanamycin supplemented BG11 plates in order to ensure that this resistance is no longer expressed. The genomic DNA was then extracted from these cells as previously described (13). The DNA fragment that contains the site-specific mutations was amplified by PCR and sequenced.

Cell growth and chlorophyll content. To measure growth rates of *Synechocystis* sp. PCC 6803 wild type and mutant strains, the cultures were grown in BG11 medium (14) to late exponential phase (0.7- 1.0 OD₇₃₀) at 30 °C. The cells were centrifuged at 4000 x g and washed twice by resuspension in BG11 medium. The 50ml-cultures were started with an initial concentration of 0.1 OD₇₃₀ and constant shaking at 140 rpm under low light (5-10 $\mu\text{mol photons m}^{-2}\text{s}^{-1}$), normal light (40-50 $\mu\text{mol photons m}^{-2}\text{s}^{-1}$) and high light (90-100 $\mu\text{mol photons m}^{-2}\text{s}^{-1}$). For photoheterotrophic growth, the cultures were supplemented with 5mM glucose. The mutants were supplemented with 30mg/L chloramphenicol. Growth rates were monitored by absorbance measurements at 730nm (A_{730}) with a UV-160U spectrophotometer (Shimadzu, Tokyo, Japan). Total chlorophyll content in the cells was performed by extractions with 100% methanol as previously described (15).

PSI trimer isolation. For extraction of thylakoid membranes, cells were grown in large quantities in BG11 medium, in the presence of glucose (5mM) at normal light intensity to 1.0 OD₇₃₀. The cells were harvested and resuspended in SMN solution (0.4 mM sucrose, 10mM NaCl and 50 mM MOPS, pH 7.0). Thylakoid membrane extraction and isolation of PSI particles was performed according to previously published methods with minor alterations (16). Chlorophyll content determination in the membranes with 80% acetone was carried out as described previously (17). For isolation of PSI complexes the membranes (containing 6mg Chl) were incubated in SMN buffer with 10mM CaCl₂ for 0.5 hr, at room temperature in the dark, in order to promote trimerization. For solubilization, n-dodecyl- β -D-maltoside (DM) was added (1.5% final concentration) to the membranes, and the sample was incubated for 15 min in the dark on ice. The non-solubilized material was removed by centrifugation at 20,000 x g for 15 min and the photosynthetic complexes were separated with a 10 to 30% gradient of sucrose with 0.05% DM in 10mM MOPS, pH 7.0, by ultracentrifugation (160,000 x g) for 18 hrs at 4°C. The band containing the PSI trimers was collected, concentrated to 1mg Chl/ml and stored in -20°C.

FTIR difference spectroscopy. Samples for FTIR were prepared by centrifugation (300000 x g for 60 min) of PS I trimers in Tris-HCl buffer (70mM; pH 7.0) containing 80 mM potassium ferrocyanide and 20 mM potassium ferricyanide. A small fraction of the resultant pellet was squeezed between two calcium fluoride windows and the thickness of the

sample was adjusted to give an absorption of about 0.8 OD unit at the maximum around 1650 cm^{-1} with approximately half of this absorption being due to the amide I absorption and the other half to the scissoring mode of water. Light-induced difference spectra were recorded on Nicolet 60SX and 860 FTIR spectrometers at a temperature of 5°C and at a resolution of 4 cm^{-1} as previously reported (11).

ENDOR Spectroscopy. PSI trimers (~0.2mg Chl) were placed in standard 4mm Suprasil quartz EPR tubes and illuminated with a white 200 W lamp for ~10sec. The light was passed through a 20-cm water filter before it reached the sample. The trimers were frozen at 77K while under illumination. ENDOR spectra of P700⁺ in samples were obtained by standard techniques on a Bruker ESP 300E EPR spectrophotometer equipped with a DICE ENDOR ESP 350 system and a Bruker ER4111 temperature controller at 120K (Mod. Freq. =12.5 kHz).

RESULTS

Physiological characterization of the mutants. The altered DNA fragments in the mutants were amplified by PCR and the mutations were confirmed by sequencing. The mutants do not show any resistance to Kanamycin and are able to grow with the absence of glucose (photoautotrophically). Single mutant PsaB F710Y does not show any changes in growth or chlorophyll content, compared to the wild type. The doubling times and chlorophyll contents obtained from the triple mutant PsaB L581Y/G585S/Y718T and the wild type are shown in Table 2. The chlorophyll content in this mutant is decreased from ~3.83 to ~2.98 $\mu\text{g Chl/OD}_{730}/\text{ml}$ in comparison to the wild type. Growth of the triple mutant is not severely altered, although doubling times are slightly increased under all conditions.

P700⁺-P700 difference spectra. Vibrational spectroscopy is a technique used for obtaining bonding information of P700 with its surrounding protein environment. Bands at 1600-1800 cm^{-1} region of the FTIR (P700⁺-P700) difference spectra, are due to vibrational modes from the C=O groups in chlorophyll. The negative bands (-) and the positive bands (+) are associated with the neutral and oxidized state of the dimer. According to the assignments from Breton et al. (11,18), negative bands at ~1638 and 1698 cm^{-1} have been assigned to the 13¹ keto C=O vibrations for Chl α' and Chl α respectively. Upon conversion

to P700⁺, these are represented by positive bands at ~1653 and 1718 cm⁻¹ (11,18). The FTIR (P700⁺-P700) difference spectra of the double (PsaB-L581Y/G585S) and triple mutant (PsaB L581Y/G585S/Y718T), reveal changes in the bonding pattern of Chl α with the protein.

Figure 3 shows the (P700⁺-P700) difference spectra from wild type and the PsaB triple mutant PSI samples. In the 1720-1630 cm⁻¹ spectral range of the difference spectra from the mutant, the positive peak at 1718 cm⁻¹, representing the Chl α ⁺ 13¹ keto C=O vibrations, is reduced by ~30%. Moreover, this signal is slightly upshifted by 1-2 cm⁻¹. The reduced state, represented by signal at 1698(-) cm⁻¹, is also reduced in the mutant but to a less extent. Moreover, a strong negative peak appears at 1668 cm⁻¹ and the positive signal at 1687 cm⁻¹, also present in the wild type, increases. These changes provide evidence that the 13¹ keto C=O vibrations of Chl α are affected by the mutations. The reduced signal at 1718(+)/1698(-) cm⁻¹ and the appearance of the 1687(+)/1668(-) cm⁻¹ could possibly be a result of a partial (30%) hydrogen bonding formation of the protein to the 13¹ keto C=O of Chl α . The 1653(+)/1638(-) difference signal, representing the 13¹ keto C=O vibrations from the oxidized and reduced states of Chl α ', does not exhibit any changes.

Differences are also observed in the 1720-1750 cm⁻¹ region of the spectra. Signals at 1742(+)/1735(-) cm⁻¹ and 1754(+)/1749(-) cm⁻¹ have been assigned to vibrational modes of the C=O of the 13² carbomethoxy group of Chl α ' and Chl α respectively (11,18). According to Figure 3, the triple mutant shows changes in the 13²-keto C=O vibrational modes of Chl α as well. Specifically, the 1754(+)/1749(-) cm⁻¹ difference signal is upshifted by 3 cm⁻¹. This indicates an increase in the freedom of vibration of C=O of the 13² carbomethoxy group in Chl α . On the contrary, the signals related to Chl α ' at this region, remain the same as in the wild type.

The P700⁺-P700 difference spectra from the wild type and the double mutant (PsaB-L581Y/G585S), are shown in Figure 4. This mutant is genetically identical to the triple mutant except for the absence of the Y718T substitution. In comparison to the wild type, the spectra of the triple mutant show exactly the same changes as the triple mutant, suggesting that the additional mutation at Tyr PsaB718 has no detectable effect on the bonding interaction of the cofactor with the protein.

Unlike the double and triple mutants, the FTIR spectra of the single mutant PsaB F710Y, shows no significant differences in comparison to the wild type (Figure 5). According to Breton et al. (11,18), the vibrational modes of the phytol ester carbonyl oxygen cannot be detected in the 1600-1800 cm^{-1} region. The data, however, can be used as evidence that, mutation PsaB F710Y does not affect the bonding patterns of ^{13}C keto C=O bond and the C=O of the ^{13}C carbomethoxy group.

ENDOR spectra of P700⁺. The ^1H -ENDOR spectra of P700⁺ can provide information on the electronic structure of P700 (10). Based on experiments done with $\text{Chl}\alpha^+$ in organic solvents, PSI in single crystals or PSI isolated from mutants, the hyperfine couplings (hfc) obtained in these spectra have been assigned to specific protons in P700 (19-21). Figures 6 and 7 show the signal splittings represented in line pairs of the double (PsaB L581Y/G585S) and triple mutant (PsaB L581Y/G585S/Y718T) in comparison to the wild type, respectively. Unfortunately, other than the line pairs 1'/1 and 2'/2, no more splittings have been detected and assigned to the low spin carrying $\text{Chl}\alpha'$ (19,21). Line pairs 3'/3 and 5'/5 are assigned to the perpendicular and parallel hyperfine tensor components of the methyl protons at position 2 of the spin carrying $\text{Chl}\alpha$. Line pairs 4'/4 and 6'/6 are assigned to the methyl protons at position 7 and the splittings at 7'/7 and 8'/8 are assigned to the 12-methyl protons. The hfc are also summarized in Table 3. According to the ENDOR spectra in Figure 7, obtained from the triple mutant PSI, the parallel hyperfine tensor components of the methyl protons at position 2 of $\text{Chl}\alpha$ increase by 0.52 MHz. Moreover, the perpendicular components of the protons at positions 7 slightly increase and the 2'/2 splittings assigned to $\text{Chl}\alpha'$, show a decrease of 22 MHz. The changes in the ENDOR spectra of the double mutant, in comparison to the wild type, are more dramatic. According to figure 6, the parallel and perpendicular hfc of the methyl protons at positions 2, 7 and 12 of $\text{Chl}\alpha$ all increase in the double mutant. The most significant increase is for line pairs 5'/5, 7'/7 and 8'/8. However, the $\text{Chl}\alpha'$ splittings, 1'/1 and 2'/2, do not show any significant change. This result suggests an effect on the electron spin distribution in P700⁺ upon PsaB mutations, with a stronger spin localization on $\text{Chl}\alpha$.

DISCUSSION

According to the crystal structure of *Synechococcus elongatus*, P700 is a heterodimer composed of Chl α and Chl α' , the 13² epimer of Chl α (2). Figure 2 shows the protein interaction of the two Chl molecules with PsaA and PsaB. PsaA forms hydrogen bonds directly or through a water molecule to the E ring of Chl α . The homologous residues in PsaB do not form such bonds. It has been suggested that this asymmetry in protein-cofactor interaction might influence the biophysical properties of P700 (9, 10). Specifically, the electron spin density localized over the heterodimer has been reported to be asymmetric favoring Chl α (10 for rev.). In this study, we have used site-directed mutagenesis in PsaB of *Synechocystis* sp. PCC 6803, to introduce amino acids that are capable of a hydrogen bonding interaction. In order to achieve symmetry in the protein environment of Chl α and Chl α' , the choice of mutations were based on the respective hydrogen bonding amino acids in PsaA. Three mutants were generated: PsaB L581Y/G585S/Y718T triple mutant, PsaB L581Y/G585S double mutant and the single mutant, PsaB F710Y.

Protein-cofactor interactions determined by FTIR Spectroscopy. FTIR difference spectroscopy was used in order to study changes of cofactor-protein binding interactions in the mutants and the presence of any possible formation of hydrogen bonds between PsaB and Chl α . The (P700⁺-P700) difference spectra give signals due to the vibrational modes from the 13¹ keto C=O and the C=O of the 13² carbomethoxy group of both Chl α' and Chl α . According to the assignments of Breton et al., (18) signals at ~1653(+)/1638(-) and 1718(+)/1698(-) cm⁻¹ in the wild type (P700⁺-P700) difference spectra, have been assigned to the 13¹ keto C=O vibrations for Chl α' and Chl α , respectively (positive and negative signals associated with oxidized and reduced states respectively). In addition, signals at 1742(+)/1735(-) cm⁻¹ and 1754(+)/1749(-) cm⁻¹ have been assigned to vibrational modes of the C=O of the 13² carbomethoxy group of Chl α' and Chl α respectively.

(P700⁺-P700) difference spectra from PSI particles of the double mutant PSI is compared to wild type in Figure 4. The positive peak at 1718 cm⁻¹, representing the Chl α' 13¹ keto C=O vibrations is reduced by ~30% in the mutant and slightly upshifted by 1-2 cm⁻¹. The reduced state, represented by signal at 1698(-) cm⁻¹, is also decreased but to a less extent. An increase of the positive signal at 1687 cm⁻¹ and the appearance of a new negative

signal at 1668 cm^{-1} are also observed in the spectra. A possible interpretation of the above change, is the existence of a heterogeneous population of the $\text{Chl}\alpha/\text{Chl}\alpha^+$. A fraction of ~70% still has a free 13^1 keto $\text{C}=\text{O}$ absorbing like in WT, while the remaining ~30% absorbs around $1687(+)/1668(-)\text{cm}^{-1}$ due to hydrogen bonding at this position. This hydrogen bonding could originate from (a) the side chain of the Tyr at PsaB718 through a water molecule or (b) through the introduced Ser and Tyr in the double mutant, possibly through a water molecule. According to the crystal structure (2), in the wild type the side chain of a Tyr faces away from the chlorophyll and due to the large distance in between, a hydrogen bond to the 13^1 keto $\text{C}=\text{O}$ of $\text{Chl}\alpha$, cannot be formed. It is possible that mutations at in the double mutant caused a rearrangement of the protein backbone, favoring such an interaction, possibly facilitated by a water molecule. The triple mutant has, in addition to the double mutation, the Tyr PsaB718 changed to the PsaA homologue, a Thr. However, the ($\text{P700}^+ - \text{P700}$) difference spectra from the double and triple mutant are almost identical showing that the Y718T replacement in the triple mutant had no effect in the ($\text{P700}^+ - \text{P700}$) difference spectra. This can be explained by the fact that the introduced Thr at that position is also capable of hydrogen bonding although some shift to the frequency of the $1687(+)/1668(-)\text{cm}^{-1}$ signal would have been expected due to the large difference in the size of the side chains of Tyr and Thr. This leads us to believe that the difference signal $1687(+)/1668(-)\text{cm}^{-1}$ is independent of the amino acid at PsaB 718 position and that the 30% population of 13^1 keto $\text{C}=\text{O}$ hydrogen bonds to the introduced Tyr and Ser, more likely through a water molecule. This interpretation can also explain the small upshift observed in the $1754(+)/1749(-)\text{cm}^{-1}$ difference signal, which represents vibrational bonds from the 13^2 carbomethoxy group of $\text{Chl}\alpha$. This is evidence that this $\text{C}=\text{O}$, not only does not hydrogen bond, but also vibrates with more freedom in the mutants. The issue of whether the changes in this region of the spectra are due to the double mutation, regardless of the PsaB718 position could be tested in the future by the formation of a triple mutant with a nonhydrogen bonding residue in place of Tyr B718. If such a mutant provides similar spectra as our double and triple mutant, then it would be certain that the Ser and Tyr in the mutants cause the alterations in the bonding pattern with $\text{Chl}\alpha$ and not Tyr B718.

The 1656(+)/1637(-) and 1717(+)/1697(-) difference signals representing the 13^1 keto and the 13^2 carbomethoxy C=O bond vibrations of Chl α' appear to be the same as in the wild type. This indicates that the mutations in PsaB did not effect the interactions of the other half of the dimer with PsaA. Single mutant PsaB F710Y, shows no significant differences in comparison to the wild type (Figure 5). In this mutant the Phe at 710 was changed to a Tyr, that is in the homologous position in PsaA and is thought to donate a hydrogen bond to the phytyl ester carbonyl oxygen of Chl α' (2). According to Breton et al. (11,18), the vibrational modes of the the phytyl ester carbonyl oxygen cannot be detected in the 1600-1800 cm^{-1} region. The data, however, can be taken as an indication that mutation PsaB F710Y does not alter the positioning of the heterodimer with respect to the protein environment.

Electron spin density distribution determined in the double and triple mutants by ENDOR spectroscopy. The electronic structure of P700 has been studied extensively during the past years. ENDOR and EPR studies, have shown that the electron spin distribution over the oxidized state of P700 (P700⁺), is asymmetrical, favoring the PsaB coordinated chlorophyll (Chl α) by ratios $\geq 4:1$ (10). However, FTIR spectroscopy, measures a more equally distributed positive charge over the two chlorophylls with ratios of 1:1 or 2:1, favoring B-side Chl α (11). FTIR determines charge distribution based on the upshifts of the C=O group vibrational frequencies upon oxidation of P700, and the amplitudes of the signals from the 13^1 keto group of Chl α and Chl α' (22,23). However, the relations between charge distribution and signal upshift or signal amplitude has not yet been well defined since the carbonyl bond frequency is very sensitive to interactions from the environment, such as hydrogen bonding. For these reasons, we have used ENDOR for determining the electron spin density of P700 in our triple mutant. The ^1H -ENDOR spectra of P700⁺ provide the hyperfine coupling constants from specific protons of the spin carrying chlorophyll, Chl α (19-21). Only two small detectable hfc's, have been assigned to the low spin carrying Chl α' (line pairs 1'/1 and 2'/2 in Figure 6 or 7). In our ENDOR spectra of our double mutant P700⁺ (Figure 6) line pairs 5'/5 (parallel hfc components of the methyl protons at position 2 of Chl α), line pairs 4'/4 and 6'/6 (methyl protons at position 7) and 7'/7 and 8'/8 (assigned to 12-methyl protons) increase. The hfc's in MHz are also summarized in Table 3. The most dramatic increase is observed in splittings 5'/5, 7'/7, 8'/8. These data indicate that the

electron spin density over $P700^+$ becomes even more asymmetric upon mutations in PsaB. This is in contrast to the effects that would be expected if a hydrogen bond to 13^1 -keto C=O, was indeed introduced (as predicted by our FTIR spectra). According to (9, 10) hydrogen bonding would stabilize the reduced state of this half of the dimer, and favor spin shift in the opposite direction (toward $Chl\alpha'$). Studies on similar mutations in PsaA, where the hydrogen bonding residues to $Chl\alpha'$ were replaced by the homologues in PsaB, show results suggesting a shift of electron spin density from $Chl\alpha$ to $Chl\alpha'$ (M. Pantelidou et al., in preparation). A possible reason for the induced asymmetric distribution of electron spin in our double PsaB mutant, would be the change in the polarity in the environment surrounding the E ring of the $Chl\alpha$. In the mutant, the nonpolar Leu was replaced by a polar Tyr and a Gly was replaced by Ser, a residue of higher polarity. Polar residues cause an increase in the dielectric constant of the nearby environment. This can weaken the interaction between local positive charges (coming from the protein) and the positive charge of $Chl\alpha^+$ and favor the electron spin density shift towards the chlorophyll molecule. However, this interpretation does not apply for the triple mutant. It seems that in this mutant the additional Y718T mutation has caused a reversion of the changes observed in the line pairs 6'/6, 7'/7 and 8'/8 of the double mutant and a decrease in the 2'/2 splittings. It should be noted that the hfcs assigned to the low spin carrying $Chl\alpha'$ (line pairs 1'/1 and 2'/2) in double mutant do not show any significant changes. However, ENDOR is unable to make a more detailed assignment of the (low) electron spin density over this half of the dimer and we therefore cannot say with certainty if indeed no changes have occurred for this chlorophyll molecule. We therefore, take the increase of the hfcs assigned to the high electron spin carrying, $Chl\alpha$, as an indication of electron spin density redistribution within the dimer with an induced localization on $Chl\alpha$. The electrons spin density shifts towards $Chl\alpha$ in both mutants but the double mutant shows stronger effects. The difference of the side chain of the introduced Thr in the triple mutant in place of Tyr at position PsaA 718, may affect the backbone of the protein surrounding $Chl\alpha$ which can be another possible reason for the changes in the electron spin density observed or the differences observed in the hfcs of the two mutants. It should be noted, however, that the $P700^+$ - $P700$ FTIR difference spectra of these mutants are very similar.

In conclusion, our results suggest that the mutations in PsaB, surrounding the E conjugated ring of Chl α , have affected interaction with the protein. An insertion of a partial hydrogen bond between ^{13}C -keto C=O and PsaB is suggested by FTIR spectroscopy. The electronic structure of P700⁺ studied by ENDOR has also been altered with an induced asymmetry favoring Chl α . The nature of this electron spin density is not completely clear. The double mutant shows stronger changes than the triple mutant, while the FTIR spectra of PSI from both mutants are very similar. The polarity of the introduced residues at the site is a possible reason for the changes observed. Furthermore, rearrangements in the backbone structure of the protein resulting from the mutations, may also play a key role. Additional mutations at this site will help illustrate the exact nature of the changes observed in our mutants. Furthermore, the single mutant PsaB Y718T would help illustrate the differences between the ENDOR spectra of our double and triple mutants.

REFERENCES

1. Chitnis P.R. (2001). *Annu. Rev. Plant Physiol. Plant Mol. Biol.*, 52, 593-626.
2. Jordan P., Fromme P., Witt H.T., Klukas O., Saenger W. and Krauß N. (2001). *Nature*, 411, 909-917.
3. Fromme P., Jordan P., Krauss N. (2001). *Biochim. Biophys. Acta*, 1507, 5-31.
4. Brettel K. and Leibl W. (2001). *Biochim. Biophys. Acta*, 1507, 100-114.
5. Xu W., Chitnis P., Valieva A., Est A., Pushkar Y.N., Krzystyniak B., Teutloff C., Zech S.G., Bittl R., Stehlik D., Zybaylov B., Shen G. and Golbeck J.H. (2003). *J. Biol. Chem.*, 278, 27864-27875.
6. Putron S., Stevens D. R., Muhiuddin I. P., Evans M. C., Carter S., Rigby S. E. and Heathcote P. (2001). *Biochemistry*, 40, 2167-2175.
7. Boudreaux B., Macmillan F., Teutoll C., Rufat A., Gu F., Grimaldi S., Bittl R., Brettel K. and Redding K. (2001). *J. Biol. Chem.*, 276, 37299-37306.
8. Guergova-Kuras M., Boudreaux B., Joliot A., Joliot P. and Redding K. (2001). *PNAS*, 98, 4437-4442.
9. Golbeck J.H. (2003). *Annu. Rev. Biophys. Biomol. Struct.*, 32, 237-256.
10. Webber A.N. and Lubitz W. (2001). *Biochim. Biophys. Acta*, 1507, 61-79.
11. Breton J., Nabedryk E. and Leibl W. (1999). *Biochemistry*, 38, 11585-11592.
12. Williams J.G.K. (1988). *Meth. Enzymol.*, 167, 766-778.
13. Smart L. B., Anderson S. L. and McIntosh L. (1991). *EMBO J.*, 10, 3289-3296.
14. Rippka R., Deruelles j., Waterbury J. B., Herdman M. and Stanier R. Y. (1979). *J. Gen. Microbiol.*, 111, 1-61.
15. MacKinney G. (1941). *J. Biol. Chem.*, 140, 315-322.
16. Sun J., Ke A., Jin P., Chitnis V. P. and Chitnis P. R. (1998). *Meth. Enzymol.*, 297, 124-139.
17. Arnon D. (1949). *Plant Physiol.*, 24, 1-14.
18. Breton J. (2001). *Biochim Biophys Acta*, 1507, 180-193.
19. Kass H., Fromme P., Witt H. T. and Lubitz W. (2001). *J. Phys Chem.*, 105, 1225-1239
20. Käss H., Fromme P. and Lubitz W. (1996). *Chem. Phys. Lett.*, 257, 197-206.

21. Krabben L., Schlotter E., Jordan R., Carbonera D., Giacometti G., Lee H., Webber A.N. and Lubitz W. (2000). *Biochemistry*, 39, 13012-13025.
22. Naberdryk E., Allen J. P., Tagushi A. K.W., Williams J.C., Woodbury N. W. and Breton J. (1993). *Biochemistry*, 32, 13879-13885.
23. Ivancich A., Artz K., Williams J.C., Allen J.P. and Mattioli T.A. (1998). *Biochemistry*, 37, 11812-11820

FIGURE LEGENDS

Figure 1. **Molecular structure of Chlorophyll α** (IUPAC numbering). Chl α' is the epimer at position 13².

Figure 2. **Interaction of P700 with the protein environment** (numbering is according to *Synechocystis* sp. PCC 6803). A. HisA676 and HisB651 are the coordinating ligands of P700. Putative hydrogen bonds between Chl α' , the water molecule and surrounding PsaA residues are shown by dotted lines on the right. The respective PsaB residues that do not hydrogen bond are shown on the right.

Figure 3. **Fourier transform infrared (FTIR) spectra of PsaB L581Y/G585S/Y718T mutant.** The (P700⁺-P700) difference spectra of the wild type (top) and PsaB-L581Y/G585S/Y718T triple mutant (bottom). Positive and negative signals are related to oxidized and reduced states of the dimer, respectively.

Figure 4. **FTIR spectra of PsaB L581Y/G585S double mutant.** The (P700⁺-P700) difference spectra of the wild type (top) and PsaB L581Y/G585S double mutant (bottom).

Figure 5. **FTIR spectra of PsaB F710Y single mutant.** The (P700⁺-P700) difference spectra of the wild type (top) and PsaB F710Y single mutant (bottom). The spectra do not show any detectable differences.

Figure 6. **Electron nuclear double resonance (ENDOR) Spectra of P700⁺ of the wild type (upper) and the PsaB L581Y/G585S double mutant (lower).** The splittings are shown with numbers and the increase of the 12-methyl proton hfcs in the mutant are indicated with dotted lines. The Larmor frequency of ¹H (not shown) is at 14.5 MHz. (Conditions: temperature=120K, modulation frequency =12.5 kHz, modulation amplitude =2G, microwave power =20 mW, gain = 10⁵, time constant =81.9 msec, 89 scans were summed)

Figure 6. Electron nuclear double resonance (ENDOR) Spectra of P700⁺ of the wild type (upper) and the PsaB L581Y/G585S/Y718T triple mutant (lower). The increase in the 4'/4 and 5'/5 line splittings is shown with dotted lines. No significant increase is observed in the 12-methyl proton hfcs (7'/7, 8'/8) in the mutant (also indicated with dotted lines).

Table 1: Mutagenic primers used for making mutations in PsaB.

PsaB F719Y	5'GCACATAACCAACGGTGTAGTGGGCTAAACCAACC3'
PsaB L581Y/G585S	5'GGATGCTGAACACCTTGAGTTGGTTGACCTTCTAC3' 5'CTAGCCATGTTCTGGATGTACAACACCTTGAGTTGG3'
PsaB L581Y/G585S/Y718T	5'GGATGCTGAACACCTTGAGTTGGTTGACCTTCTAC3' 5'CTAGCCATGTTCTGGATGTACAACACCTTGAGTTGG3' 5'GCAATTAGGAATGCCGCAGTGGTGAGCACATAACC3'

Table 2: Physiological characterization of the *PsaB* triple mutant, L581Y/G585S/Y718T^a

Strains	Chlorophyll Content ($\mu\text{g}/\text{OD}_{730}/\text{ml}$)	Doubling Time (hours)				
		With Glucose			Without Glucose	
		Low Light ^b	Normal Light ^b	High Light ^b	Normal Light	High Light
Wild type	3.83 \pm 0.15	25.4 \pm 3.5	13.3 \pm 1.8	15.6 \pm 3.8	92.2 \pm 6.4	64.4 \pm 7.1
<i>PsaB</i> triple mutant	2.98 \pm 0.29	33.8 \pm 2.0	16.2 \pm 0.1	15.9 \pm 0.1	99.1 \pm 2.0	68 \pm 0.1

^a Average of three independent measurements

^b Low, normal and high light conditions are 5-10, 40-50 and 90-100 $\mu\text{mol photons m}^{-2}\text{s}^{-1}$ respectively

Table 3: Proton hyperfine couplings in MHz of P700⁺ from the wild type and the mutants in *Synechocystis* sp. PCC 6803^a

Strains	PsaA Chl (1'/1)	PsaA Chl (2'/2)	A _⊥ (2) (3'/3)	A _∥ (2) (5'/5)	A _⊥ (7) (4'/4)	A _∥ (7) (6'/6)	A _⊥ (12) (7'/7)	A _∥ (12) (8'/8)
Wild type	0.89	1.79	2.48	3.59	3.26	4.32	5.26	6.14
PsaB L581Y/G585S/Y718T	0.88	1.57	2.44	4.11	3.38	4.34	5.24	6.10
PsaA L581Y/G585S	0.88	1.71	2.53	4.22	3.49	4.46	5.50	6.77

^a The error for each measurement is ±0.05 MHz

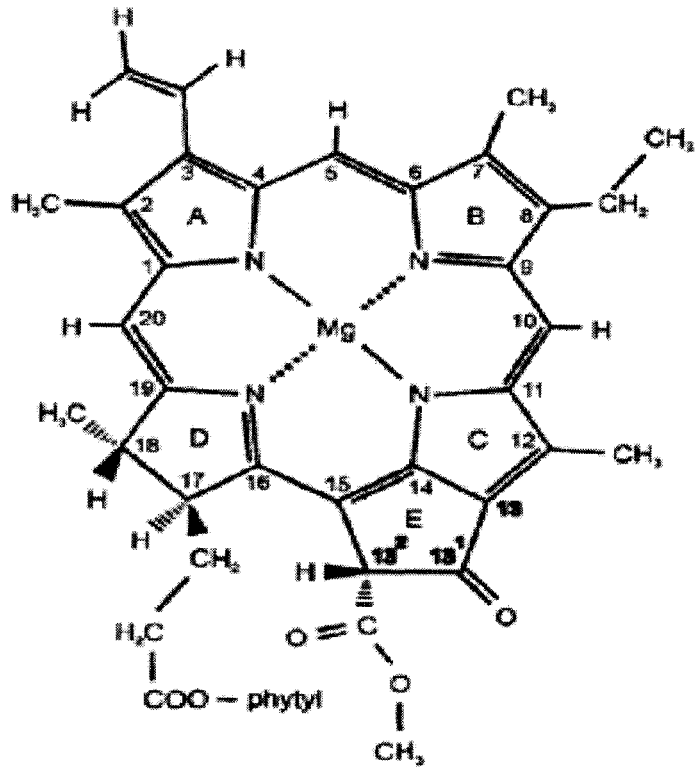


Figure 1

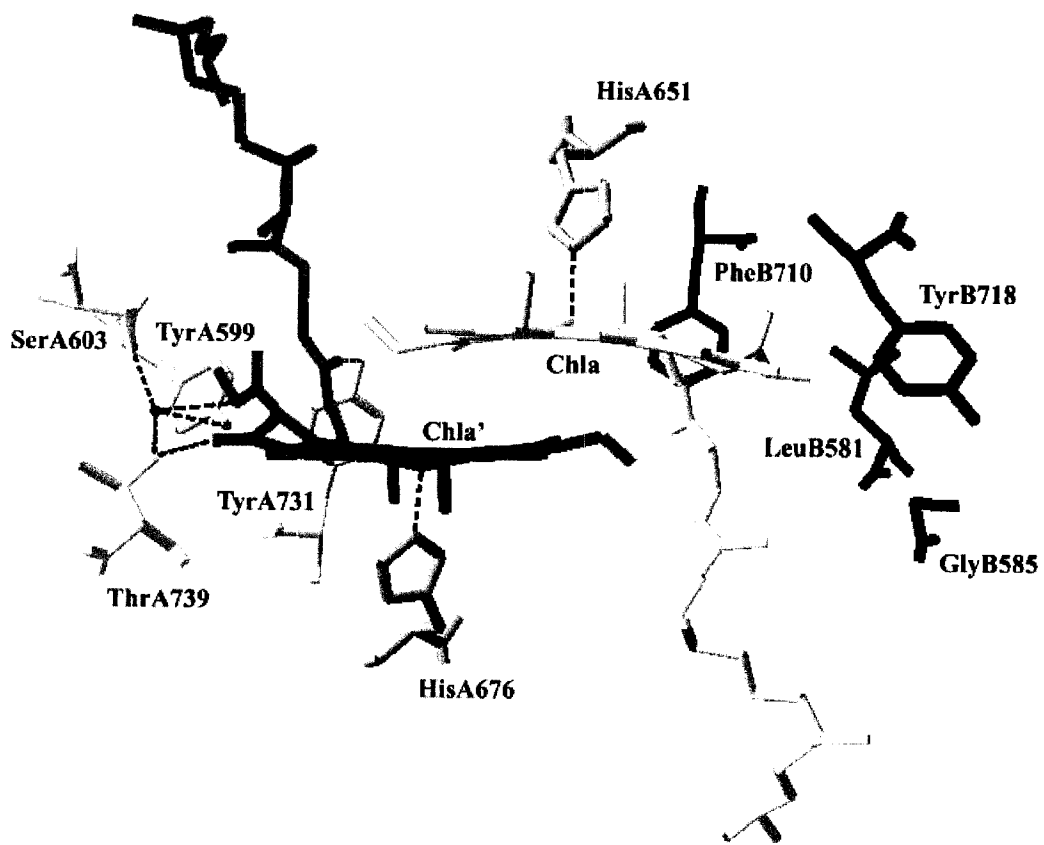


Figure 2

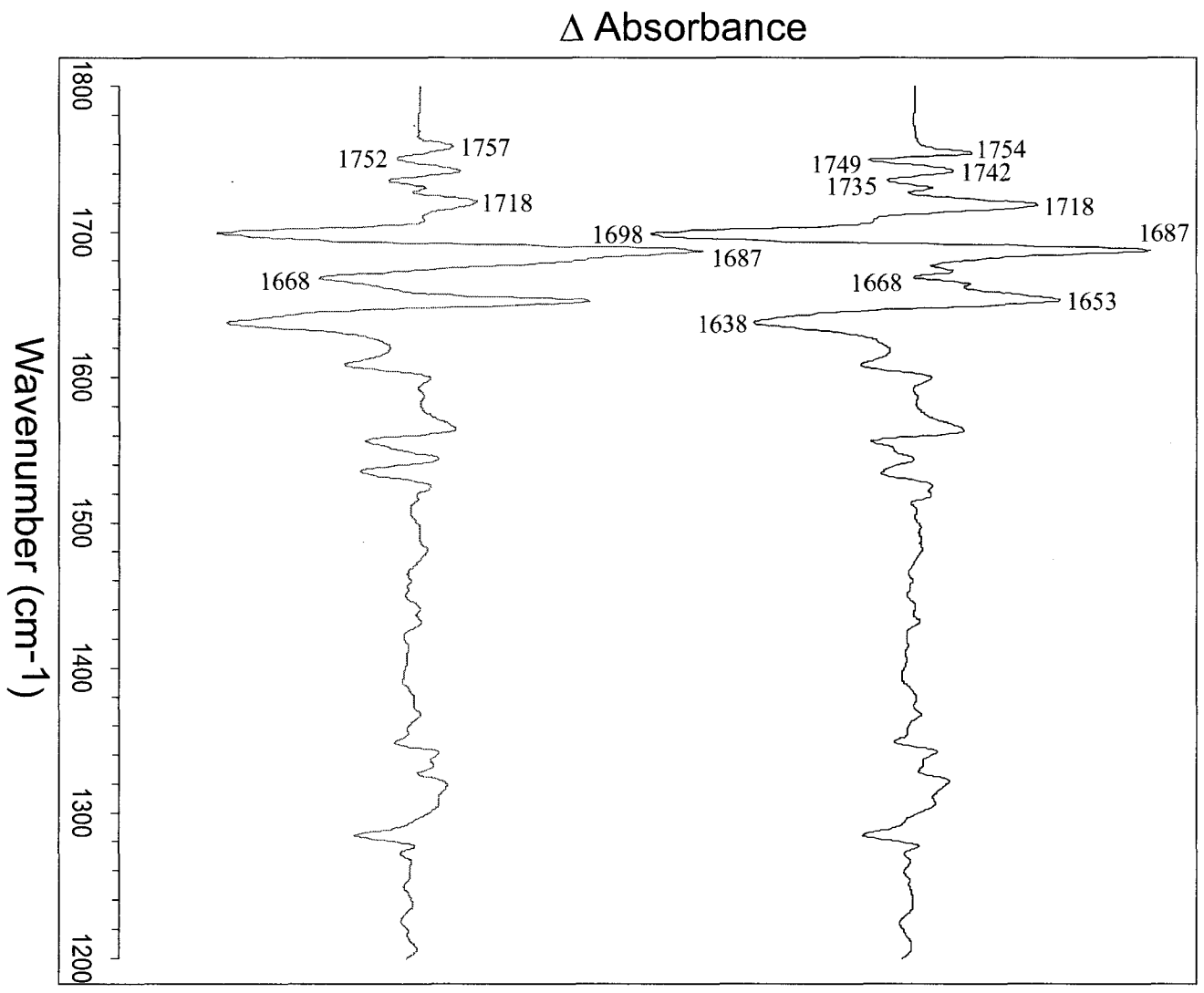


Figure 3

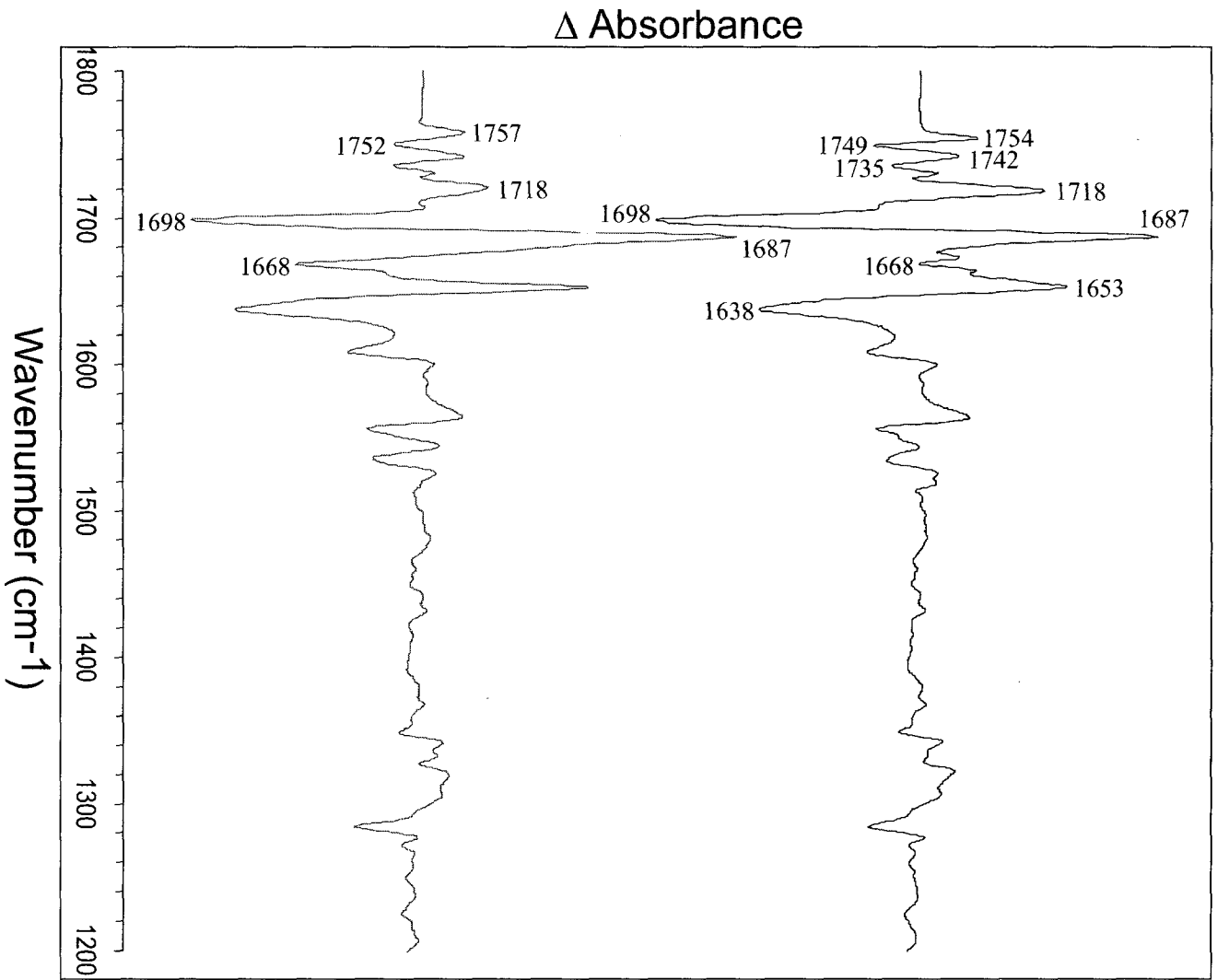


Figure 4

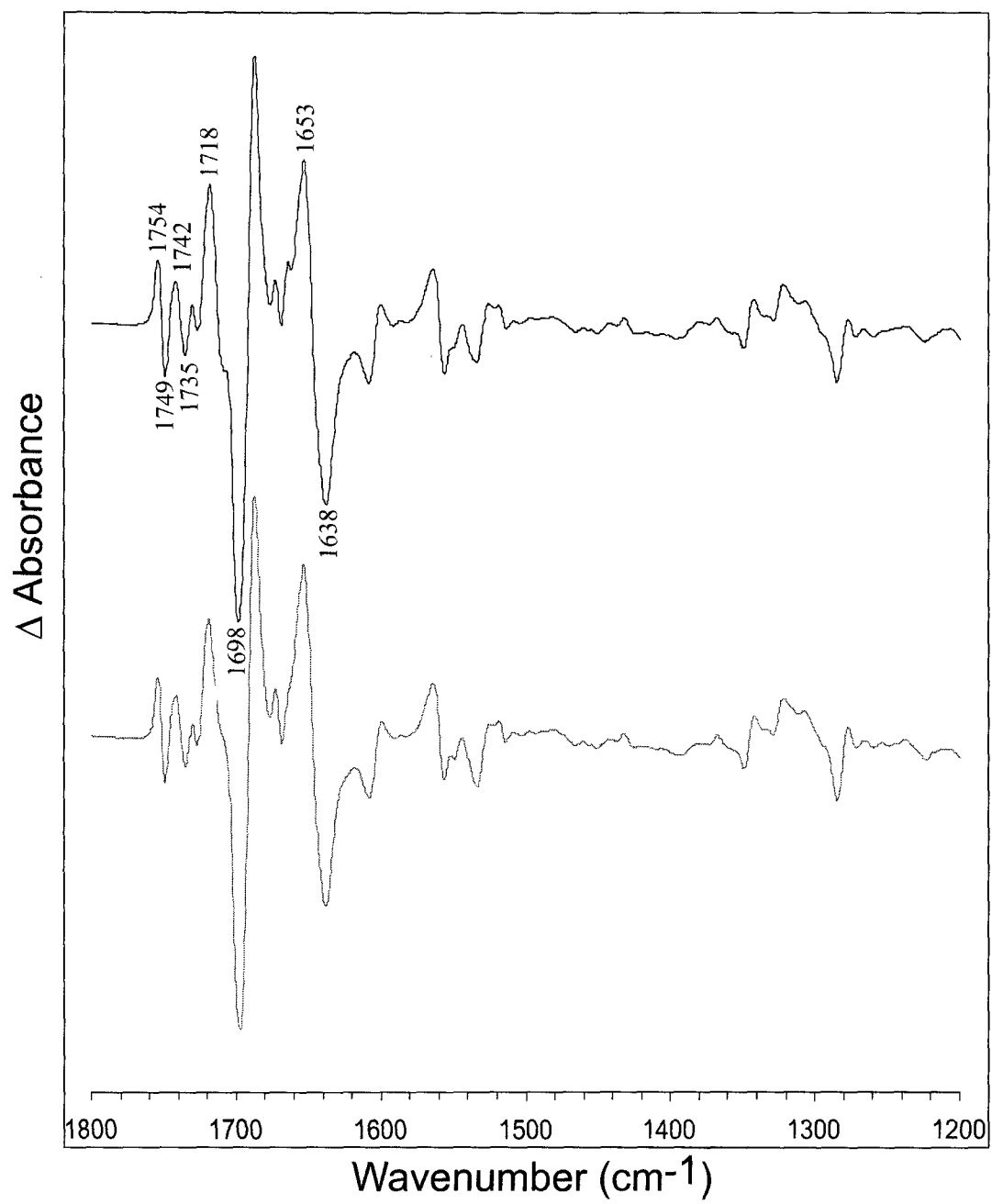


Figure 5

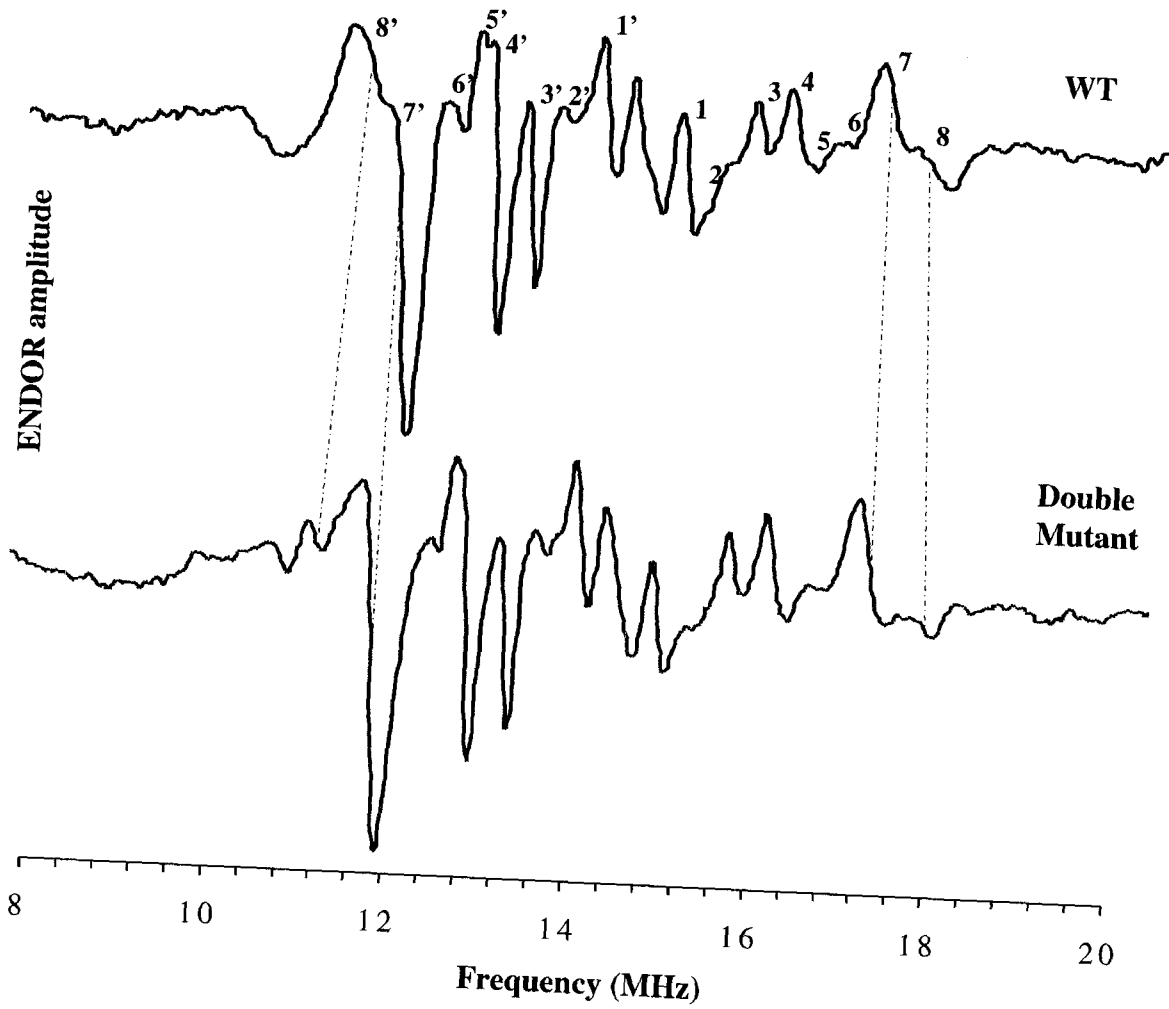


Figure 6

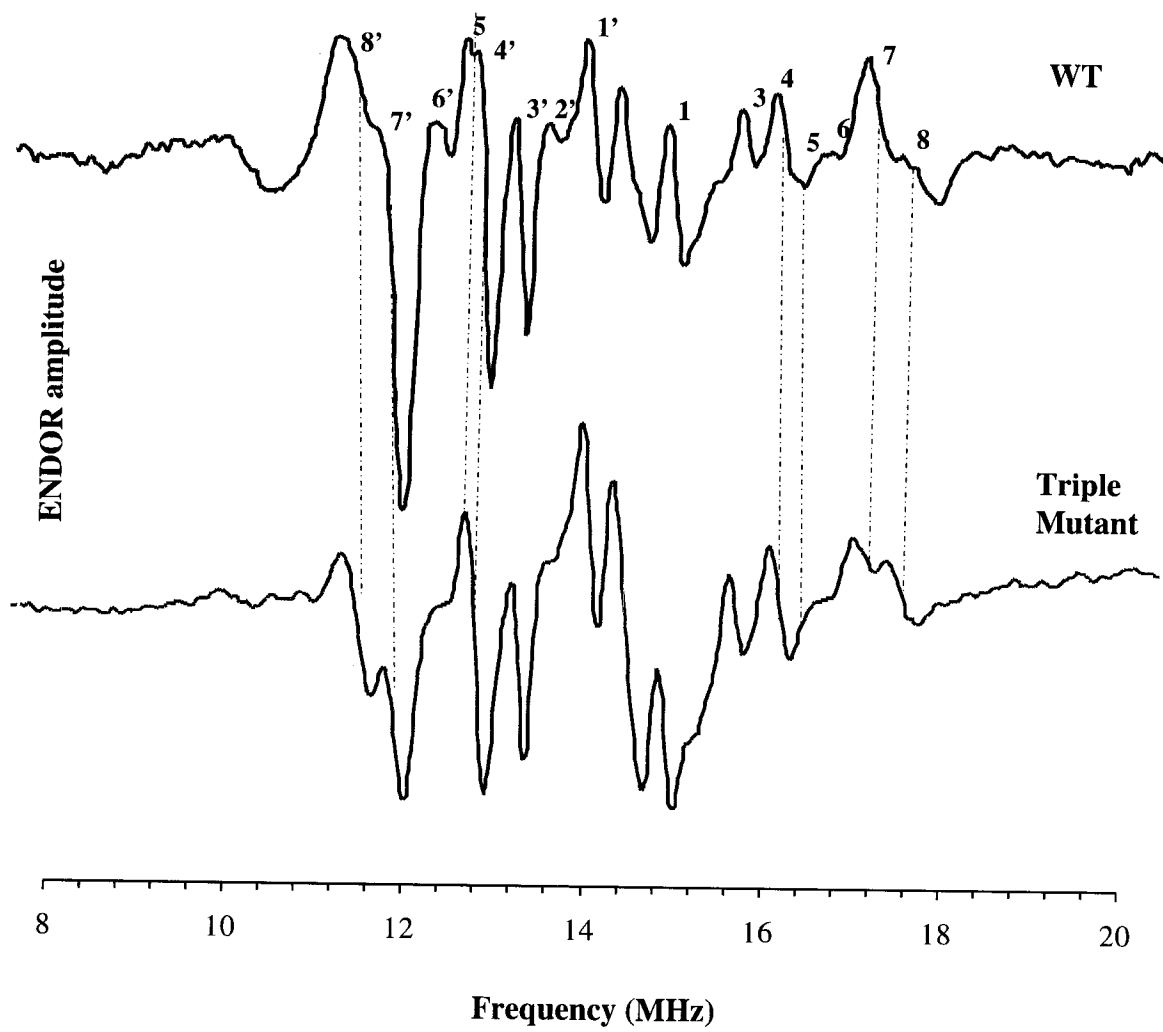


Figure 7

CHAPTER 5: GENERAL CONCLUSIONS

Photosystem I, one of the two photoreaction centers in *Synechocystis* sp. PCC 6803, is a protein-cofactor complex located in the thylakoid membrane of the cells. Its function involves the oxidation of plastocyanin and the reduction of ferredoxin, through a light-driven electron transport across the thylakoid membrane. Cyanobacterial PSI consists of 12 protein subunits, 96 chlorophyll α molecules, 22 beta-carotenes, two phylloquinones and three iron-sulfur clusters. PsaA and PsaB, the largest subunits, protect the electron transfer chain (ETC) cofactors. These cofactors are: P700, the primary electron donor chlorophylls, another pair of molecules of Chl α (A_0), two phylloquinone molecules (A_1) and three iron-sulfur clusters F_X , F_A and F_B . When light energy harvested by the antenna chlorophylls is eventually trapped in P700, excited P700* is formed. P700* donates an electron to A_0 and A_0^- -P700⁺ is formed. The electron is then transferred to A_1 and then to the three iron-sulfur clusters F_X , F_A and F_B . This electron eventually reaches ferredoxin. P700⁺ goes back to its ground state by an electron uptake from plastocyanin. The cofactors are arranged in two branches, symmetrically surrounded by PsaA and PsaB. Whether the electron transfer follows a direction involving one or both branches is not completely clear. Many studies have been performed during the past few years, in order to elucidate this issue. P700, the primary electron donor of PSI, can potentially play a key role in electron directionality down the branches of PSI. Whether the electron spin density is symmetrically distributed or mostly over one half of the dimer, has also been a controversial issue. In this study we have affected the interaction of P700 with the protein environment to determine the effects the dimer's the biophysical properties.

P700 is a heterodimer. It is composed of chlorophyll α (Chl α) and the C13² epimer of Chl α (called Chl α'). PsaA coordinates Chl α' and PsaB, on the other hand, coordinates Chl α , the other half of P700. There are hydrogen bonds present between some residues of PsaA and Chl α' . Thr at PsaA 739 (numbering is according to *Synechocystis*), donates a hydrogen bond to the 13¹ keto oxygen the Chl α' and to a water molecule. This water molecule, which can be hydrogen bonded to residues Ser A603, Tyr A599 and Gly A735, forms a hydrogen bond to the bridging oxygen of the 13² carbomethoxy group of Chl α' .

Moreover, Tyr A731 is within hydrogen bond distance with P700⁺ with the phytyl ester-carbonyl oxygen of Chl α' . The homologous positions in PsaB, are occupied by different amino acids and no hydrogen bonds are formed with Chl α . In this study we have used site-directed mutagenesis in *psaA* and *psaB* genes to make (1) PsaA mutants that do not longer hydrogen bond to Chl α' and (2) PsaB mutants that can hydrogen bond to Chl α . We then studied the mutants to determine whether changes in the interaction with the protein have altered the spectroscopic properties of P700.

The bonding interaction of P700⁺/P700 with the protein was studied by fourier transform infrared (FTIR) spectroscopy. Mutant PsaA T739F and triple mutant PsaA Y599L/S603G/T739Y showed evidence for rupture of the hydrogen bonding to the 13¹ keto oxygen the Chl α' . In the triple mutant, the additional double mutation also affected the bonding interaction to the bridging oxygen of the 13² carbomethoxy group of Chl α' , but to a less extent. Electron nuclear double resonance spectroscopy (ENDOR) was used in order to determine the electron spin density distribution over P700⁺. In the past this has been reported to be asymmetric mostly favoring B-side Chl α . According to our results, the triple mutant showed a redistribution of the spin, with a small, shift towards Chl α' . FTIR analysis of the PsaB double mutant ((PsaB L581Y/G585S) and triple mutant (PsaB L581Y/G585S/Y718T), demonstrated an insertion of a partial (30%) hydrogen bond to the 13¹-keto C=O of Chl α , while the other side of the dimer (Chl α') still remained hydrogen bonded to PsaA. However, the electronic structure of P700⁺ in our PsaB mutants and particularly the double mutant, as studied by ENDOR, revealed an even more asymmetric electron spin distribution, with a shift towards B side Chl α .

The research presented in this dissertation demonstrates the importance of protein interactions in determining the spectroscopic properties of P700. The mutations affecting the hydrogen bonding to PsaA have shown to induce a small shift towards that side of the molecule and a small reduction of the electron spin density asymmetry determined by ENDOR. In contrast, (partial) hydrogen bonding insertion in PsaB mutants by substitution with hydrogen bonding residues has induced increased asymmetric spin favoring Chl α . Therefore, other factors, such as the change in the polarity of the environment surrounding this side of P700 or changes in the backbone of the protein induced by the mutations could

have a strong effect on the electron spin above Chl α and increase its localization over this half of the dimer. More mutations in *psaB* as well as generation of mutants with both *psaA* and *psaB* changed, will help indicate the nature of the introduced hydrogen bonding in PsaB and electronic structure of P700⁺.

In conclusion, we have demonstrated that the interaction of P700 with the protein in the surrounding environment plays a very important role in the dimer's properties. Specifically, the electron spin distribution over the chlorophyll dimer is affected by this interaction. In the future, it also will be interesting to also study the effects of the mutations performed in this work on the electron transfer after P700 such as phylloquinone A₁.

APPENDIX. DISRUPTION OF *crtX* GENE, ENCODING A HYPOTHETICAL ZEAXANTHIN GLYCOSYL TRANSFERASE IN *SYNECHOCYSTIS* SP. PCC 6803.

SUMMARY

The carotenoid biosynthetic pathway in *Synechocystis* sp. PCC 6803 has not been completely elucidated yet. One of the carotenoids that accumulate significantly in this organism is zeaxanthin, a xanthophyll. Zeaxanthin mono or diglycosides have never been detected in *Synechocystis*. Nevertheless, the open reading frame slr1125 is thought to encode for a zeaxanthin glycosyl transferase (CrtX). To study the role of this gene in the carotenoid biosynthetic pathway, *crtX* was disrupted by insertion of an antibiotic cassette. Pigment analysis of the mutant by High Performance Liquid Chromatography showed no alterations in the carotenoid composition. Furthermore, the mutation did not seem to affect the growth or photosystem stoichiometry in the cells and light sensitivity was not increased.

INTRODUCTION

Carotenoids are isoprenoid polyene molecules found in many organisms such as algae, fungi, photosynthetic or nonphotosynthetic bacteria and higher plants (1). They are classified as oxygen free carotenes (such as β -carotene) and xanthophylls, that contain oxygen in the form of hydroxyl or epoxy group. The xanthophylls are also found linked through a glycosidic bond to sugar moieties, and are called carotenoid glycosides. These molecules are highly polar and although their function is not known, they are thought to be associated with membrane fluidity (2). In photosynthetic organisms, carotenoids mostly interact with chlorophyll binding proteins and are found to have a protective function. During photosynthesis, in addition to their contribution to light absorption, their role is to provide photooxidative protection through quenching the triplet excited states of chlorophyll and the damaging singlet oxygen (1).

The carotenoid biosynthetic pathway in the photosynthetic bacterium *Synechocystis* sp. PCC 6803, has been studied extensively in the past years but it is still not completely known. More than 10 enzymes are thought to be involved in this pathway but only five enzymes have been identified so far (3-8). According to Figure 1, the pathway starts with

condensation of two geranyl geranyl pyrophosphate molecules by a phytoene synthase (encoded by *crtB*) and through a series of steps catalyzed by *crtP* (phytoene desaturase), *crtQ* (ζ -carotene desaturase), *crtR* (β -carotene hydroxylase) and *crtO* (β -carotene ketolase) four carotenoids accumulate significantly, zeaxanthin, echinenone and myxoxanthophyll (7, 9). The latter was reported to be a ramosylated xanthophyll (7, 9) but more recent studies have indicated that the sugar moiety is a dimethylated fucose, instead, and it is therefore now called myxol 2'- α -L-fucoside (10).

Zeaxanthin, a β , β -carotene-3,3'-diol, is synthesized from β -carotene through the action of β -carotene hydroxylase, an enzyme encoded by *crtR* (Figure 1). Zeaxanthin glycoside has not been detected in *Synechocystis* but its formation is possible. The open reading frame slr1125 (according to Cyanobase (<http://www.kazusa.or.jp/cyano.html>)) has homology with *crtX* the gene encoding for zeaxanthin glucosyl transferase in *Erwinia uredovora*. This phytopathogenic bacterium, utilizes the glycosylation enzyme for production of zeaxanthin- β -diglucoside (11). Zeaxanthin glucosyl transferase has been also identified and studied in the nonphotosynthetic bacterium, *Erwinia herbicola*. This enzyme catalyzes the formation of zeaxanthin mono and diglucosides (12). Further studies have also indicated that the glucosylation is achieved through a UDP-binding domain on the enzyme (13). Zeaxanthin glycosylation has not been studied in *Synechocystis*. In the present study, we have disrupted the *crtX* gene in *Synechocystis* sp. PCC 6803, by insertion of a spectinomycin resistance cassette. HPLC analysis of the pigments in the mutant showed that the carotenoid composition has not been altered.

EXPERIMENTAL PROCEDURES

Cell growth and chlorophyll content. To measure growth rates of *Synechocystis* sp. PCC 6803 wild type and mutant strains, the cultures were grown in BG11 medium (14) to late exponential phase (0.7- 1.0 OD₇₃₀) at 30 °C. The cells were centrifuged at 4000 x g and washed twice by resuspension in BG11 medium. The 50ml-cultures were started with an initial concentration of 0.1 OD₇₃₀ and constant shaking at 140 rpm under low light (5-10 $\mu\text{mol photons m}^{-2}\text{s}^{-1}$), normal light (40-50 $\mu\text{mol photons m}^{-2}\text{s}^{-1}$) and high light (90-100 $\mu\text{mol photons m}^{-2}\text{s}^{-1}$). For photoheterotrophic growth, the cultures were supplemented with 5mM

glucose. The mutants were supplemented with 50mg/L spectinomycin. Growth rates were monitored by absorbance measurements at 730nm (A_{730}) with a UV-160U spectrophotometer (Shimadzu, Tokyo, Japan). Total chlorophyll content in the cells was performed by extractions with 100% methanol as previously described (15).

Generation of the crtX mutant. The *crtX* gene was cloned from the wild type *Synechocystis* sp. PCC 6803 based on the sequence provided by Cyanobase (<http://www.kazusa.or.jp/cyano/cyano.html>). The forward and reverse primers that were used for amplification of *crtX* were 5'GCATAGAGTTGGATTTACAGCC3' at genome position 85659 and 3'TATTGAGGCATTCCAACGTGG5' at position 87158. The fragment was ligated into pGEM-T vector system and was inactivated by insertion of the spectinomycin resistance gene cassette at the *Hind*III restriction site in the gene (Figure 3). The resulting recombinant plasmid was used for transformation of wild type *Synechocystis* sp. PCC6803. The DNA-cell mixture was spread on a BG11 plate with 5mM glucose at low light intensity ($5-10 \mu\text{mol photons m}^{-2}\text{s}^{-1}$). For initial selection of the transformants, BG11 plate was supplemented with 25 $\mu\text{g/ml}$ spectinomycin. The antibiotic concentration was gradually increased to 50 $\mu\text{g/ml}$. Finally, total genomic DNA was isolated from the mutant and wild type cells as described (13), and the fragment of interest was amplified by PCR was performed. The primers used were 5'AATTTATGGCTGAGTTGGGGC3' and 3'TTTCTGGGTGATTTTGGCCACAG5' at positions 87088 and 87162, proximal to the *Hind*III restriction site where the spectinomycin cassette was inserted (arrows shown in Figure 3). The amplified DNA fragments were separated by agarose gel electrophoresis (Figure 4) and isolated using the Qiaquick purification kit from Qiagen. The mutant genotype was verified by sequencing the ends of the amplified fragments.

77K Fluorescence emission spectra. Cell cultures were grown in the presence of 5mM glucose under light conditions of $40-50 \mu\text{mol photons m}^{-2}\text{s}^{-1}$ and harvested at approximately 0.7 OD_{730} . Cells containing 5 μg of chlorophyll were diluted in 50ul water containing 50% (v/v) glycerol prior to freezing in liquid nitrogen. The low temperature fluorescence emission spectra were obtained by using a SLM 8000C spectrofluorometer as previously described (16), with the excitation wavelength set at 440nm, the excitation slit width at 4nm and the emission slit width at 2nm.

Pigment extraction. *Synechocystis* sp. PCC6803 was harvested at 1.0 OD growth phase. The cells were centrifuged at 4000xg and water was removed from the pellet. First extraction was performed with 100% acetone and the green supernatant was collected. This extraction was repeated until all pigments are extracted (color of solvent is clear) and a last extraction with hexane was performed. The solvent was then evaporated with N₂ gas and the carotenoids were stored in -80. The pigment extraction procedure was performed under dim light.

HPLC analysis of pigments. Pigments were dissolved in 2:1 (v/v) isopropanol/dichloropethane solvent before injection. The pigment analysis was done by high performance liquid chromatography by a Shimadzu UV-Spectrophotometer LC-10A with a Beckman ODS5 4.6 by 250mm. We used a combination of isocratic and gradient programs for chromatography. An isocratic elution with acetonitrile/water [97.5:2.5 (v/v) containing ammonium acetate (10mM), solvent A] was run for 5 min at a flow rate of 0.6 ml/min. A linear gradient from solvent A to solvent B [acetonitrile/dichloromethane/water, 70:30:1 (v/v/v) containing ammonium acetate (10mM)] and an increase in flow rate from 0.6 to 1.2 ml were applied from 5 to 25 min. Then solvent B was run from 25 to 60 min at a flow rate of 1.2 ml/min, followed by a linear gradient from solvent B to A with a flow rate of 0.6 ml/min from 60 to 65 min.

RESULTS

Genotype of the crtX mutant. The primers used to test the mutant were designed at positions near the *Hind*III restriction site, where the spectinomycin cassette (2kb) was inserted. Figure 4 shows the PCR amplification of that region in the wild type and the *crtX* mutant. The incorporation of the Spectinomycin resistance cartridge is indicated by the presence of the 2074 bp fragment. Moreover, the 74bp fragment that was produced by the wild type was absent in the mutant, and showed complete segregation.

Phenotypic characterization. The *crtX* mutant and wild type cells were grown photoheterotrophically and autotrophically under different light intensities. The mutant grew with similar doubling time as the wild type under all conditions (data not shown). When DCMU was added to the cells, the mutant grew a little slower than the wild type but the

difference does not appear to be significant. Therefore, the *crtX* mutant grew with similar rates as the wild type and the cyclic electron transport around PSI is not a limiting factor in this mutant.

PSI and PSII content. Figure 5 shows the 77K fluorescence emission spectra of whole cells based on equal chlorophyll amounts. Chlorophylls of PSII emit fluorescence at 685 and 695 nm, whereas chlorophylls of PSI emit at ~720nm. The emission spectra in figure 5 show that the mutation did not affect the photosystem stoichiometry. *crtX* mutant showed similar amounts of PSI and PSII relative to the wild type.

*Carotenoid composition of *crtX* mutant.* According to Figure 6, the HPLC spectra obtained at 450nm for the mutant, show the accumulation of 4 carotenoids: zeaxanthin (peak 1), myxoxanthophyll (peak 2), echinenone (peak 5) and β -carotene (peak 6). Chlorophyll was also detected as peaks 3 and 4. The carotenoids were identified based on their retention times and characteristic absorption spectra (also shown in Figure 6). Carotenoid standards used for zeaxanthin, myxoxanthophyll and β -carotene were also used in order to verify the identity of the carotenoid species found in our samples. According to the spectra obtained from both the mutant and the wild type (not shown), based on peak areas, the carotenoid composition remained the same.

DISCUSSION

Xanthophyll glycosides are highly polar molecules that are synthesized upon glycosylation of a xanthophylls with a sugar moiety. Zeaxanthin diglycosides have been studied in nonphotosynthetic organisms such as *Erwinia uredovora* and *Erwinia herbicola*. The function of these glycosides is still not completely known. *crtX* in *Synechocystis* sp. PCC 6893 is a gene thought to encode a glycosyl transferase. It shows good homology with *crtX* of *Erwinia uredovora*. However, zeaxanthin glycosides have never been detected in *Synechocystis*. In this study we have disrupted *slr1125* by insertion of a spectinomycin resistance cassette and the carotenoid composition was studied in the mutant. HPLC analysis showed that the zeaxanthin levels, as well as the content of the other carotenoids that accumulate significantly in the cells, have not been altered by the inactivation of the gene. Furthermore, the PSI and PSII levels did not change in the mutant. Its growth remained the

same with the wild type even under high light conditions. We therefore conclude that this gene does not seem to have a significant function regarding the glycosylation of zeaxanthin or any other xanthophyll in *Synechocystis*.

REFERENCES

1. Armstrong G. A. (1997). *Annu. Rev. Microbiol.*, 51, 629-659.
2. Phander H. (1976). *Pure Appl. Chem.*, 47, 121-128.
3. Martinez-Ferez I., Fernandez-Gonzalez B., Sandmann G. and Vioque A. (1994). *Biochim. Biophys. Acta*, 1218, 145-152.
4. Martinez-Ferez I. and Vioque A. (1992). *Plant Mol. Biol.*, 18, 981-983.
5. Breitenbach j., Fernandez-Gonzalez B., Vioque A. and Sandmann G. (1998). *Plant Mol. Bio.*, 36, 725-732.
6. Masamoto K., Misawa N., Kaneko T., Kikuno R. and Toh H. (1998). *Plant Cell Physiol.*, 39, 560-564.
7. Lagarde D and Vermaas W. (1999). *FEBS Lett.*, 454, 247-251.
8. Fernandez-Gonzalez B., Sandmann G. and Vioque A. (1997). *J. Biol. Chem.*, 272, 9728-9733.
9. Lagarde D., Beuf L. and Vermaas W. (2000). *Appl. Env. Microbiol.*, 66, 64-72.
10. Takaichi S., Maoka T. and Masamoto K. (2001). *Plant Cell Physiol.*, 42, 756-762.
11. Misawa N., Nakagawa M, Kobayashi K., Yamano S., Izawa Y., Nakamura K. and Harashima K. (1990). *J. Biol. Chem.*, 172, 6704-6712.
12. Hundle B. S., Beyer P., Kleinig H., Englert G. and Hearst J. E. (1991). *Photochem and Photobiol.*, 54, 89-93.
13. Hundle B. S., O'Brien D. A., Alberti M., Beyer P. and Hearst J. E. (1992). *Proc. Natl. Acad. Sci. USA*, 89, 9321-9325.
14. Rippka R., Deruelles j., Waterbury J. B., Herdman M. and Stanier R. Y. (1979). *J. Gen. Microbiol.*, 111, 1-61.
15. MacKinney G. (1941). *J. Biol. Chem.*, 140, 315-322.
16. Shen G. Z. and Bryant D. A. (1995). *Photosynth. Res.*, 44, 41-53.

FIGURE LEGENDS

Figure 1: **Simplified carotenoid biosynthetic pathway.** Carotenoids that accumulate in *Synechocystis* sp. PCC6803 : myxoxanthophyll, echinenone, beta-carotene and zeaxanthin, taken from Lagarde et al. (1999).

Figure 2: **Glycosylation of Zeaxanthin in *Erwinia uredovora* by CrtX (Misawa et al., 1990).**

Figure 3: **Construction of the *crtX* mutant strain of *Synechocystis* sp. PCC 6803.** The inactivation of the *crtX* gene by insertion of the 2kb spectinomycin cassette at a *HindIII* restriction site. The primers used are indicated with arrows.

Figure 4: **DNA agarose gel electrophoresis of the mutant and wild type fragments.**

Lane#1 of the gel is the wild type *Synechocystis* sp. PCC 6803 PCR product (~74bps) and lane #2 is the *crtX* mutant PCR product (~2074bps). The presence of the 2074bp and the absence of the 74 bp DNA fragment, that occurs in the wild type, shows that the mutant *crtX* was completely segregated.

Figure 5: **The 77k fluorescence emission spectra of wild type and *crtX* mutant strains.**

PSII and its accessory pigments have emission maxima at 685 and 695 nm whereas PSI at 721nm. The PSI and PSII ratio remains the same in the mutant as in the wild type.

Figure 6: **Pigment analysis by High Performance Liquid Chromatography.** The chromatogram at 450nm is shown on top. Peaks 1, 2, 5 and 6 were identified to be zeaxanthin, myxoxanthophyll, echinenone and β -carotene. The typical retention times and absorption spectra at 450nm (shown below) were used in order to identify the carotenoids.

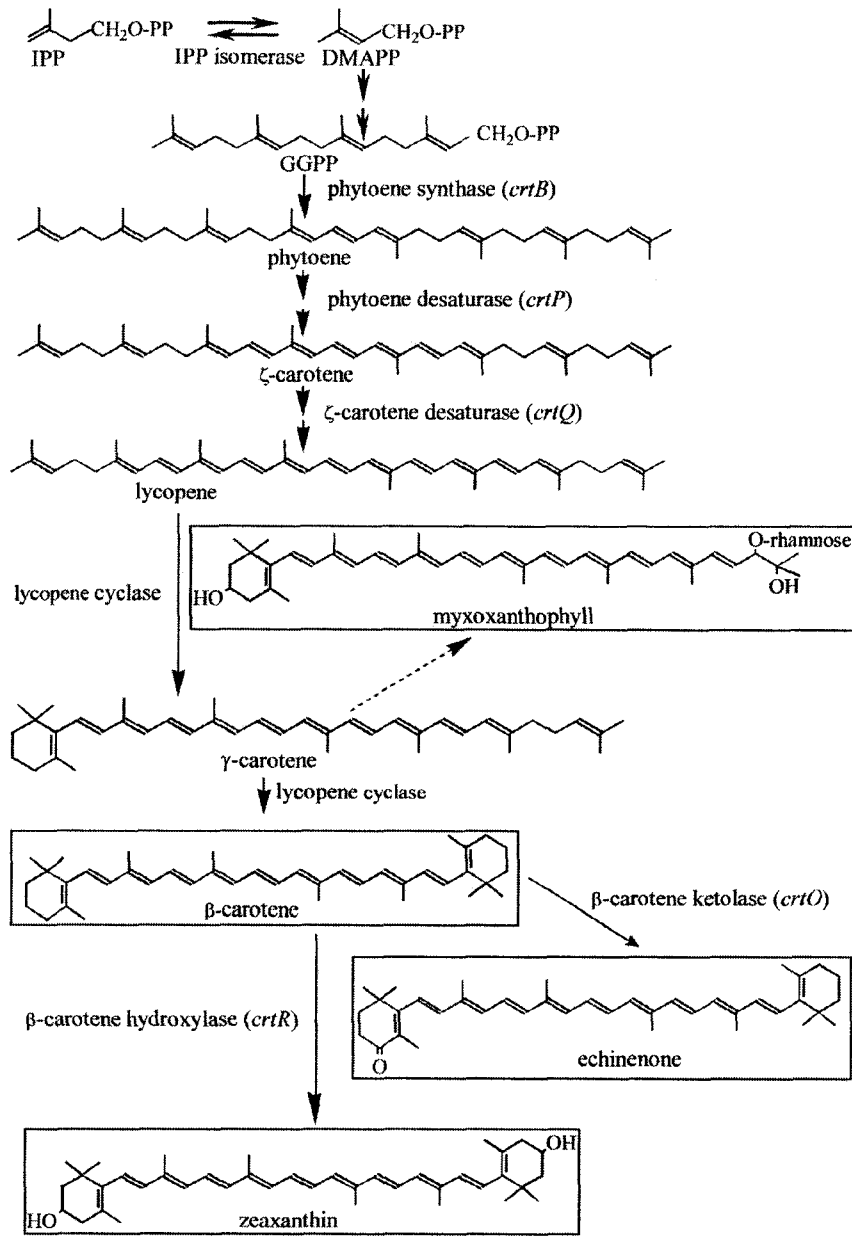


Figure 1

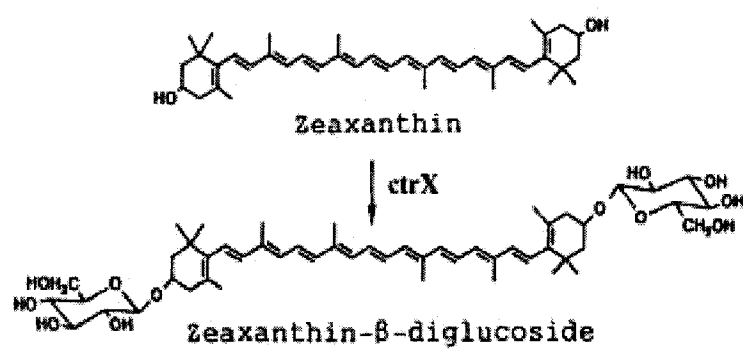


Figure 2

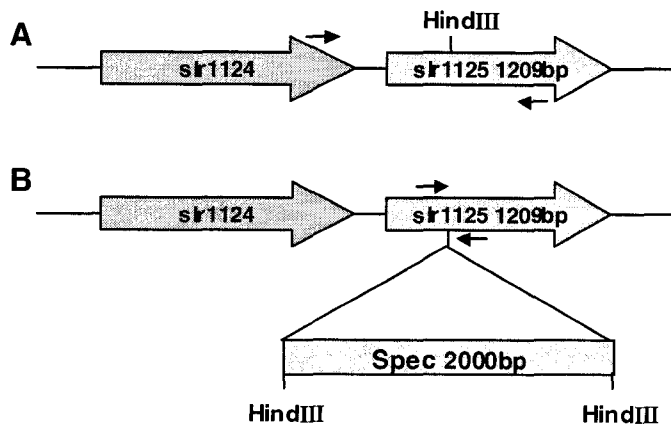


Figure 3

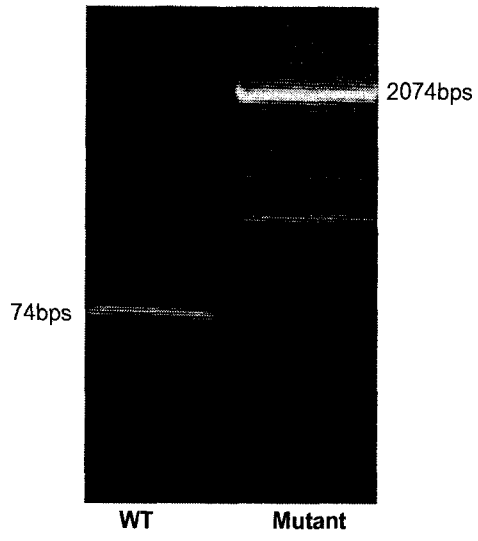


Figure 4

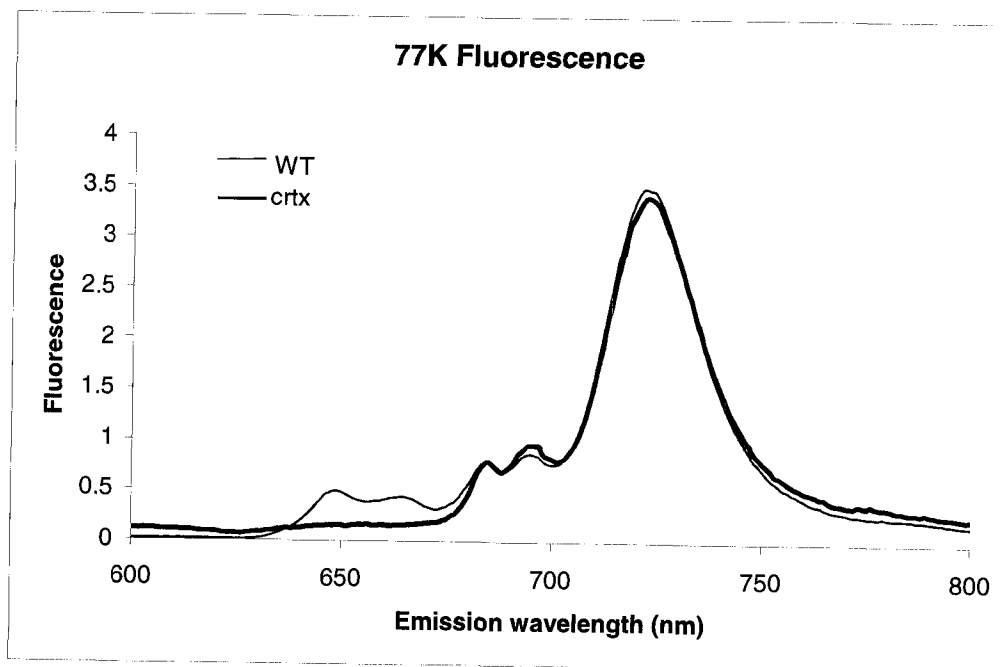


Figure 5

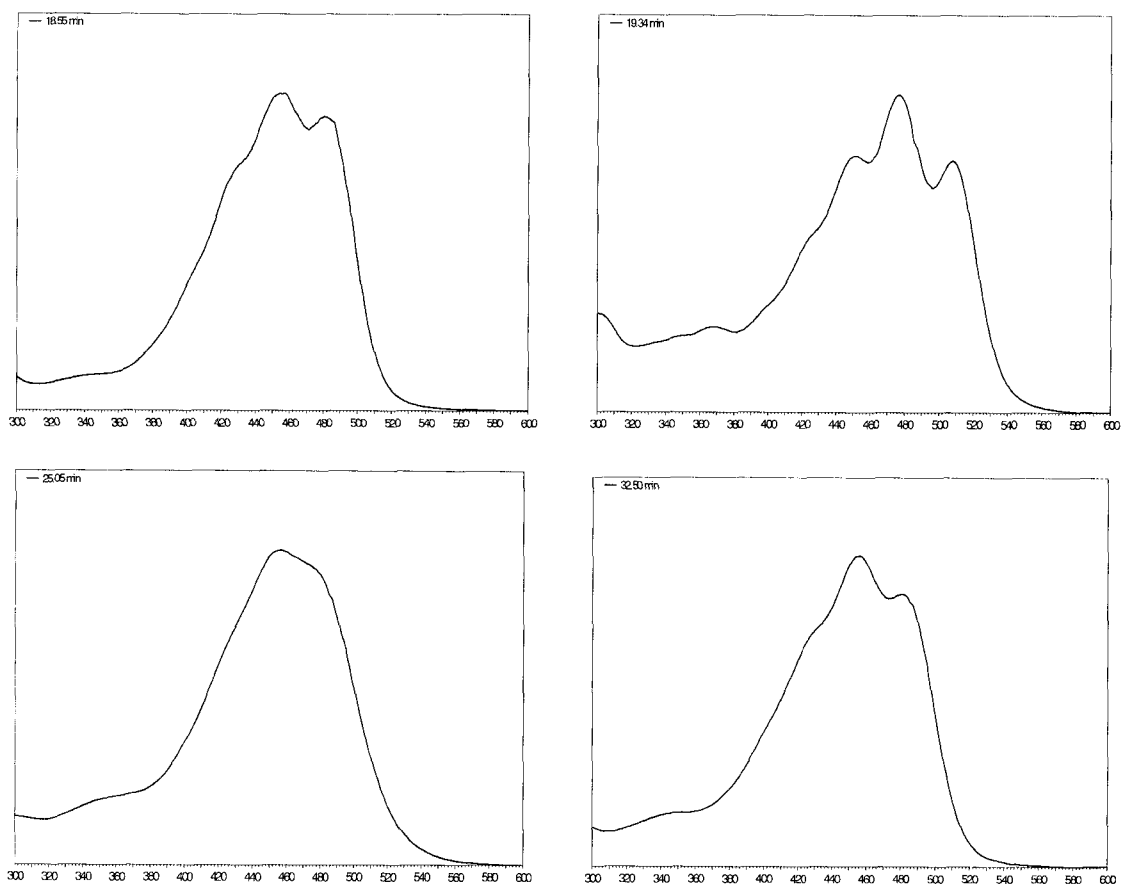
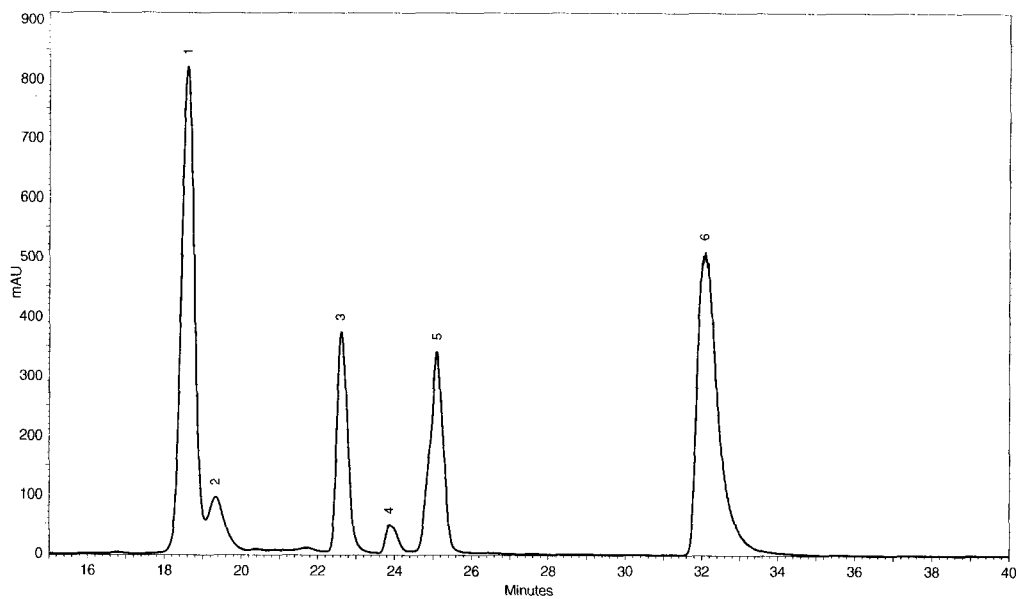


Figure 6

ACKNOWLEDGEMENTS

First I would like to thank my major professor, Dr. Parag Chitnis. It has been a great experience to have him as a mentor during my PhD training. His guidance and good advice has helped me learn a great deal in how to be a good scientist. He has taught me how to approach a scientific project by forming the right strategic plans. Most importantly, he has helped me become more organized by planning my work carefully and consistently. I thank him for his good support during my graduate career.

I would also like to thank my POS committee members: Dr. Basil Nikolau, Dr. Steve Rodermel, Dr. Robert Thornburg and Dr. David Oliver. Through our POS meetings and during the preliminary exam I was provided with good advice and ideas that helped me obtain a better understanding of my work. I am also very thankful to Dr. Arun Barua, a recent member of my POS committee, who also has helped our lab a great deal in developing a method of analysis of cyanobacterial pigments by HPLC.

Next, I would like to express my thanks to Dr. Jacques Breton and Dr. Kevin Redding for inviting me to their labs to perform some of my experimental work. I thank both of them for their help and especially for the stimulating discussions concerning our work. I also thank Tanya Konovarova, at the University of Alabama, who has helped a great deal with performing ENDOR analysis of my samples.

I owe a great deal to Wu Xu and Huadong Tang, because they taught me most of the experimental techniques I used in this work. Wu and Tang: thank you for being great teachers. I am also grateful to the rest of the members of our lab: Wade Johnson, Yingchun Wang, Dondra Bailey and Mike Hitchler for being a great influence and support during my work.

Finally, I would like to express my thanks to my family. To my parents, George and Dina, I owe all of my success in obtaining my doctorate degree. They have provided me with the opportunity to come this far and for that I will always be grateful. Their love, support and encouragement has helped me go through the hard times, especially during these last few months. I would not have been able to do this without them. Also, I thank my sister Rania, for her continuous support and good advice. Finally, to all of my close friends here in

Ames and back home, I owe so much. Thanks, for your support during these past few years and most of all for the wonderful memories I take with me.